TRENDS OF CLIMATIC EXTREMES AND THEIR CORRELATION WITH WILDFIRE OCCURENCES IN MARGALLA HILLS NATIONAL PARK, ISLAMABAD

By

Mir Khizar Rafique

Department of Earth and Environmental Sciences

Bahria University, Islamabad

2026

TRENDS OF CLIMATIC EXTREMES AND THEIR CORRELATION WITH WILDFIRE OCCURENCES IN MARGALLA HILLS NATIONAL PARK, ISLAMABAD

A thesis submitted to Bahria University, Islamabad in partial fulfillment of the requirement for the degree of M.S in Environmental Sciences

Mir Khizar Rafique

01-262242-039

Department of Earth and Environmental Sciences

Bahria University, Islamabad

2026

APPROVAL FOR EXAMINATION

Scholar's Name: Mir Khizar Rafique **Registration No.** 64129

Program of Study: MS ENVIRONMENTAL SCIENCE

Thesis Title: **Trends of climatic extremes and their correlation with wildfire occurrences in Margalla hills national park, Islamabad**

It is to certify that the above scholar's thesis has been completed to my satisfaction and, to my belief, its standard is appropriate for submission for examination. I have also conducted plagiarism test of this thesis using HEC prescribed software and found similarity index ___ that is within the permissible limit set by the HEC for the MS degree thesis. I have also the thesis in a format recognized by the BU for the MS thesis.

Principal Supervisor's Signature: _____

Date:

Name: Dr. Asma Jamil

AUTHOR'S DECLARATION

I, **"Mir Khizar Rafique"** hereby state that my MS thesis titled **"Trends of climatic extremes and their correlation with wildfire occurrences in Margalla hills national park, Islamabad"** is my own work and has not been submitted previously by me for taking any degree from **Bahria University Islamabad** or anything else in the country/world. At any time if my statement is found to be incorrect even after my graduation, the University has a right to withdraw/cancel my MS degree.

Name of scholar: Mir Khizar Rafique

Date:

PLAGIARISM UNDERTAKING

I, solemnly declare that research work presented in the thesis titled **"Trends of climatic extremes and their correlation with wildfire occurrences in Margalla hills national park, Islamabad"** is solely my research work with no significant contribution from any other person. Small contribution/help wherever taken has been duly acknowledged and that complete thesis has been written by me.

I understand the zero-tolerance policy of the HEC and Bahria University towards plagiarism. Therefore, I as an Author of the above titled thesis declare that no portion of my thesis has been plagiarized and any material used as reference is properly referred to/cited.

I undertake that if I am found guilty of any formal plagiarism in the above titled thesis even after award of MS degree, the university reserves the right to withdraw/revoke my MS degree and that HEC and the university have the right to publish my name on the HEC/University website on which names of scholars are placed who submitted plagiarized thesis.

Scholar/Author's Sign: _____

Name of the Scholar: Mir Khizar Rafique

ACKNOWLEDGEMENT

First and foremost, I am grateful to God, the Most Gracious and the Most Merciful, for His blessings.

I would like to express my sincere gratitude to my supervisor, Dr. Asma Jamil and my co-supervisor Dr. Muhammad Zia UR Rahman Hashmi for their invaluable guidance, constructive feedback, knowledge, and continuous support throughout this research. I am also thankful to Dr. Syed Umair Ullah Jamil, Head of the Department of Earth and Environmental Sciences, and all faculty members. Special thanks to Dr. Waqar Ali and Dr. Ammad Waheed for their guidance and support throughout my research journey. I sincerely acknowledge the Pakistan Meteorological Department (PMD), Capital Development Authority (CDA), and Islamabad Wildlife Management Board (IWMB) for providing the data and information required for this research.

Finally, I extend my heartfelt gratitude to my parents, family, friends, and colleagues for their prayers, unconditional support, encouragement, and assistance throughout my studies and research. Their support has been an invaluable source of strength in completing this thesis.

ABSTRACT

Climate change, fuel load, and human activities are the three major components of wildfire, but the relationship between long-term change in climatic extremes and fire activity is yet to be tested in the protected mountain landscapes of Pakistan. This study compared the climatic changes of the last 30 years in Margalla Hills National Park (MHNP) near Islamabad with the fire record of the park during 1996 to 2025. The daily maximum and minimum temperature, precipitation, relative humidity and wind speed were analysed, and 27 core Expert Team on Climate Change Detection and Indices for temperature and precipitation extreme were computed using ClimPACT2 Package in RStudio. The Modified Mann-Kendall test, Sen's slope estimator and Innovative Trend Analysis were applied to examine trends at monthly, seasonal and annual scales; associations between fire frequency and burned area were quantified using Spearman's rank correlation. While warming was reported in Islamabad and the Potohar Plateau, both maximum and minimum temperature decreased (slope −0.0279°C/yr and −0.027°C/yr respectively) with ITA showing significant cooling in later years, while precipitation and humidity increased and winds were mostly calm. Fire frequency and burned area both decreased significantly, with burned area decreasing at a higher rate than fire frequency, meaning that fire size has decreased but not necessarily the number of fires; the number of fires increased significantly in the summer with Sen's slope of 0.048 recently from July to September. The strongest relationships were at the lower end of the temperature spectrum, with more burned area being correlated with warmer coldest nights (rho = 0.49, $p < 0.01$), and fewer frost days being correlated with less burned area, while winter heavy-rainfall days and June rainfall totals were both correlated with reduced burned area, and the heat index was not significantly correlated. Because climate affects fire primarily through fuel dryness, rather than ignition, which remains predominantly human-driven, MHNP serves as a cooler microclimate than its warmer surroundings. This study thus contributes to a deeper understanding of the climate wildfire nexus and provides an essential baseline for evidence-based forest management, climate adaptation, and disaster risk reduction. Future efforts must prioritize early resource deployment and strict access controls, supported by future research to develop a locally calibrated Pakistan's fire-weather index.

TABLE OF CONTENTS

APPROVAL FOR EXAMINATION....ii

AUTHOR'S DECLARATION....iii

PLAGIARISM UNDERTAKING....iv

ACKNOWLEDGEMENT....v

ABSTRACT....vi

ABBREVIATIONS....xii

CHAPTER 1

INTRODUCTION AND LITERATURE REVIEW

1.1 Background....1

1.2 Climate extremes in a warming world....2

1.3 Wildfire as a climate-sensitive disturbance....3

1.4 Climate variability and wildfire in Pakistan....5

1.5 The Margalla Hills National Park-A study context....7

1.6 Literature review....8

1.7 Statement of the problem....17

1.8 Research questions....17

1.9 Objectives of the study....18

1.10 Significance of the study....18

CHAPTER 2

METHODOLODY

2.1 Study area....20

2.1.1 Climate....21

2.2 Methodological work flow....22

2.3 Data collection....23

2.3.1 Meteorological data....23
2.3.2 Wildfire data....23
2.4 Software used....24
2.5 Data preprocessing....24
2.6 Normality analysis....25
2.7 Data quality assessment....27
2.7.1 Goodness-of-fit distribution analysis....27
2.8 Homogeneity assessment....28
2.8.1 Pettitt's test....29
2.8.2 Mann–Whitney U test....29
2.8.3 Breakpoint verification....30
2.8.4 Homogeneity assessment of difference series....30
2.8.5 Wind speed homogenization....31
2.9 Lag-1 Spearman rank autocorrelation analysis....32
2.10 Descriptive statistics....32
2.11 Temperature and precipitation indices....33
2.11.1 ETCCDI climate extreme indices....33
2.12 Humidity related index: heat index....36
2.13 Wind speed....38
2.13.1 Calm days and windy days....38
2.14 Trend analysis....39
2.14.1 Modified Mann–Kendall test....39
2.14.2 Spearman's rank correlation coefficient....40
2.14.3 Innovative trend analysis (ITA)....41
2.15 Correlation analysis....42
2.15.1 Climate variables, ETCCDI indices vs wildfire....42
2.15.2 Heat index and wind extremes vs. wildfire....43
CHAPTER 3
RESULTS AND DISCUSSION

3.1 Results of normality tests....44
3.2 Goodness-of-fit distribution analysis....45
3.3 Homogeneity outcomes of climate data....48
3.4 Homogenization....49
3.5 Results of autocorrelation (serial dependence)....51
3.6 Descriptive statistics results....53
3.7 Trend analysis of wildfire activity....57
3.7.1 Annual trends....57
3.7.2 Seasonal trends....59
3.7.3 Monthly trends....60
3.8 Trends in climatic variables....62
3.8.1 Trends in temperature maximum....63
3.8.2 Trends in temperature minimum....64
3.8.3 Trends of temperature based ETCCDI....66
3.8.4 Trends in precipitation....69
3.8.5 Precipitation based ETCCDI trends....70
3.8.6 Trends in relative humidity....73
3.8.7 Heat index results....74
3.8.8 Trends in wind speed....76
3.8.9 Wind speed indices....77
3.9 Correlation Results....79
3.9.1 Correlation between temperature extremes and wildfire Activity....78
3.9.2 Correlation of precipitation extremes and wildfire activity....80
3.9.3 Correlation between RH, heat index and wildfire activity....81
3.9.4 Correlation between wind extremes and wildfire activity....82
CONCLUSION....84
RECOMMENDATIONS....86
REFERENCES....87
APPENDIX....105

LIST OF TABLES

Table 2.1 ETCCDI climate extreme indices.....34

Table 2.2 Heat Index risk categories.....37

Table 3.1 Non-Significant results of Normality tests.....45

Table 3.2 Test statistics for homogeneity of climate parameters.....49

Table 3.3 Common breakpoints: Raw and Difference series.....50

Table 3.4 Spearman's lag-1 Autocorrelation stats.....51

Table 3.5 Descriptive statistics climate and fire parameters (1996-2025).....55

Table 3.6 Trend statistics of wildfire.....58

Table 3.8 Significant climate-wildfire correlation (1996-2025).....77

LIST OF FIGURES

Figure 1.1 Fire behavior triangle……..…….....4

Figure 1.2 Spatial distribution of wildfires in Pakistan, 2000-2023….……...….6

Figure 1.3 Global map of average annual area burned, 1960-2000….……...12

Figure 1.4 Satellite map of active fires in Margalla Hills…….……...…...14

Figure 1.5 Duration of forest fires on Margalla Hills, 2002-2011….…….15

Figure 3.1. Histogram and quantile matching graphs for temperature maximum.....44

Figure 3.2 Comparative Goodness-of-Fit and Probability Distribution Analysis for Event Frequency and Precipitation Data.....47

Figure 3.3 Homogenization.....50

Figure 3.4 Innovative Trend Analysis annual fire activity.....58

Figure 3.5 Line graphs of temperature minimum.....65

Figure 3.6 ITA graphs- temperature minimum.....65

Figure 3.7 Sen's slope for temperature's extreme indices (1996-2025).....67

Figure 3.7 ITA- precipitation.....69

Figure 3.8 Sen's slope for precipitation extreme indices-multi scale (1996-2025).…….72

Figure 3.9 ITA- relative humidity.....73

Figure 3.10 Seasonal heat index box plot.....75

Figure 3.11 Heat index (year x month).....75

Figure 3.12 Line graphs of wind speed.....77

Figure 3.13 Stacked area chart of wind speed indices.....78

Figure 3.14 Monthly distribution of wind speed indices.....78

ABBREVIATIONS

AD	Anderson–Darling Statistic
AIC	Akaike Information Criterion
AMJ	April–May–June (Pre-Monsoon Season)
CDA	Capital Development Authority
CL	Confidence Limit
CMIP5	Coupled Model Intercomparison Project Phase 5
CV	Coefficient of Variation
DJFM	December–January–February–March (Winter Season)
ECA&D	European Climate Assessment & Dataset
ECDF	Empirical Cumulative Distribution Function
EQM	Empirical Quantile Matching
ETCCDI	Expert Team on Climate Change Detection and Indices
IPCC	Intergovernmental Panel on Climate Change
IQR	Interquartile Range
ITA	Innovative Trend Analysis
IWMB	Islamabad Wildlife Management Board
JAS	July–August–September (Monsoon Season)
JB	Jarque–Bera Statistic
KPK	Khyber Pakhtunkhwa
MHNP	Margalla Hills National Park
MK	Mann–Kendall
MMK	Modified Mann–Kendall
MODIS	Moderate Resolution Imaging Spectroradiometer
NASA	National Aeronautics and Space Administration
NDMA	National Disaster Management Authority
RH	Relative Humidity
SD	Standard Deviation
SR	Spearman's Rank Correlation

LIST OF APPENDICES

A1. Normality test results for monthly climate data.....105

A2. Normality test results for yearly climate data.....105

A3. Normality test results for monthly and yearly fire data.....106

B1. Goodness-of-Fit results for climate data 106

B2. Goodness-of-Fit results for fire data 107

C. Descriptive statistics results for climate data.....107

D1. ITA results for fire and climate data.....108

D2. Mann–Kendall test statistics ETCCDI indices (1996-2025).....110

E. Spearman’s correlations results.....110

CHAPTER 1

INTRODUCTION AND LITERATURE REVIEW

1.1 Background

Wildland fire is a global phenomenon that arises from the interaction of climate and weather, fuels and human activity, and its behaviour cannot be understood by reference to any one of these components alone (Flannigan et al., 2009). Forests have carbon sequestration, moderate local temperature, slope stability and water provisioning functions, and large scale disturbances affect more than the stand they inhabit. Fire is unique among ecological disturbances in that it is a natural ecological process, a hazard to life and property, and a source of atmospheric carbon that contributes to warming and, consequently, to fire (Bowman et al., 2009).

Fire patterns are influenced by temperature, rainfall, humidity and extreme heat and fire ecology models show that these factors interact to determine fuel moisture, atmospheric dryness and likelihood of ignition, which in turn influences fire activity frequency and severity (Flannigan et al., 2009). The important changes in recent decades are that the background climate on which fire seasons are occurring is changing. Jolly et al., (2015) found that fire weather seasons became longer over about 25% of vegetated land surface between 1979 and 2013, suggesting an increase in the time period when fuels are ready to burn. Questions that were previously asked in a year to year manner are now increasingly phrased in terms of a directional change.

Given this turn, the importance of assessment of climatic extremes has increased in particular. The mean annual temperature and total annual rainfall are useful summary statistics, but can mask the occurrence of shorter, more intense events that impact landscape flammability and wildfire occurrence (Xing et al., 2023). A slight increase or decrease in the annual mean can have a smaller effect on fire activity than a single dry spell of a few weeks, or a few days of unusually high temperatures, or a season of consistently low humidity (Jones et al., 2022). Effort has therefore been expended to develop standardised measures of extremes which can be compared between regions and time periods, and these are now the common currency of climate extremes research. Such indices are important for the study of wildfire because fire conducive conditions are

frequently related to thresholds and extended periods of climatic stress and not just to a gradual change in average conditions. For instance, an upward trend in the number of extremely warm days, in the length of dry periods or in the length of warm spells could lead to an increase in fuel dryness even if the annual averages are not significantly different. An analysis of extremes is thus a more direct method of detecting changes in climatic conditions that may enhance the potential for fire.

In this wider context, Pakistan is a very vulnerable country. Rafaqat et al., (2022) found that climatic conditions explained the most variance in wildfire occurrences in the country, more than did fuel and topography, suggesting that the country's fire pattern is more climate-driven than ignition-driven. Moreover, Nafees et al., (2024) noted that decreased precipitation and frequent heatwaves have exacerbated the risk of wildfires in the Northern Highlands and have hindered vegetation recovery. However, the systematic investigation of the link between climate extremes and fire activity in protected areas of Pakistan is in its infancy and is the motivation for the present work.

1.2 Climate extremes in a warming world

The evidence of fluctuations in the occurrence and magnitude of extreme events is now extensive. The IPCC (2021) documents a rise in the frequency of hot extreme events and severity across most continental regions, episodes of extreme cold have become less frequent and less severe since the 1950s, and human activity is considered as the primary cause of these trends. In addition, the same assessment records that human influence has likely enhanced the likelihood of compound extreme events, such as fire weather in some areas of all inhabited continents. The importance of such statements for the present study is that they indicate that the changes studied are present in the tails of the distributions, where fire risk is concentrated (Kalashnikov et al., 2026). The extremes of temperature and precipitation do not happen in isolation and they often combine for the most harmful effects. For example, a warm winter followed by a dry summer could lead to soil moisture deficits that are significantly greater than either anomaly would cause. Given this, focus has shifted to compound and sequential events, where the sequence of anomalies is as important as the magnitude of the anomalies themselves (Seneviratne et al., 2021). Moreover, warmer air also pulls more moisture out of plants and soil. So even if the same amount of rain falls, fuels end up drier than they used to under cooler conditions meaning drying can get worse even when rainfall stays the same (Abatzoglou & Williams, 2016). The temporal scale of analysis is also important because climatic conditions relevant to

wildfire can vary considerably within a year. Average conditions for the year may mask the presence of extreme heat, low humidity, high winds or extended dry spells, and average conditions in a season may mask the presence of particularly severe conditions in a given month. Monthly, seasonal and annual analysis can therefore be used to complement each other to identify long-term changes and to capture variations occurring at different times of the year to capture variations occurring at different times of the year when climatic conditions are most conducive to wildfire. A second set of variables has been studied less than the variables affecting the fire directly, but both affect the fire indirectly: relative humidity and wind speed. These variables, when combined, give information on the dryness of the atmosphere and fire behaviour that cannot be adequately represented by temperature and precipitation. Dry, fine fuels (dry grass, fallen leaves) lose moisture faster at low relative humidity. The wind aids the fire in several ways: it supplies oxygen, pushes the flames towards unburned fuel and carries burning embers ahead of the main fire. This finding corresponds with the results of Rafaqat et al., (2022), who identified specific humidity and vapour pressure among the key predictors of fire occurrence in Pakistan. Since these variables are routinely recorded at meteorological stations, their neglect in trend studies appears to reflect convention rather than any judgement about their importance, and the present study therefore treats humidity and wind speed as analytical variables of equal standing with temperature and precipitation.

1.3 Wildfire as a climate-sensitive disturbance

Wildfire occurrence depends on the simultaneous presence of three conditions, namely available fuel, an ignition source, and weather that lets the fire burn and spread Since ignition in most inhabited landscapes is predominantly human in origin, variation in fire activity from year to year is frequently governed by the third condition. This distinction is important when wildfire activity is measured through both the number of fire events and the area affected. Climatic conditions may not necessarily determine whether an ignition occurs, particularly where human activities provide frequent ignition sources, but they can influence whether an ignition develops into a sustained fire and how extensively it spreads. Thus, changes in temperature, moisture, and wind may be reflected differently in fire frequency and burned area (Pokhrel et al., 2026). Tariq et al., (2022) found that human activities account for a large proportion of forest fires in Margalla Hills which supports the proposition that ignition is rarely the limiting factor in populated

landscapes and that climatic variation therefore determines whether ignitions develop into significant events.

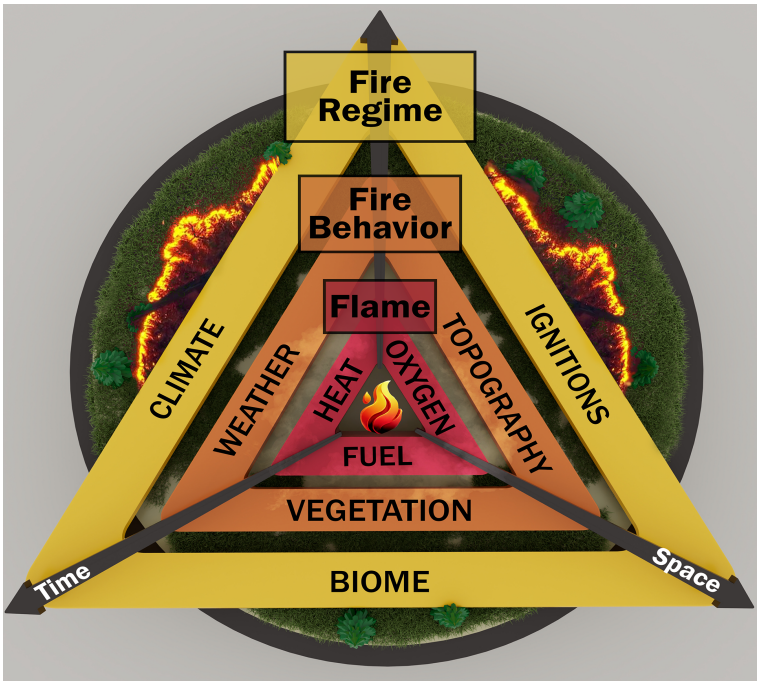


Figure 1.1. Fire behavior triangle. Source: Ethan brain.

The case of the western United States is a good example of this. Westerling et al., (2006) demonstrated that warming and an earlier onset of spring were associated with increased forest wildfire activity, thereby linking the timing of snowmelt and the length of the dry season to the burned area recorded in subsequent months. Building on this work, Abatzoglou and Williams (2016) attributed a substantial share of the observed increase in fuel aridity to human-caused climate change and concluded that anthropogenic influence had doubled the cumulative forest fire area since 1984. In addition, Williams et al., (2019) documented how rising temperatures and increasing vapour pressure deficits have extended fire seasons and increased burned area in California. Goss et al., (2020) found that the risk of severe autumn fire conditions has increased in the same area as a result of climate change.

Forecasts for other temperate systems are similar. Turco et al., (2018) calculated future summer burned area for Mediterranean Europe at different warming levels, namely 1.5°C, 2°C, and 3°C**,** and concluded that burned area is projected to increase substantially, with the magnitude of increase rising with the level of warming even with non-stationary changes in the climate–fire relationship due to vegetation productivity. Taken together,

these studies demonstrate that a climatic signal in fire records can be detected and, under favourable data conditions, partially attributed.

Nevertheless, the strength of the climate–fire relationship is not uniform across regions. In humid forests, there's usually plenty of fuel but the problem is it's often too moist to burn. So warming there tends to raise fire risk by drying things out; in arid systems, where fuel production itself depends on rainfall, a wetter year may increase fire activity in the following season by generating additional biomass (O et al., 2020). Thus, results from one biome cannot be applied to another without verification and local studies must be conducted. This is relevant directly to the subtropical, monsoon-influenced system studied here, which is more similar to neither the Mediterranean nor the boreal systems that have been the subject of the international literature.

1.4 Climate variability and wildfire in Pakistan

Pakistan experiences a markedly seasonal climate in which the majority of annual precipitation over the northern districts arrives during the monsoon, while the pre-monsoon period from April to June is characterised by high temperatures, low humidity and limited rainfall (Abbas et al., 2025). Since this window coincides with the accumulation of dry litter following winter leaf fall, it is the time when fire is most likely in the sub-mountainous forests of the north (Nafees et al., 2024). Changes in the timing, duration, or severity of dry periods may therefore affect wildfire occurrence and behavior, even if the number of fire ignitions remains unchanged.

Climate extremes-related research in Pakistan has increased significantly in the last decade, but has been largely focused on precipitation and hydrological impacts, with little focus on fire. Abbas et al., (2023) investigated the country-wide seasonal variations of extreme precipitation and observed that the warming tendency affects monsoon precipitation with unprecedented intensity, which contributes to severe flooding. Although flooding and wildfire are often regarded as opposing hazards, both have been linked to the same underlying hydroclimatic mechanism: as atmospheric warming increases the air's capacity to hold and evaporate moisture, precipitation is increasingly delivered in fewer, more intense events punctuated by longer dry intervals, during which vegetation desiccates and fuel loads accumulate, thereby elevating wildfire risk (Swain et al., 2025).

National-scale fire research has developed principally through satellite-based analysis. Rafaqat et al., (2022) investigated the spatiotemporal pattern and drivers of wildfire across Pakistan for the period from 2001 to 2020, and reported that elevation, population, specific humidity, vapour pressure and vegetation index were the most influential predictors, with climatic conditions contributing the largest share of explanatory power at the national level. Building on such work, Shahzad et al., (2024) compared machine learning algorithms for predicting vegetation fire detections across Pakistan using data compiled from 2001 to 2022, and reported accuracies for forest fire prediction that confirm the value of long climatic and environmental time series. In contrast, Nafees et al., (2024) approached the question from a management perspective in the Northern Highlands and emphasised the compounding effect of reduced precipitation and recurrent heat episodes on both fire risk and post-fire recovery.

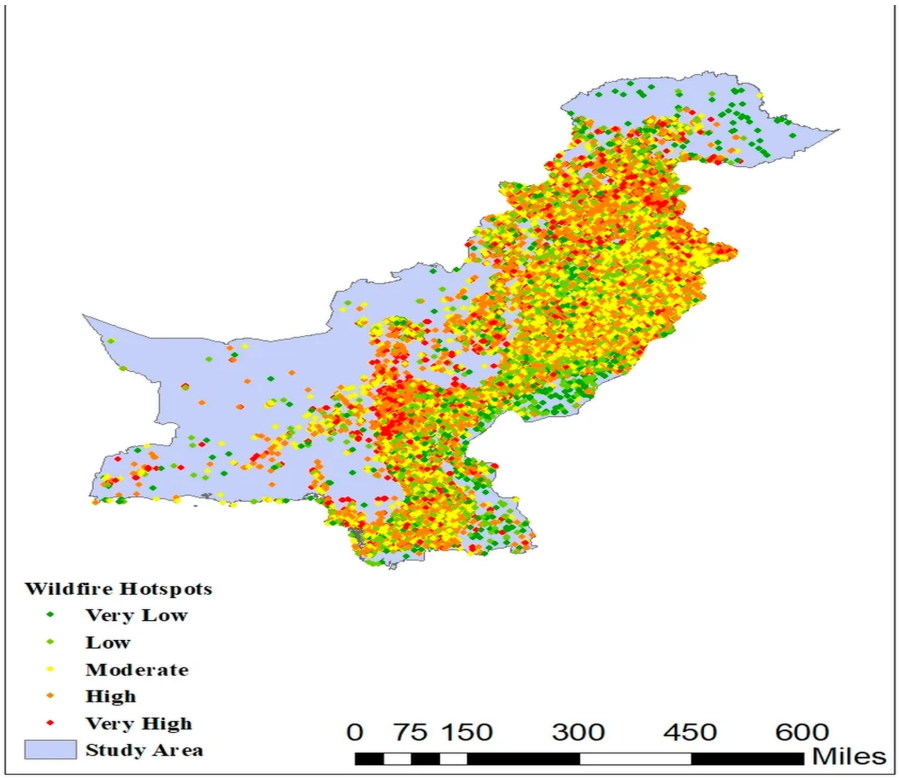


Figure 1.2. Spatial distribution of wildfires in Pakistan, 2000-2023. (Rafaqat et al., 2022)

Furthermore, the national record of heat extremes has attracted growing concern. Since the physiological burden of heat depends on humidity as well as on air temperature, the heat index has been adopted in operational practice as a measure of apparent temperature (Rothfusz, 1990). Although the heat index was developed for human health

applications rather than for fire science, its combination of temperature and humidity into a single quantity makes it a plausible summary of the atmospheric conditions that also govern fine fuel moisture, and its behaviour over time in fire-prone districts has not been widely examined.

1.5 The Margalla Hills National Park-A study context

Margalla Hills National Park (MHNP) was established in 1980 and forms the northern boundary of the Islamabad Capital Territory and represents the southernmost extension of the Himalayan foothills. The Margalla Hills comprise the Margalla Hills range (12,802 ha), Shakarparian (1,376 ha) and Rawal Lake (1,702 ha) and are bounded by approximately 33°40′ N latitude and 72°45′ E to 72°52′ E longitude (Rais et al., 2021; Batool & Javaid, 2018). Because of its wide range of elevations, slopes, and aspects, the park contains a mixture of deciduous, coniferous, and mixed vegetation. This diversity creates considerable variation in fuel types and moisture conditions across the park (Tariq et al., 2021a).

The park is an ecologically important zone that is rich in biodiversity yet vulnerable to anthropogenic pressure and natural hazards, particularly wildfire (Rafaqat et al., 2022). It is unique among protected areas because it is located directly near a large urban center, has high recreational use, is traversed by roads and trails, and borders residential communities that use forest resources. Since human presence supplies the ignitions that convert favourable fire weather into actual fire events, the proximity of the park to Islamabad makes its fire pattern particularly sensitive to any climatic change that lengthens or intensifies the receptive period (Tariq et al., 2022).

In addition, the topography of the park amplifies fire behaviour in ways that are well documented in fire science. Steep slopes allow flames to reach the vegetation above more quickly, while narrow valleys can direct and strengthen winds. Exposed limestone areas create breaks in the landscape that can make it difficult for firefighting teams to reach and control the fire (Tariq et al., 2021a). Because firefighting resources are limited and some parts of the park are difficult to reach, even a moderate increase in hot, dry, or windy conditions may lead to a much larger increase in the area burned. Therefore, the park provides a useful setting for examining how climatic conditions influence wildfire risk while also considering the role of human caused ignitions. The combination of persistent human ignition pressure and variable climatic conditions also makes it possible

to examine whether changes in the climatic environment are reflected in both the frequency of wildfire events and the extent of burned area over time.

1.6 Literature review

Studies on temperature extremes have yielded a fairly uniform global pattern, with warming being more pronounced for warm nights and warm days than for cold days as well as cold nights. The IPCC (2021) assessment confirms that the observed rise in the occurrence of hot extremes in most land regions is very likely to be due to climate change caused by human activity, and has been supported by a large number of index-based regional studies carried out over many decades.

Sillmann et al., (2013) evaluated the representation of climate extremes indices within the CMIP5 multimodel ensemble and confirmed that the standardised indices provide a workable basis for comparison between observed and modelled conditions, which has since supported the use of the same indices in observational trend studies. On the basis of this framework, regional analyses have been conducted in various parts of South Asia, and the overall picture is broadly in line with the worldwide pattern, but with significant local variation. However, mountainous areas often differ from lowland areas because the elevation, snow cover and aspect influence the local energy balance differently from a national aggregate (Nafees et al., 2024).

The temperature indices most relevant to fire research are those that reflect the maximum temperature and duration of hot conditions. The annual maximum of daily maximum temperature is a measure of heat intensity, the number of days above the ninetieth percentile is a measure of how often extreme heat occurs, and the warm spell duration index quantifies the duration of a given period of unusually hot conditions (Alexander et al., 2006). Since fuel drying is a process that takes time, indices which are more sensitive to the duration of warm conditions might have more explanatory power than those sensitive to the peak of warm conditions. An extreme heat day is likely to dry only fine fuels (e.g. leaf litter and small twigs) while a prolonged warm spell has the potential to dry both fine and coarser fuels, which may allow fire to burn and spread (Flannigan et al., 2009). This agrees with findings from Nafees et al., (2024), who reported that in the Northern Highlands of Pakistan, fire risk was elevated more strongly by recurring periods of heat than by isolated temperature extremes.

Precipitation indices tend to be less spatially coherent than temperature indices, since rainfall is shaped more strongly by local convective activity and circulation patterns than temperature is (Alexander et al., 2006). The record length used can also change the picture considerably: Pal and Al-Tabbaa (2011) identified that the trends in seasonal and annual rainfall for each region varied when using a long time series (1871–2005) as compared to a shorter time series (1954–2003), and that some regions had no significant trend over the long time series but a significant trend over the short time series. Abbas et al., (2023) explored the seasonal variability in extreme precipitation over Pakistan and reported that monsoon precipitation has intensified under a warming climate, contributing to more severe flooding though their results also showed this intensification was uneven, with some regions registering significant increases in wet-day frequency while others registered significant decreases across different sub-periods. These results indicate that any precipitation extremes national-scale trends should be interpreted with care, as there may be significant regional and temporal variations.

Common indices used in this area include the yearly frequency of wet days, peak one- and five-day precipitation and days exceeding specified thresholds and number of consecutive wet and dry days (Zhang et al., 2011). Of these, the duration indices are of particular interest in fire research as the length of the longest dry spell gives a direct measure of the length of the period over which fuels may be drying without replenishment. Additionally, under a warming climate, projections for the broader Central and South Asian region (including northern Pakistan) suggest a concurrent rise in both the intensity of rainfall and the length of dry spells, which would further favor increased fire potential even if annual precipitation is unchanged (Rai et al., 2024).

Notably, precipitation series are often non-normal, with a distribution shape that is usually right-skewed (e.g., gamma distribution) and not Gaussian. This non-normality is a well-documented reason for preferring resistant and non-parametric statistical techniques over standard parametric methods in climate data analysis, including trend estimation, and it also motivates fitting an appropriate parametric distribution to the data as an alternative approach to handling skewness (Lanzante, 1996).

The comparability of extremes research across regions depends on the use of a common set of definitions, and this need has been addressed primarily by the Expert Team on Climate Change Detection and Indices (ETCCDI). Zhang et al., (2011) found temporal changes in extreme indices of climate are increasingly based on relative thresholds that

refer to features in the tails of meteorological distributions rather than on fixed physical thresholds that have little relevance outside the region for which they are defined. Zhang explains the distinction between absolute and percentile-based indices carries practical consequences. An absolute index, such as the count of days on which maximum temperature exceeds twenty-five degrees Celsius, is easy to read but is meaningful only where that threshold is meaningful for that climate. A percentile-based index like the number of days above the ninetieth percentile of the reference period will adjust automatically to the local situation and can thus be compared between a temperate mountain valley and a subtropical plain. Since the present study concerns a location with a subtropical semi-arid to sub-humid climate, both categories are retained, the absolute indices for local interpretability and the percentile indices for external comparison.

The ETCCDI framework offers standardized methods for the calculation of percentile thresholds, with a 5-day window around each calendar day. This is to make the thresholds smooth across the seasons and avoid jumps in the index values from one day to the next. The need for following these standard procedures is important because it enables climate extremes to be calculated on a consistent basis over regions, which facilitates comparison of climate extremes, and enables researchers to determine if climate models are able to accurately represent climate extremes (Klein Tank et al., 2009).

Rothfusz (1990) formalised the heat index as an apparent temperature and it has been widely adopted by meteorological services, including those of South Asia. The reason for this is related to the physiology of the body: the more humid the environment, the less effective the evaporative cooling, and the more uncomfortable a particular temperature will be in a humid environment compared to a dry one. The index was developed to protect health, but its application to fire science is based on the same physical relationship but in reverse. Fine fuel moisture responds to the environment, and how fast it responds is related to temperature and humidity (Matthews, 2014). The time-series of the heat index can then be interpreted as an integrated measure of the moisture environment of the atmosphere, and the direction of change in the heat index can be compared with the direction of change in the temperature and humidity indices to check if both variables are trending in similar or contrasting directions. This is indirectly supported by the work done by Rafaqat et al., (2022) who reported that specific humidity and vapour pressure were among the strongest predictors of fire occurrence in Pakistan.

But caution should be taken in interpreting trends in heat index. Higher humidity levels tend to lower the fire risk, while higher humidity levels increase the heat index. Thus, rising heat index does not necessarily mean rising wildfire risk, and this relationship should be evaluated on a case-by-case basis and not assumed. This complexity could be one reason why the heat index has not been widely studied in the context of wildfires, especially in fire-prone subtropical areas.

The variables that influence the occurrence of wildfires are also used in operational fire-danger systems, since fire is more likely to occur during periods of high temperature, high drought severity, strong wind, low relative humidity and low rainfall (Zacharakis & Tsihrintzis, 2023). Wind is especially significant because it has the greatest influence on fire spread, not fire initiation, and its influence increases with wind speeds above moderate. Therefore, a small increase in wind speed during the season can result in a disproportionately large increase in burned area per fire, which is relevant to practice as Tariq, Shu, Saddiqui et al., (2021) determined that burned area increased rapidly after a fire once it had become established.

Relative humidity mainly affects wildfire risk by influencing fuel moisture. The moisture content of fine fuels (grass, needles, leaf litter) can change rapidly with humidity, so low afternoon humidity can influence whether a new fire continues to spread or dies out (Lewis et al., 2024). This aligns with the findings of Rafaqat et al., (2022), who used national scale models and found humidity-related factors to be significant predictors of wildfire occurrence. Since relative humidity is routinely measured along with temperature and rainfall, its exclusion from regional trend analyses cannot be easily explained by a lack of data. However, wind data can be very difficult to analyse. The data may contain gaps that can be interpreted as climate change signals, but are instead due to changes in the measurement conditions, such as anemometers, vegetation or buildings (Venema et al., 2018; Wan et al., 2010). Therefore, wind trends should be assessed carefully and checked for homogeneity before analysis to avoid misleading results. This consideration is taken into account in the present study.

The best empirical evidence for the relationship between climate and wildfire is found in temperate forests in the Mediterranean and North America. Westerling et al., (2006) identified a non random rise in the count of large wildfires in the western United States that was linked to higher spring and summer temperatures and earlier snow melt.

These changes were also linked to a longer fire season. Their study helped establish a quantitative link between climate change and wildfire activity. Later, Abatzoglou and Williams (2016) examined the role of human-caused climate change by comparing observed conditions with model simulations. They discovered that anthropogenic climate change has caused a greater than 50% contribution to fuel aridity since the 1970s and a doubling of the cumulative area burned by wildfire since 1984. The impacts of human-induced warming on wildfires in California were also reported by Williams et al., (2019) and Goss et al., (2020), who observed a higher likelihood of extreme autumn fire-weather conditions in the region. At the global scale, Jolly et al., (2015) reported the average length of fire-weather season hiked about 19% between 1979 and 2013. Projection studies build on this relationship by examining how wildfire activity may change under future warming. Turco et al., (2018) modelled summer burned area across Mediterranean Europe under different warming scenarios and found consistent increases in burned area. Their results also showed that limiting future warming could substantially reduce the projected area burned, highlighting the importance of climate change for future wildfire risk.

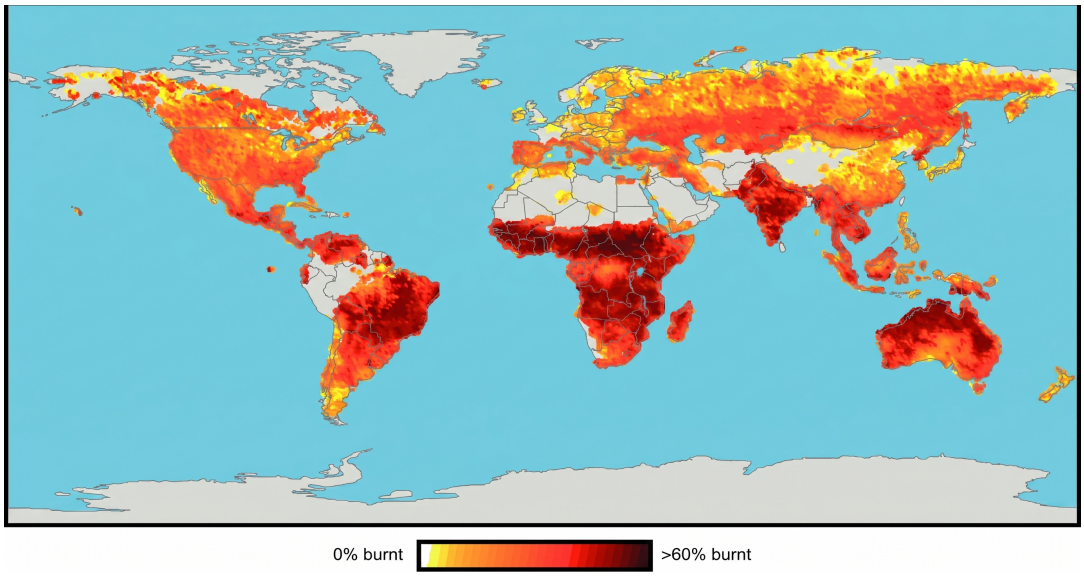


Figure 1.3. Global map of average annual area burned, 1960-2000 (Flannigan et al., 2009)

However, these studies also show that reliable climate–fire analysis depends on long and consistent fire records, good meteorological coverage, and conditions where fuel moisture strongly influences fire activity (Dupuy et al., 2020). Such conditions may be less common in developing regions, where fire records and climate observations can be limited. Therefore, these methods cannot always be applied directly and may need to be

adapted to local data conditions. This is particularly relevant to the present study, where the available fire records are more limited than those used in many of the studies discussed above.

Research conducted in the Indian Himalaya provides the closest available analogue to the setting of the present study, since the vegetation, the monsoon-driven seasonality and the predominance of anthropogenic ignition are broadly comparable. Mina et al., (2023) evaluated the correlation between fire events and climate parameters in Uttarakhand and found that maximum, average, and diurnal range of temperature showed positive and significant relationship with fire events while relative humidity showed negative and insignificant relationship. The seasonal pattern reported in the region is also applicable. Fire activity was highest during the pre-monsoon period, when dry leaf litter, increasing temperatures, lower humidity, and greater human activity related to grazing and fuelwood collection create favorable conditions for fire (Charak et al., 2026). Pokhrel et al., (2026) reported a similar pattern in Langtang National Park, Nepal, where maximum temperature was identified as the main climatic factor influencing burned area. Studies in the western Himalaya have reported increasing fire activity and significant relationships between burned area and climatic variables. For instance, Bar et al., (2021) observed a positive trend in burned area and moderate positive correlation with temperature and precipitation for Uttarakhand while Kumar and Kumar (2022) identified temperature as an important factor influencing fire occurrence. These findings indicate that climate contributes to Himalayan wildfire activity, although its influence varies across locations and interacts with other factors.

Wildfire research in Pakistan has largely focused on geospatial analysis, susceptibility mapping, and machine-learning-based prediction. At the national scale, Rafaqat et al., (2022) examined the spatial and temporal patterns and drivers of wildfires from 2001 to 2020 using machine-learning models based on climatic, topographic, and vegetation-related variables. They identified elevation, population, specific humidity, and as important drivers, with their relative influence varying across locations and seasons. Similarly, Shahzad et al., (2024) evaluated several machine-learning algorithms for predicting vegetation fire detections using data from 2001–2022 and found that the random forest model achieved the highest accuracy for forest fires (87.5%). These studies demonstrate the value of long-term environmental data for understanding and predicting wildfire activity in Pakistan. However, they do not specifically examine MHNP or assess

long-term trends in humidity, heat-related conditions, and other climatic extremes within the park.

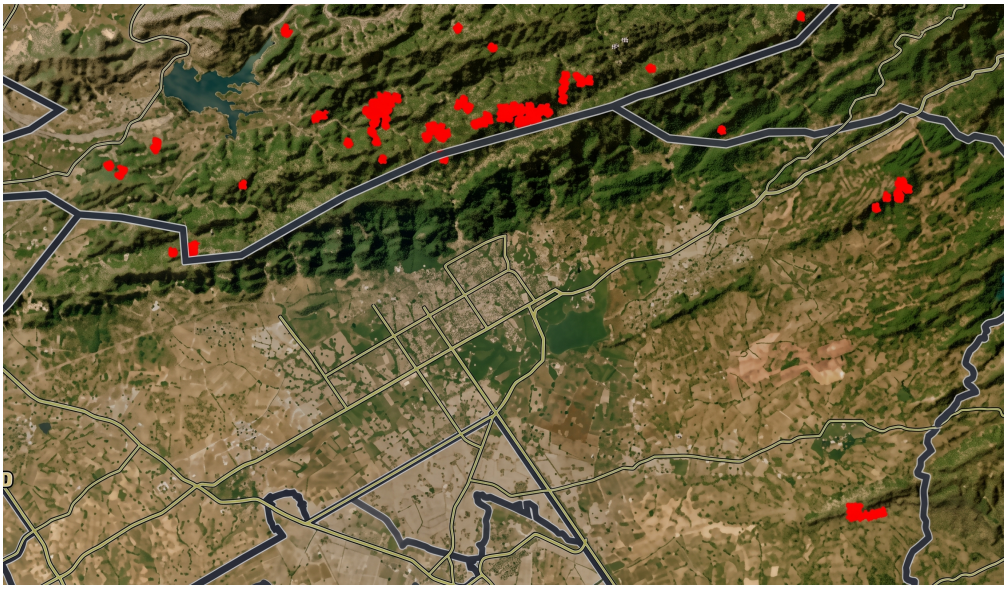


Figure 1.4. Satellite map of active fires in Margalla Hills Source: (The Friday Times, 2024)

Within the park itself, three studies are of particular relevance. Tariq et al., 2021a developed a methodology for analysing the spatial pattern of fire danger using Landsat imagery, considering climatic, vegetation, topographic and anthropogenic variables across a large set of recorded fire locations, and observed that burned area increased at a rate of approximately twenty-six hectares per day as fire duration lengthened. In parallel, Tariq et al., 2021b applied Sentinel-derived spectral indices together with radar imagery to assess burned areas from wildfires and prescribed fires between 2015 and 2020, thereby establishing a remote sensing basis for burned area estimation within the park.

Although hot, dry conditions set the stage for fire in Margalla Hills National Park (MHNP), most ignitions there are attributed to people rather than natural causes such as lightning. Spatio-temporal modelling of fire history from 1990 to 2019 found that fire probability in the Margalla Hills was related to accessibility and human behaviour, with fires mainly distributed in urban areas (Tariq et al., 2022). Related work found that distance to roads, along with forest density, temperature and wind speed, was highly correlated with fire severity (Tariq et al., 2021). Within this pattern, several specific activities are repeatedly reported. The first is careless recreational use of the park. Hikers, picnickers and campers are reported to ignite fires unintentionally by discarding lit

cigarettes into dry grass or by not fully extinguishing campfires (Abubakar, 2018). The second is deliberate burning by residents of surrounding villages, often described as retaliation for restrictions on grazing livestock inside the park, or for not being hired for seasonal daily-wage fire-patrol work (Junaidi & Shahid, 2021). The third is that fires have also been linked to attempts to conceal illegal tree felling (Abubakar, 2018). The chairperson of the Islamabad Wildlife Management Board has stated that roughly 80–90% of fires in the park are set by people (Junaidi & Shahid, 2021; Qudratullah 2024).

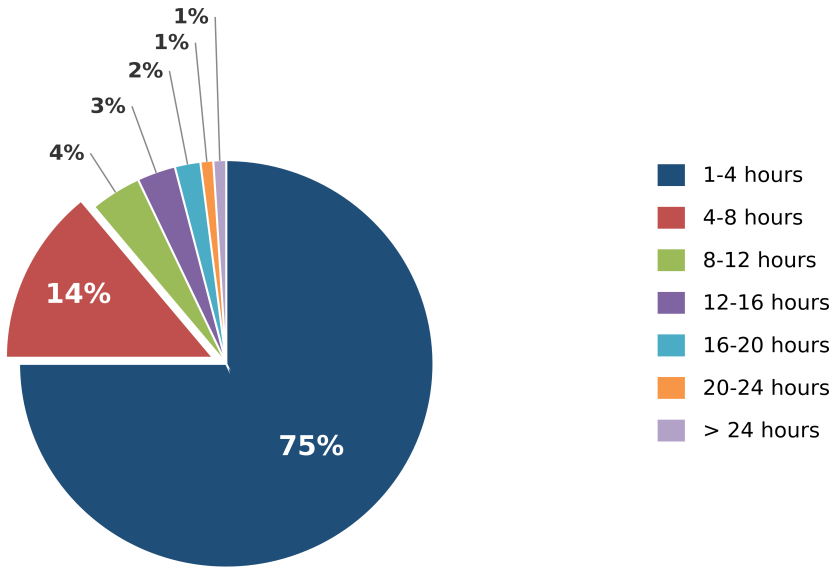


Figure 1.5. Duration of forest fires on Margalla Hills, 2002-2011 (Khalid et al., 2015).

Taken together, these studies indicate that human activity influences fire ignition, while climatic conditions affect fire spread and severity. However, most existing research treats climate as a background factor and covers relatively short periods. In contrast, the present study examines changes in climatic conditions over a 30-year period and their relationship with wildfire activity, thereby extending the existing research on the Margalla Hills. It should also be noted that the park's fire records are based on administrative reports rather than a dedicated monitoring system, so reporting may vary over time. As a result, increases in reported fire frequency may partly reflect changes in reporting practices. Hence, fire event trends should be treated with greater caution than burned area trends. Satellite-based active fire and burned area products can contribute to this problem and serve as an independent means for comparing administrative records (Giglio et al., 2018; Schroeder et al., 2014).

Non-parametric methods are widely used for detecting trends in climatic data because these datasets often do not meet the assumptions required by parametric tests. The Mann–Kendall test is often applied to detect significant monotonic trends, and Sen's slope estimator quantifies the magnitude of the trend based on the median of all pairwise slopes, which is less influenced by outliers than the median slope (Sen, 1968). Their combined use is well established in climate trend studies and has been applied successfully to meteorological data in different regions (Gocic & Trajkovic, 2013). The classical Mann Kendall test is however sensitive to serial correlation. Hamed and Rao (1998) demonstrated that a positive autocorrelation can lead to a higher probability of identifying a significant trend if there is not one. They therefore proposed a modification that adjusts the variance of the test statistic to account for autocorrelation. Since climatic data at monthly and seasonal scales can exhibit serial dependence, the modified Mann–Kendall test is more appropriate when such dependence is present.

In addition to rank-based tests, graphical approaches have gained ground in recent years. The innovative trend analysis developed through Şen's (2012) research is based on dividing a series into two equal parts and plotting the sorted values of the two halves against each other to determine the position of the points relative to the one-to-one line, which is used to determine whether there is a trend or not. Since the method imposes no distributional or independence assumptions, it may be applied where rank-based tests are compromised, and it possesses the further advantage of revealing whether a trend affects low, medium and high values differently. In contrast to the Mann–Kendall test, which returns a single monotonic verdict, the graphical method distinguishes trends confined to particular parts of the distribution, which is informative in extremes research. Correlation analysis is another important part of the present study. When the variables are non-normally distributed, as is often the case when climatic indices are related to wildfire counts, Spearman's non-parametric correlation is preferable to Pearson's linear correlation because it measures monotonic relationships, which do not depend on normality or linear relationship (Weaver et al., 2017). However, results from multiple index–variable comparisons should be interpreted carefully because a large number of tests can increase the likelihood of finding significant relationships by chance.

A climatic series is considered homogeneous when its variations reflect only natural changes in weather and climate. However, station relocation, instrument replacement, changes in observation practices, and changes around the station can introduce artificial breaks (Venema et al., 2018). Identifying these breaks before trend analysis is important because the choice of homogenization method can influence the results (Domonkos et al., 2021). Various statistical tests and software tools are available for detecting such discontinuities (Wang & Feng, 2013). Serial dependence is another important concern, as autocorrelation can affect trend-test results. Therefore, when autocorrelation is detected, this study applies the variance-correction approach of Hamed and Rao (1998), as prewhitening may remove part of the actual trend along with the serial dependence.

1.7 Statement of the problem

Despite recurring wildfires in Margalla Hills National Park (MHNP), the long-term influence of climatic variability and extremes on wildfire activity remains poorly understood. Existing studies have largely emphasized spatial patterns over limited periods (Tariq et al., 2021a, 2021b; Tariq et al., 2022), leaving long-term trends in climate extremes, wildfire frequency, burned area, and their statistical relationships insufficiently investigated. Moreover, inadequate consideration of data homogeneity and serial correlation may undermine the reliability of trend assessments. This lack of integrated and statistically robust evidence limits predictive fire management and effective wildfire preparedness in MHNP, highlighting the need for a comprehensive analysis covered by this study.

1.8 Research questions

The research questions below were formulated from the stated research problem:

i. Over the 1996–2025 period, did the mean and indicators representing unusually high or low temperature, rainfall, humidity, and wind conditions change significantly at annual, seasonal, and monthly scales?
ii. Which of the standardised extreme climate indices show the strongest trends and when?
iii. Is there a measurable trend in the count of fire events and the total burned area during the same time period?

iv. To what extent do the identified climatic trends correlate statistically with the observed pattern of wildfire activity?

1.9 Objectives of the study

Following from these questions, the study pursues two principal objectives:

i. To study the annual, monthly and seasonal variations of climatic parameters including temperature, precipitation, humidity and wind speed in Margalla Hills National Park during 1996-2025 as well as extreme climate indices; and
ii. To examine the relationship between the observed trends in mean and extreme climate and the frequency and pattern of past wildfire occurrences in Margalla Hills National Park during the same thirty years.

1.10 Significance of the study

This study holds theoretical, methodological, and practical significance for understanding wildfire dynamics in Margalla Hills National Park (MHNP). Academically, it addresses an important gap by shifting the focus of regional wildfire research from spatial patterns to multi-decadal temporal dynamics (1996–2025) and examining whether broader climate–wildfire relationships are evident at the local scale. Methodologically, the study provides a comprehensive assessment by incorporating standardized extreme climate indices and less-studied variables such as relative humidity, wind speed, and heat index, while applying rigorous statistical diagnostics including homogeneity testing and autocorrelation correction to validate trend estimates. Practically, the findings may help identify high-risk seasons and climatic conditions, support wildfire monitoring and preparedness, and guide targeted, climate-informed wildfire management in MHNP; institutionally, the study also overcomes existing data silos by consolidating meteorological data with fragmented fire records across agencies such as IWMB and CDA into a single, unified database. Environmentally, these insights provide the empirical foundation to protect the park's native biodiversity, preserve forest cover, and maintain its ecological role as a cooling microclimate and carbon sink for Islamabad. Socio-economically, identifying these high-risk windows allows agencies such as IWMB and CDA to allocate firefighting resources pre-emptively rather than reactively, reducing emergency suppression costs and protecting residential communities along the park's wildland-urban interface. The study also establishes a 30-year baseline that can support future research and climate adaptation planning in the region, including

the empirical groundwork needed for future researchers to develop a locally calibrated Pakistani fire-weather index.

CHAPTER 2

METHODOLOGY

2.1 Study area

This research was carried out for MHNP, which lies in the northern part of Islamabad Capital Territory (ICT), Pakistan. This study was specifically for Margalla Hills range that is the largest vegetative part of the park. It represents the southernmost extension of the Himalayan foothills and is recognized as one of Pakistan's most ecologically significant protected areas because of its biodiversity, forest ecosystems, and conservation importance (Government of Pakistan, 2020; Chandio et al., 2019).

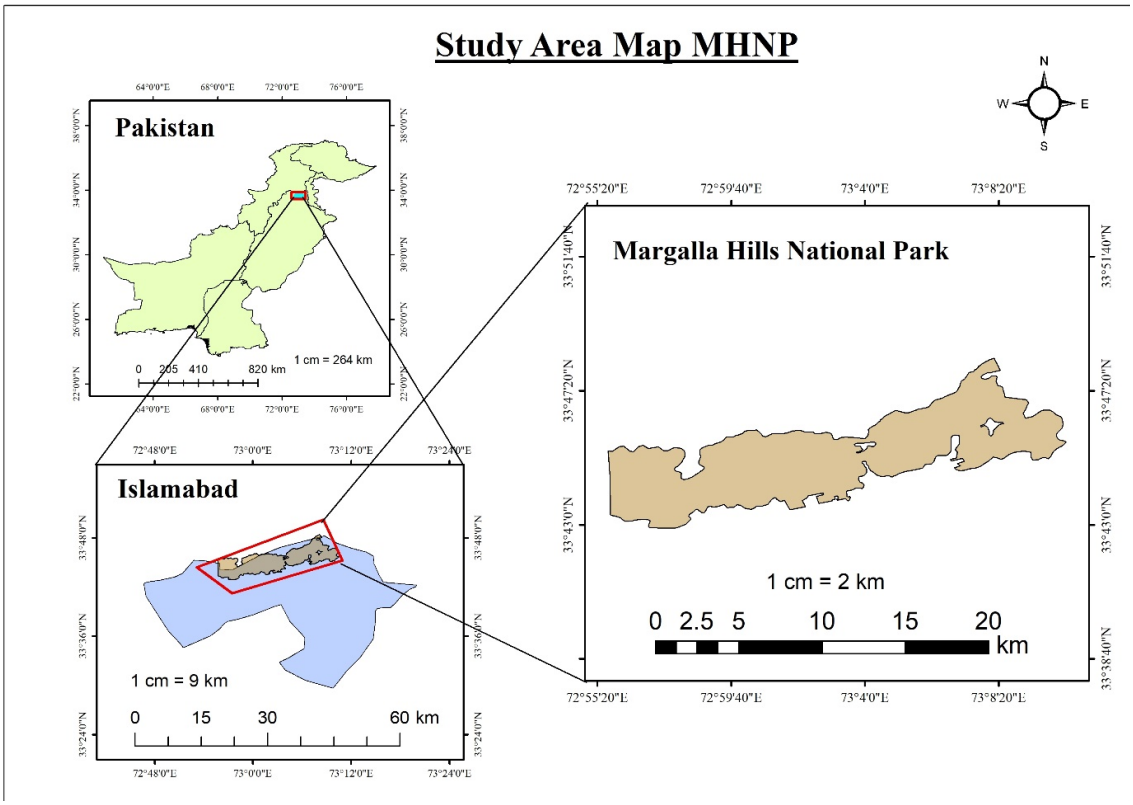


Fig 2.1. Study area map

Geographically, MHNP extends approximately between 72°45′ E to 72°52′ E longitude and 33°41′N and 33°49′N latitude. The total area of the park has been reported between approximately 15,883 and 17,386 ha depending on the adopted boundary delineation and management framework (Aslam & Yasmeen, 2021). The park contains diverse topographic features, including steep slopes, narrow valleys, rocky escarpments, and exposed limestone formations.

The park ranges in elevation from approximately 450 m above sea level in its western section to 1604 m at Tilla Charouni, the highest point of the Margalla Hills. (Government of Pakistan, 2020). These variations in elevation strongly influence local climatic conditions, vegetation distribution, fuel moisture availability, and wildfire behaviour. Complex mountainous terrain can accelerate wildfire spread because slope inclination increases flame contact with adjacent vegetation and promotes faster uphill fire propagation.

2.1.1 Climate

Margalla Hills National Park is situated in the subtropical semi-arid to sub-humid climatic zone which is under the influence of South Asian monsoon system. Marked seasonal climatic variation occurs in the area, with dry and hot conditions before the monsoon, rainfall during the summer monsoon, and relatively cool winters (Sarfaraz et al., 2014). During the 30-year study period (1996–2025), the average annual precipitation was approximately 1,200 mm, with most rainfall occurring through the monsoon months (July to September). In contrast, pre-monsoon period (May–June) is generally characterized by prolonged dry conditions, elevated temperatures, and reduced atmospheric humidity, producing favourable environmental conditions for wildfire ignition and vegetation drying (Ministry of Climate Change and Environmental Coordination, 2025). The vegetation of MHNP is dominated by subtropical dry evergreen forests with the presence of moist broad-leaved species (Rais et al., 2021).

Maximum air temperatures frequently reach approximately 38–40°C during the pre-monsoon season, whereas minimum winter temperatures may decline below 3°C. Such seasonal variability influences fuel moisture conditions and fire weather behaviour (Government of Pakistan, 2022). Wildfire occurrence is rarely controlled by a single climatic factor; instead, it results from interactions among temperature, precipitation deficit, humidity, wind conditions, and available vegetation fuel. The combination of

steep terrain, seasonal climatic extremes, and combustible vegetation creates favorable conditions for wildfire ignition and propagation. Consequently, MHNP provides an appropriate study area for investigating relationships between long-term climatic variability, climate extremes, and wildfire dynamics.

2.2 Methodological work flow

Considering the aims, objectives, and scope of the study, the following methodology was employed to carry out the research.

2.3 Data collection

To assess the association between climatic variability and wildfire activity in Margalla Hills National Park, secondary data was used. A 30-year period from 1996 to 2025 was analyzed. The data that were collected were organized into two categories: meteorological data and wildfire inventory data.

2.3.1 Meteorological data

Daily meteorological observations were obtained from the Pakistan Meteorological Department (PMD). Five climatic variables were obtained from the Islamabad meteorological station:

- Daily temperature maximum (°C)
- Daily temperature minimum (°C)
- Precipitation in mm
- Relative air humidity in %
- Wind velocity (m/s)

The PMD dataset constituted approximately 90% of the complete climatic record and served as the primary source of meteorological observations throughout the study period.

Missing observations within the PMD dataset were supplemented using NASA Earth observation data corresponding to the geographic coordinates of the Islamabad meteorological station. To support data verification and homogeneity assessment,

meteorological records from four neighbouring stations—Rawalpindi, Wah Cantt, Taxila, and Kahuta were also obtained from NASA archives and combined to produce a regional composite reference series.

2.3.2 Wildfire data

Historical wildfire information for MHNP was compiled for the same 30-year period (1996–2025). Two wildfire variables were considered throughout the study:

- Number of wildfire events
- Total area affected (ha)

Because no single continuous wildfire database exists for MHNP, the wildfire inventory was developed by integrating multiple data sources. Official wildfire records and damage information were requested from the Capital Development Authority (CDA) together with the Islamabad Wildlife Management Board (IWMB). These records were then cross-checked with published scientific literature and documented historic wildfire reports to create a consistent wildfire inventory for the study area for the entire study period.

2.4 Software used

Data processing and statistical analysis were performed throughout this study in three software platforms. Both meteorological and wildfire data were initially organized, formatted, temporally aggregated and preprocessed using Microsoft Excel. The quality-controlled daily meteorological observations were applied in the calculation of ETCCDI indices using the ClimPACT package. All statistical analyses, graphical visualization, and trend assessment were performed using RStudio version 2026.08.1, including goodness-of-fit analysis, homogeneity testing, autocorrelation analysis, descriptive statistics, trend analysis, and correlation analysis.

2.5 Data preprocessing

Prior to statistical analysis, all datasets were standardized to ensure consistency and reliability. Meteorological observations obtained from the Pakistan Meteorological Department (PMD), supplementary NASA datasets, and wildfire records collected from different administrative sources were converted into a uniform tabular format in

Microsoft Excel. The datasets were arranged chronologically to establish a continuous observation period from 1996 to 2025.

The meteorological variables were matched with the wildfire variables, namely number of fire events and total area affected. For consistency, all variables were expressed in standard units: precipitation in mm, temperature in °C, relative humidity in %, wind speed in m/s, and burned area in ha. The daily observations were summarized for the monthly, seasonal and annual data for further statistical analysis. The following seasonal scheme was adopted for data aggregation:

- Winter period: December–March
- Spring (pre-monsoon) period: April to June
- Summer (monsoon) period: July to September
- Autumn (post-monsoon) period: October to November

For cumulative variables, including precipitation, wildfire events, and burned area, values were summed within each temporal period. Continuous meteorological variables, including maximum temperature, relative humidity, temperature minimum, and speed of wind, were summarized using arithmetic means.

Data quality assessment was subsequently performed to identify missing observations, duplicate records, and obvious data-entry inconsistencies. Missing values in the PMD dataset were replaced using corresponding NASA observations, while remaining inconsistencies were corrected prior to analysis. Outlier screening was conducted using the Interquartile Range (IQR) method to identify potential recording errors while preserving genuine extreme climatic events (Mahmood & Jia, 2016). The aim of the study was to assess climate extremes and only erroneous values were removed while retaining those extreme observations that were statistically valid.

2.6 Normality analysis

The distributional characteristics of the meteorological variables and wildfire records were evaluated prior to selecting the statistical methods for subsequent analyses. Since many environmental variables had skewed distributions and extreme observations, normality tests were applied to ascertain whether data met the assumptions of parametric statistical procedures (Lee et al., 2016; Uhm & Yi, 2023).

Daily observations were aggregated into monthly and annual datasets before analysis. Monthly aggregation represented seasonal variability, whereas annual

aggregation represented long-term inter-annual variability. To begin with, data distributions were visually analyzed by means of histograms and Quantile–Quantile (Q–Q) plots. The shape of the distribution was assessed with histograms using 40 frequency bins, and quantiles were compared with theoretical normal quantiles using Q–Q plots. Aryadoust and Jia (2026) recommend combining graphical methods, such as histograms and Q–Q plots, with formal statistical tests to provide a more comprehensive assessment of data normality.

Four statistical normality tests were used in conjunction with the visual assessment. The null hypotheses for each test were that the data were normally distributed. Deviations from normality were assessed using the Anderson–Darling test, focusing on the distribution tails (Berlinger et al., 2021).

The statistic of test was obtained as

$$A^2 = -n - \frac{1}{n}\sum_{i=1}^{n}(2i-1)\left[\ln F(Y_i) + \ln\left(1 - F\left(Y_{n+1-i}\right)\right)\right] \tag{2.1}$$

In this notation, n denotes the sample size, Y_i represents the ordered observations, and $F(Y_i)$ denotes the function of cumulative distribution.

The Lilliefors version of the Kolmogorov–Smirnov test was applied because the mean and variance of the population were unknown and had to be estimated from the sample (Tomšik, 2019). The corresponding test statistic is given here

$$D = max\left|F^{¿}(x) - S_n(x)\right| \tag{2.2}$$

Here, $F^{¿}(x)$ is the function of theoretical cumulative distribution, while $S_n(x)$ represents the function of empirical cumulative distribution.

The Jarque–Bera procedure assessed departures from normality through the sample skewness and kurtosis. The test statistic was determined to be:

$$JB = \frac{n}{6}\left(S^2 + \frac{(K-3)^2}{4}\right) \tag{2.3}$$

In this notation, S represents sample skewness and K represents sample kurtosis (Bera, 1981; Tomšik, 2019)

The Cramér–von Mises statistic was applied to assess how closely the empirical distribution agreed with the theoretical cumulative distribution.

$$W^2 = \frac{1}{12n} + \sum_{i=1}^{n} \left[F\left(Y_i\right) - \frac{2i-1}{2n} \right]^2 \quad (2.4)$$

here n is the size of sample, Yi is the ith ordered data, and F(Yi) is the function of theoretical cumulative distribution computed at the ordered data Yi (Lee et al., 2016).

A significance threshold of 5% was adopted for all normality tests. Values below 0.05 led to rejection of the null hypothesis, whereas values of 0.05 or greater did not provide sufficient evidence to reject it.

2.7 Data quality assessment

Before conducting advanced statistical modeling, a rigorous data quality assessment was performed to evaluate the completeness and underlying statistical properties of the collected data.

2.7.1 Goodness-of-fit distribution analysis

Prior to statistical analysis, the probability distribution of each climatic and wildfire variable was evaluated to determine the most appropriate statistical model. Environmental datasets commonly deviate from normality because they contain skewed distributions, zero values, and occasional extreme events. Consequently, identifying the underlying probability distribution was necessary before applying subsequent statistical procedures (Gul et al., 2021).

Missing observations were removed before distribution fitting. Variables that require strictly positive values, such as Gamma and Weibull distributions, were prepared by applying a constant shift to datasets containing negative values (e.g., minimum temperature), ensuring that all observations satisfied the mathematical assumptions of the respective distributions (Yonus et al., 2023). Wildfire variables were also included in the distribution-fitting procedure.

The R package fitdistrplus was applied to evaluate four possible probability distributions (Delignette-Muller & Dutang, 2015):

i. **Normal probability distribution**
ii. **Gamma probability distribution**
iii. **Weibull probability distribution**
iv. **Lognormal probability distribution**

The probability density functions employed in the distribution fitting are given by the following.

Normal distribution

$$f(x)=\frac{1}{\sigma\sqrt{2\pi}}\exp\left[\frac{-(x-\mu)^2}{2\sigma^2}\right] \tag{2.5}$$

Here, μ is the mean and σ represents standard deviation. The N distribution is symmetric and therefore less appropriate for modelling heavy-tailed data, particularly some rainfall and wind speed data for this study.

Gamma distribution

$$f(x)=\frac{x^{k-1}e^{-x/\theta}}{\Gamma(k)\theta^k} \tag{2.6}$$

In this equation, k gives shape parameter, θ represents the scale parameter, and $\Gamma(k)$ denotes the gamma function.

Weibull distribution

$$f(x)=\frac{k}{\lambda}\left(\frac{x}{\lambda}\right)^{k-1}\exp\left[-\left(\frac{x}{\lambda}\right)^k\right] \tag{2.7}$$

Here, k represents the shape parameter and λ represents the scale parameter.

For the lognormal model, the logarithm of the observations was assumed to exhibit a normal distribution (Haseeb et al., 2025).

The Anderson–Darling (AD) statistic together with the Akaike Information Criterion (AIC) was used to select the most suitable distribution for each variable. The Anderson–Darling statistic assesses the agreement of the theoretical and observed distributions, placing more weight on the tails of the distribution than the AIC does (Berlinger et al., 2021; Akaike, 1974). The distribution with the lowest AIC and the smallest Anderson–Darling statistic was considered the most appropriate representation of the data.

Histograms containing fitted density curves and Q–Q plots were also examined as graphical checks of the selected distributions (Delignette-Muller & Dutang, 2015). These

visual assessments were used to confirm the agreement between the observed and theoretical distributions before proceeding with further statistical analyses.

2.8 Homogeneity assessment

Long-term climatic datasets may contain artificial discontinuities arising from changes in instrumentation, station relocation, observation practices, or environmental modifications surrounding the monitoring station. These non-climatic shifts can distort long-term variability and lead to misleading trend estimates if left uncorrected. Therefore, homogeneity assessment was performed prior to trend analysis to identify abrupt changes within the meteorological time series (Aguilar et al., 2003; Caussinus & Mestre, 2004).

The five meteorological variables were assessed for homogeneity over 1996–2025. Pettitt's test and the Mann–Whitney U test were applied to the monthly, seasonal, and annual series (Kartal et al., 2024). These methods were selected because they do not require normally distributed data and are robust for climatic datasets containing outliers and skewed distributions.

The seasonal classification used throughout this study was maintained for seasonal analysis. The seasonal groups were (December to March) as Winters, (April to June) as Spring, (July to September) as Summers, and (October to November) as Autumn. (Ministry of Climate Change and Environmental Coordination, 2025; Khan & Gadiwala, 2013)). During temporal aggregation, cumulative variables (precipitation) were summed, whereas continuous variables (temperature, humidity, and wind speed) were represented by arithmetic means.

2.8.1 Pettitt's test

To determine one abrupt point of change in each climatic series of time, Pettitt's test was used. The test evaluates every possible partition of the dataset and identifies the point where observations before and after the partition differ most significantly.

The Pettitt statistic is expressed as

$$U_t = \sum_{i=1}^{t} \sum_{j=t+1}^{N} sgn\left(x_i - x_j\right) \tag{2.8}$$

where:

The x_i and x_j are observations, t is the candidate change point, N denotes the total number of observations and sgn is a sign function (Kocsis et al., 2020). The time when the absolute value of *Ut* was the maximum was taken as the most likely time to be a breakpoint. A result was interpreted as significant for $p < 0.05$.

2.8.2 Mann–Whitney U test

To confirm the breakpoints detected by Pettitt's test, another test the Mann–Whitney U was performed iteratively across each time series. At each candidate breakpoint, the dataset was partitioned into two chronological segments corresponding to the periods before and after the breakpoint. The Mann–Whitney U statistic was calculated as

$$U = R_1 - \frac{n_1(n_1+1)}{2} \tag{2.9}$$

R_1 denotes the rank sum of the first group, while n_1 indicates the total observations within that group. A p-value was calculated for each partition and the partition with the smallest statistically significant p-value was the most likely breakpoint (Emerson, 2023; Yaseen et al., 2020).

2.8.3 Breakpoint verification

To minimize false detection of artificial change points, breakpoint confirmation required agreement between both homogeneity tests. A breakpoint was considered valid only when:

i. Both Pettitt's and Mann–Whitney U procedures produced significant results ($p < 0.05$)
ii. both tests identified the same breakpoint.

Only confirmed breakpoints were considered potential inhomogeneity requiring further evaluation.

2.8.4 Homogeneity assessment of difference series

To distinguish climatic shifts from station-related discontinuities, the homogeneity analysis was repeated using 'difference series'. Difference series were

constructed by subtracting the composite average of four neighbouring stations (Rawalpindi, Wah Cantt, Taxila, and Kahuta) from the corresponding Islamabad station observations. The use of reference or difference series derived from neighbouring stations is a standard approach in climatological homogenization because it helps distinguish artificial station-related shifts from genuine regional climatic variability (Aguilar et al., 2003; Menne & Williams, 2009; Domonkos, 2024). The same Pettitt and Mann Whitney procedures described above were applied to these difference series. Only breakpoints detected simultaneously in both the original observations and the difference series were considered evidence of true station inhomogeneity. Among all climatic variables, only wind speed exhibited a common statistically significant breakpoint in both datasets, occurring in Winter 2010. Consequently, homogenization was performed only for the wind speed series.

2.8.5 Wind speed homogenization

The identified wind speed discontinuity was corrected using Empirical Quantile Matching (EQM). EQM is a non-parametric homogenization technique that adjusts the complete empirical distribution of observations rather than correcting only the mean, thereby preserving the statistical characteristics of the dataset (Chen et al., 2021).

The daily wind speed series was divided into pre-break and post-break periods using the confirmed breakpoint of Winter 2010. The empirical cumulative distribution function (ECDF) was first obtained for the observations preceding the identified break. Each pre-break observation was then assigned its corresponding percentile within this distribution and mapped to the equivalent percentile of the post-break distribution (Della-Marta & Wanner, 2006).

The change is represented by:

$$x^{¿} = Q_{post}\left(F_{pre}(x)\right) \tag{2.10}$$

where;

Empirical cumulative distribution function of the pre-break period is F_{pre}, Q_{post} denotes the quantile function of the post-break period, x denotes the original observation, $x^{¿}$ refers to the homogenized value.

The adjusted observations that were recorded as 0 were changed to the smallest non-zero wind speed recorded during the post-break period to ensure physical consistency due to wind speed not being able to be negative.

The full daily data set was first adjusted using the EQM adjustment. Daily observations were then homogenized and monthly averages were calculated. The same procedure was then repeated for the monthly series to ensure consistency across temporal scales.

The homogenized wind speed dataset was used in all subsequent statistical analyses, while the remaining climatic variables were retained in their original form because no statistically verified in-homogeneities were detected.

2.9 Lag-1 Spearman rank autocorrelation analysis

To determine whether successive observations exhibited serial dependence, a Lag-1 Spearman Rank Autocorrelation analysis was performed for the 30-year period (1996–2025). The analysis included precipitation, temperature max, wind speed, temperature min, relative humidity, number of fire events, and affected area. Monthly, seasonal and annual datasets were analysed.

Because the climatic series were non-normal and the wildfire records contained extreme observations, a non-parametric Spearman rank approach was selected instead of conventional parametric autocorrelation measures. Spearman's method evaluates the relationship between consecutive observations using their ranks rather than their original values, making it more robust to non-normal distributions and less sensitive to outliers (de Winter et al., 2024).

For each time series, observations were shifted by one time step, such that each value was correlated with the immediately preceding observation. Serial dependence was evaluated using the Spearman ranked autocorrelation coefficient (lag-1).

The lag-1 Spearman coefficient was calculated as

$$r_s = 1 - \frac{6 \sum d_i^2}{n\left(n^2 - 1\right)} \tag{2.11}$$

The notation is defined as follows:

r_s denotes the Spearman rank autocorrelation coefficient, d_i represents the rank difference between successive paired observations, n represents the count of paired observations. The coefficient ranges −1 to +1. Positive values suggest the presence of

positive serial dependence, Negative values reflect negative dependence, and values approaching zero indicate minimal or no serial correlation. Statistical significance was evaluated using asymptotic p-values, with $p < 0.05$ taken as significant.

2.10 Descriptive statistics

Descriptive statistics were used to characterize climatic and wildfire records over 1996–2025. The variables included all five climatic variables, fire-event count, and affected area, each examined at monthly, seasonal, and annual scales.

For every variable, the range, standard deviation, variation coefficient, mean, skewness, and kurtosis were computed. The minimum and maximum values described the observed range of each variable, while the mean represented the average climatic or wildfire condition during the study period. Standard deviation was used to quantify the dispersion of observations around the mean (Elhassnaoui, 2021).

To facilitate comparison among variables with different units, the coefficient of variation (CV) was calculated as

$$CV = \frac{SD}{\acute{x}} \times 100 \tag{2.12}$$

Where SD = standard deviation, $\acute{x}$ is the arithmetic mean.

Skewness was calculated to evaluate the symmetry of the data distribution, whereas kurtosis was used to assess the occurrence of extreme observations relative to a normal distribution (Ouyang et al., 2024). These descriptive statistics provided an overview of climatic variability and wildfire behaviour before trend analysis.

2.11 Temperature and precipitation indices

To understand the long-term changes in the local climate, specific indices were calculated from the temperature and rainfall data.

2.11.1 ETCCDI climate extreme indices

The 27 core ETCCDI indices were calculated for 1996–2025 to assess long-term behavior in the extremes of precipitation and temperature. These standardized measures provide a common basis for examining extreme-event variability and climate change across locations (Dunn et al., 2024).

The ETCCDI indices were produced with ClimPACT and Rstudio software, with the quality-controlled daily meteorological observations checked for missing values, outliers, and inconsistent observations before being used in the statistical analyses described in the following sections. The percentile thresholds (10^{th}, 90^{th}, 95^{th}, and 99^{th}) were calculated using the 1996-2025 study period as the reference (base) period, as is standard practice for ETCCDI indices in ClimPACT2 (Alexander & Herold, 2016).

Following quality control, all 27 core ETCCDI indices were calculated according to the standard ETCCDI definitions. Table 2.1 lists the indices together with their units and definitions. The set comprised 16 temperature indices and 11 precipitation indices, providing broad coverage of climate extremes in MHNP.

Table 2.1 ETCCDI climate extreme indices.

Index	Name	Description	Units
TXx	Hottest day	Monthly and annual highest value of daily maximum temperature	°C
TNx	Warmest night	Monthly and annual highest value of daily minimum temperature	°C
TXn	Coldest day	Monthly and annual lowest value of daily maximum temperature	°C
TNn	Coldest night	Monthly and annual lowest value of daily minimum temperature	°C
TX10p	Cool days	Percentage of days when daily maximum temperature is below the 10th percentile	%
TN10p	Cool nights	Percentage of days when daily minimum temperature is below the 10th percentile	%
TX90p	Warm days	Percentage of days when daily maximum temperature is above the 90th percentile	%
TN90p	Warm nights	Percentage of days when daily minimum temperature is above the 90th percentile	%
FD	Frost days	Annual count of days when daily minimum temperature < 0°C	days
SU	Summer days	Annual count of days when daily maximum temperature > 25°C	days
ID	Ice days	Annual count of days when daily maximum temperature < 0°C	days
TR	Tropical nights	Annual count of days when daily minimum	days

Index	Name	Description	Units
		temperature > 20°C	
WSDI	Warm spell duration index	Annual count of days within periods of at least six consecutive days when daily maximum temperature exceeds the 90th percentile	days
CSDI	Cold spell duration index	Annual count of days within periods of at least six consecutive days when daily minimum temperature is below the 10th percentile	days
GSL	Growing season length	Annual count between the first period of at least six consecutive days with mean temperature > 5°C and the first period after 1 July with at least six consecutive days with mean temperature < 5°C	days
DTR	Diurnal temperature range	Annual mean difference between daily maximum and minimum temperatures	°C
PRCPTOT	Annual total wet-day precipitation	Annual total precipitation from wet days (≥ 1 mm)	mm
SDII	Simple daily intensity index	Ratio of annual total precipitation to the number of wet days (≥ 1 mm)	mm day^{-1}
Rx1day	Maximum 1-day precipitation	Monthly and annual maximum 1-day precipitation amount	mm
Rx5day	Maximum 5-day precipitation	Monthly and annual maximum consecutive 5-day precipitation amount	mm
R10mm	Heavy precipitation days	Annual count of days with precipitation ≥ 10 mm	days
R20mm	Very heavy precipitation days	Annual count of days with precipitation ≥ 20 mm	days
R25mm	Extremely heavy precipitation days	Annual count of days with precipitation ≥ 25 mm	days

Index	Name	Description	Units
CDD	Consecutive dry days	Maximum number of consecutive days with precipitation < 1 mm	days
CWD	Consecutive wet days	Maximum number of consecutive days with precipitation ≥ 1 mm	days
R95p	Very wet days	Annual total precipitation from days exceeding the 95th percentile	mm
R99p	Extremely wet days	Annual total precipitation from days exceeding the 99th percentile	mm

The temperature group comprised TXx, ID, TXn, TNn, TNx, TX10p, TX90p, TN90p, FD, TN10p, SU, GSL, TR, WSDI, CSDI, and DTR; the precipitation group comprised PRCPTOT, Rx1day, R10mm, R20mm, SDII, R25mm, CDD, CWD, Rx5day, R95p, and R99p.

Standard ETCCDI methodology was followed to calculate percentile thresholds (TX10p, TN90p, TX90p, and TN10p) with a 15-day moving window that includes the day of interest and the seven days before and after. A wet day was considered as one with precipitation of ≥1.0 mm for the precipitation indices. Percentile thresholds for R95p and R99p were computed only using wet-day data (Cooley & Chang, 2021). The indices were then aggregated to monthly, seasonal and annual data sets after their calculation, following the same seasonal classification used in this study. Because the Growing Season Length (GSL) index is based on changes in temperature over the entire year, it was calculated only on an annual basis following the ETCCDI definition. The calculated ETCCDI indices were subsequently used for the climate extreme analyses presented in the Results chapter. Subsequent statistical analyses involving these indices followed the methodology described within the corresponding parts of this chapter.

2.12 Humidity related index: heat index

Daily Heat Index (HI) values were calculated from air temperature and relative humidity for 1996–2025 to represent their combined contribution to human thermal stress.The Heat Index is the apparent or "feels like" temperature that the human body would feel if it were exposed to the combined effects of the highest temperature and moisture of the air (Xu et al., 2025).

Mean daily relative humidity was the average of morning and evening relative humidity measurements, and daily Heat Index was computed. The Heat Index equation was only used if the daily temperature maximum was ≥27°C and the relative humidity was ≥40%. Because hourly humidity observations were unavailable, mean daily relative humidity was used for the calculation. Previous studies have reported that using daily maximum temperature together with mean daily relative humidity may slightly overestimate heat stress compared with hourly observations (Diaconescu, 2023; Awasthi et al., 2026). Daily maximum temperature was first converted from degrees Celsius to degrees Fahrenheit. The Heat Index (HI) in Fahrenheit was then determined by the Rothfusz regression equation (Lu & Romps, 2022):

The variables in the equation are defined below:

$$HI_F = -42.379 + 2.04901523\,T + 10.14333127\,RH - 0.22475541\,TRH - 0.00683783\,T^2 - 0.05481717\,R$$

(2.13)

HI_F refers to the Heat Index expressed in Fahrenheit, T indicates the air temperature in Fahrenheit, RH represents relative humidity (%).

When relative humidity was below 13% and air temperature ranged from 80°F to 112°F, the corresponding low-humidity adjustment was applied (Rothfusz, 1990):

$$Adjustment_1 = \frac{(13 - RH)}{4}\sqrt{\frac{17 - |T - 95|}{17}} \tag{2.14}$$

A separate adjustment was applied for relative humidity above 85% when temperature fell between 80°F and 87°F:

$$Adjustment_2 = \frac{(RH - 85)}{10} \times \frac{(87 - T)}{5} \tag{2.15}$$

If the low-humidity condition is met:

HI= HI_F –¿ $Adjustment_1$

If the high-humidity condition is met:

H= $HI_F + Adjustment_1$

The final Heat Index values were converted back to degrees Celsius for subsequent analyses. Daily Heat Index values were classified according to the National Disaster Management Authority heat risk categories (NDMA, 2025).

Table 2.2 Heat Index risk categories.

Heat Index (°C)	Category
<27	Safe
27–32	Caution
33–40	Extreme Caution
41–51	Danger
52–92	Extreme Danger
≥93	Beyond Threshold

The number of days within each category was subsequently aggregated to monthly, seasonal, and annual temporal scales.

2.13 Wind speed

To evaluate the role of wind in the local climate, daily wind data was reviewed and grouped into different categories.

2.13.1 Calm days and windy days

To evaluate temporal changes in wind conditions, daily wind speed observations for 1996–2025 were classified into Calm Days and Windy Days using quality-controlled daily wind speed records. The European Climate Assessment & Dataset (2025) calm climate index (CCI) criterion was adopted, with calm days defined as those having mean wind speed of ≤ 2. m/s.The wind speed threshold used for Windy Days was set as > 5.5 m s^{-1} (20 km h^{-1}) as it is the lower limit of moderate to strong westerly winds reported during the wildfire season in Pakistan, which varies according to local climatic conditions (National Disaster Management Authority, 2025).

Three wind categories were defined:

Calm Days: wind speed < 2 m/s

Moderate Days: 2 - 5.5 m/s

Windy Days: wind speed > 5.5 m/s

For each month, season, and year, the number of days belonging to each category was counted. To facilitate comparison among different time periods, the percentage frequency of each category was calculated as

$$Category\ Percentage = \frac{Number\ of\ Days \in Category}{Total\ Valid\ Days} \times 100$$

where the denominator denotes the total count of valid daily observations within the corresponding period.

Yearly, seasonal and monthly percentages of Calm Days and Windy Days were subsequently used in the statistical analyses presented in later sections.

2.14 Trend analysis

Temporal trends were evaluated with the Modified Mann–Kendall (MMK) test, Spearman's rank correlation and Innovative Trend Analysis (ITA. These analyses were conducted separately for monthly, seasonal, and annual records.

The analysis covered the five climatic variables, wildfire-event count and affected area, and the climate indices developed for this study. Trends in the ETCCDI temperature and precipitation indices were assessed using MMK with Sen's slope, Spearman's rho, and ITA. Because Heat Index, Calm Days, and Windy Days were study-specific measures, and best represented by stacked area graph, box plots and heat map, so annual Heat Index trends were tested with MMK and Sen's slope, whereas Calm Days and Windy Days were evaluated using linear regression.

2.14.1 Modified Mann–Kendall test

The Modified Mann–Kendall (MMK) procedure was applied to determine long-term trends in the climatic series and wildfire measures. The non-parametric method was chosen because it is capable of handling serial autocorrelation that is often found in hydro-climatic time series, and it is also robust against non-normal distributions and extreme observations (Hamed & Rao, 1998; Wang et al., 2020).

Trend analysis covered temperature minimum, relative humidity, temperature maximum, precipitation, wind speed, climatic indices, fire-event count, and affected area

over 1996–2025. Monthly, seasonal, and annual datasets were analysed using the seasonal classification adopted throughout this study.

MMK test statistic:

The Modified Mann–Kendall statistic is the same one employed in the Mann–Kendall test.

$$S=\sum_{i=1}^{n-1}\sum_{j=i+1}^{n} sgn\left(x_j-x_i\right), \tag{2.15}$$

Where

$$sgn\left(x_j-x_i\right)=\begin{cases}1, & x_j>x_i\\ 0, & x_j=x_i\\ -1, & x_j<x_i\end{cases}$$

The variance is then adjusted for serial correlation as

$$V^{'}(S)=V(S)\times\frac{n}{n_s^{'}}, \tag{2.16}$$

where $V^{'}(S)$ is the corrected variance, $V(S)$ is the original Mann–Kendall variance, and $n_s^{'}$ is the effective sample size, which accounts for autocorrelation. A p-value below 0.05 was used to determine whether a significant trend exists.

Sen's slope was estimated using the following expression:

$$\beta=Median\left(\frac{x_j-x_i}{j-i}\right), j>i \tag{2.17}$$

Here, x_i and x_j are observations at times i and j. Sen's slope is the median of the slopes obtained from all possible observation pairs. Positive values indicate increasing change, whereas negative values indicate decreasing change (Sen, 1968; Collaud Coen et al., 2020).

For graphical presentation, a simple linear regression line was additionally fitted using:

$$y=mx+c, \tag{2.18}$$

In this notation, y is the climatic or wildfire response, m is the regression slope, x represents time, and c is the intercept. R^2 was used to express the proportion of variability explained by the fitted regression. Regression lines were used for visualization purposes

only and were presented together with Sen's slope for variables exhibiting statistically significant trends.

2.14.2 Spearman's rank correlation coefficient

Spearman’s ranked correlation additionally applied to evaluate whether each variable showed a monotonic relationship with time. The analysis included the homogenized climatic variables, all indices and wildfire metrics for the monthly, seasonal, and annual datasets. Spearman's rank correlation coefficient was included as one of the methods for trend comparison because previous work has shown that Spearman’s method has comparable statistical power to the Mann–Kendall method for identifying monotonic changes in long-term hydrological series (Yue et al., 2002a; Rahman et al., 2017).

Correlation coefficient was computed as:

$$r_s = 1 - \frac{6\sum d_i^2}{n\left(n^2-1\right)} \tag{2.19}$$

The symbols are defined as: r_s denotes correlation coefficient, d_i represents the difference in ranks for paired observation and n denotes the total observations.

The coefficient can take values ranging from −1 to +1, with positive coefficients indicating an upward monotonic pattern and negative coefficients suggest a decreasing one. Statistical significance was assessed at the 95% ($p \leq 0.05$) and 99% ($p \leq 0.01$) confidence levels (Ahmad et al., 2015).

2.14.3 Innovative trend analysis (ITA)

ITA was used to uncover trends that are not apparent in traditional statistical analyses. ITA is not based on the assumption of normality, serial independence, or large sample size as is the case with the traditional trend tests. The 30-year record was split into two equal 15-year segments: 1996–2010 and 2011–2025. Each half was sorted independently in ascending order and plotted against one another using Cartesian coordinates. A 1:1 reference line represented the absence of trend. Points located above the line indicated increasing trends, whereas points below the line indicated decreasing trends (Alifujiang et al., 2020; Şen, 2017).

The ITA slope was calculated as

$$S=\frac{2\left(M_2-M_1\right)}{n} \tag{2.20}$$

Where M_1 represents the mean of the first half, M_2 denotes the average of the second half and n represents the total observations. To evaluate changes across different magnitudes, observations were classified into low, medium, and high groups using the 10th and 90th percentile thresholds (Wang et al., 2020). The statistical significance of ITA trends for both climatic and wildfire variables was evaluated using Şen's confidence limits as 95% and 99% calculated as

$$CL=\pm Z\left(\frac{2\sqrt{2}}{n\sqrt{n}}\sigma\sqrt{1-\rho}\right) \tag{2.21}$$

The notation is as follows: n denotes the number of observations, Z represents the standard normal distribution's critical value, σ denotes the standard deviation and ρ represents the correlation coefficient between the two ordered halves. The trend was deemed significant if the calculated ITA slope was outside the respective confidence limits (Šrajbek et al., 2025).

2.15 Correlation analysis

To understand how climate affects fires, statistical tests were used to measure the links between weather patterns and wildfire activity.

2.15.1 Climate variables, ETCCDI indices vs wildfire

Correlation analysis was conducted with monthly, seasonal and annual data from 1996 to 2025 to investigate the relationships between climatic conditions, climate extremes and wildfire activity. The analysis included five climatic variables, ETCCDI, fire-event count, and affected area. Spearman's rank correlation was selected because it is distribution-free and performs well when environmental data are skewed or contain extreme observations. The correlation coefficient was calculated using the following expression:

$$r_s=1-\frac{6\sum d_i^2}{n\left(n^2-1\right)} \tag{2.22}$$

Here, ρ denotes Spearman's coefficient, d denotes the rank difference for paired observations, and n is the number of paired observations.

The analysis comprised the following components:

a) Relationships between each climatic variable and the wildfire variables (number of fire events and area affected)

b) Relationships between ETCCDI temperature and precipitation indices and wildfire measures at monthly, seasonal, and annual scales.

Coefficients range between −1 and +1, indicating positive or inverse associations. (Mehmood et al., 2024). Statistical significance was assessed at the 95% ($p < 0.05$) and 99% ($p < 0.01$) levels. The resulting correlation matrices were presented as heat maps to facilitate interpretation of the relationships among climatic variables and wildfire characteristics. The correlation matrices for the ETCCDI indices and wildfire variables were also visualized using heat maps to facilitate interpretation of relationships between climate extremes and wildfire dynamics (Muhammad et al., 2025).

2.15.2 Heat index and wind extremes vs. wildfire

A separate correlation analysis was conducted to examine the association of the calculated Heat Index and wind-speed indices with wildfire variables (Calm Days and Windy Days) and wildfire activity, as temperature, humidity, and wind are key meteorological factors influencing wildfire occurrence and spread (Hamadeh et al., 2017).

Monthly, seasonal, and annual Heat Index, Calm Days, and Windy Days values were correlated with the wildfire measures using Spearman's rank correlation, with the same significance criteria applied above. The resulting correlation coefficients were summarized using heat maps to facilitate comparison with the primary climate wildfire correlation analysis.

CHAPTER 3

RESULTS AND DISCUSSION

3.1 Results of normality tests

The all observed quantiles of climate and fire did not align with the theoretical quantiles of the normal distribution, as illustrated in Figure 3.1 as one of the findings. Likewise, the histograms provide visual evidence that the data are skewed rather than normally distributed.

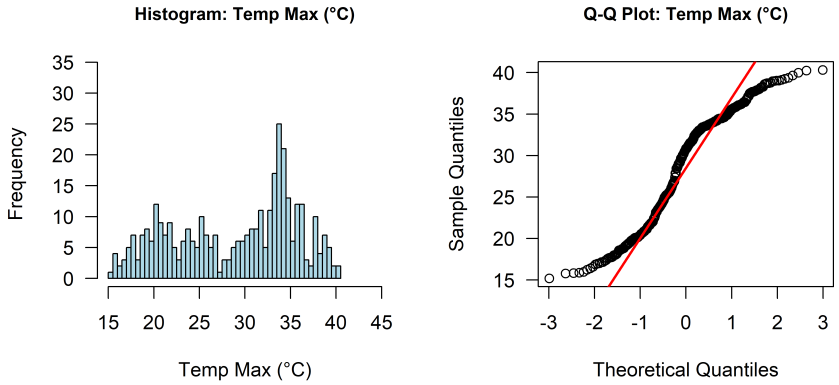


Figure 3.1. Histogram and quantile matching graphs for temperature maximum.

Normality was assessed for all climate and wildfire variables using four statistical tests: Anderson–Darling, Kolmogorov–Smirnov, Jarque–Bera, and W^2. At the significance level of $\alpha = 0.05$, the results from all four tests showed that nearly all variables across both datasets were not normally distributed, with the exception of variables at the annual scale in Table 3.1. At the annual scale, precipitation, maximum temperature maximum, relative humidity and temperature minimum all had p-values above 0.05 in the four normality tests; therefore, normality was not rejected for these variables. For the annual wildfire area affected (ha), the Jarque–Bera test was the only test to produce a non-significant result ($p = 0.0583$), whereas the Anderson–Darling, Kolmogorov–Smirnov, and W^2 tests all remained significant, indicating that the variable still departed from a normal distribution. The complete Q-Q plots, histograms and results of normality are given in appendix A.

Table 3.1 Non-Significant results of Normality tests.

Variable	A^2	*p*	*D*	*p*	*JB*	*p*	W^2	*p*
Precipitation (mm)	0.41	.323	0.135	.178	1.0	.593	0.062	.340
Temperature Max (°C)	0.19	.891	0.071	.963	0.8	.663	0.027	.879
Temperature Min (°C)	0.47	.231	0.098	.649	1.2	.542	0.077	.221
Relative Humidity (%)	0.37	.400	0.136	.165	1.1	.565	0.065	.315
Area Affected (ha)	—	—	—	—	5.7	.058	—	—

Note. A^2 *= Anderson–Darling statistic; D = Kolmogorov–Smirnov (Lilliefors) statistic; JB = Jarque–Bera statistic;* W^2 *= Cramér–von Mises statistic*

Overall, the results show that the climate and wildfire datasets do not meet the normality assumption required for parametric statistical analyses, justifying the use of non-parametric methods in the subsequent analyses. Hydroclimatic variables also have similar characteristics to the variables discussed above, with precipitation, temperature extremes, and other environmental variables frequently having skewed or heavy-tailed distributions, due to natural variability and the potential for extreme events to occur, rather than Gaussian distributions (Nerantzaki & Papalexiou, 2022; Reinders & Muñoz, 2024). The near-normal behaviour observed for a small number of annual variables is likely the result of temporal classification, which minimizes short-term variations and reduces the impact of extreme values. Therefore, the use of non-parametric statistical methods is appropriate for the present study and provides a more reliable basis for the subsequent trend and correlation analyses.

3.2 Goodness-of-fit distribution analysis

This section evaluates the goodness-of-fit metrics for each climate and wildfire variable to identify the most accurate probability distribution model in direct comparison to the standard normal distribution.

Non-normal probability distributions repeatedly provided a closer fit than the normal distribution across the analyzed environmental and wildfire datasets. The Weibull distribution was the optimal model for precipitation, maximum temperature, and humidity. This difference was most pronounced for precipitation, where the Weibull model (AD = 0.49, AIC = 4047) fit the data far better than the normal distribution (AD =

25.24, AIC = 4492). The Weibull distribution also outperformed the normal distribution for maximum temperature (Weibull AD = 7.64, AIC = 2373 vs. Normal AD = 8.65, AIC = 2393) and humidity (Weibull AD = 4.25, AIC = 2605 vs. Normal AD = 8.08, AIC = 2659). Minimum temperature presented the only split result: the normal distribution yielded a lower Anderson-Darling statistic (10.22 vs. Weibull 11.71), while the Weibull distribution produced the lowest Akaike Information Criterion (2492 vs. Normal 2504). For wind speed and the number of wildfire events, the lognormal distribution offered the closest fit. Wind speed data aligned best with the lognormal model (AD = 8.47, AIC = 280), which was a measurable improvement over the normal model (AD = 14.18, AIC = 428). Likewise, the number of wildfire events fit the lognormal distribution (AD = 0.28, AIC = 275) much closer than the normal distribution (AD = 1.56, AIC = 293).

The gamma distribution provided the best fit for the area affected by wildfires (AD = 0.42, AIC = 341), directly outperforming the normal distribution (AD = 1.27, AIC = 362). Establishing that these datasets deviate from normality dictates the statistical procedures required for the subsequent modeling phases. As detailed in the text, Figure 3.2 show two representative examples (one climate variable and one fire variable). The complete set of visual plots for all tested distribution fits can be found in Appendix B.

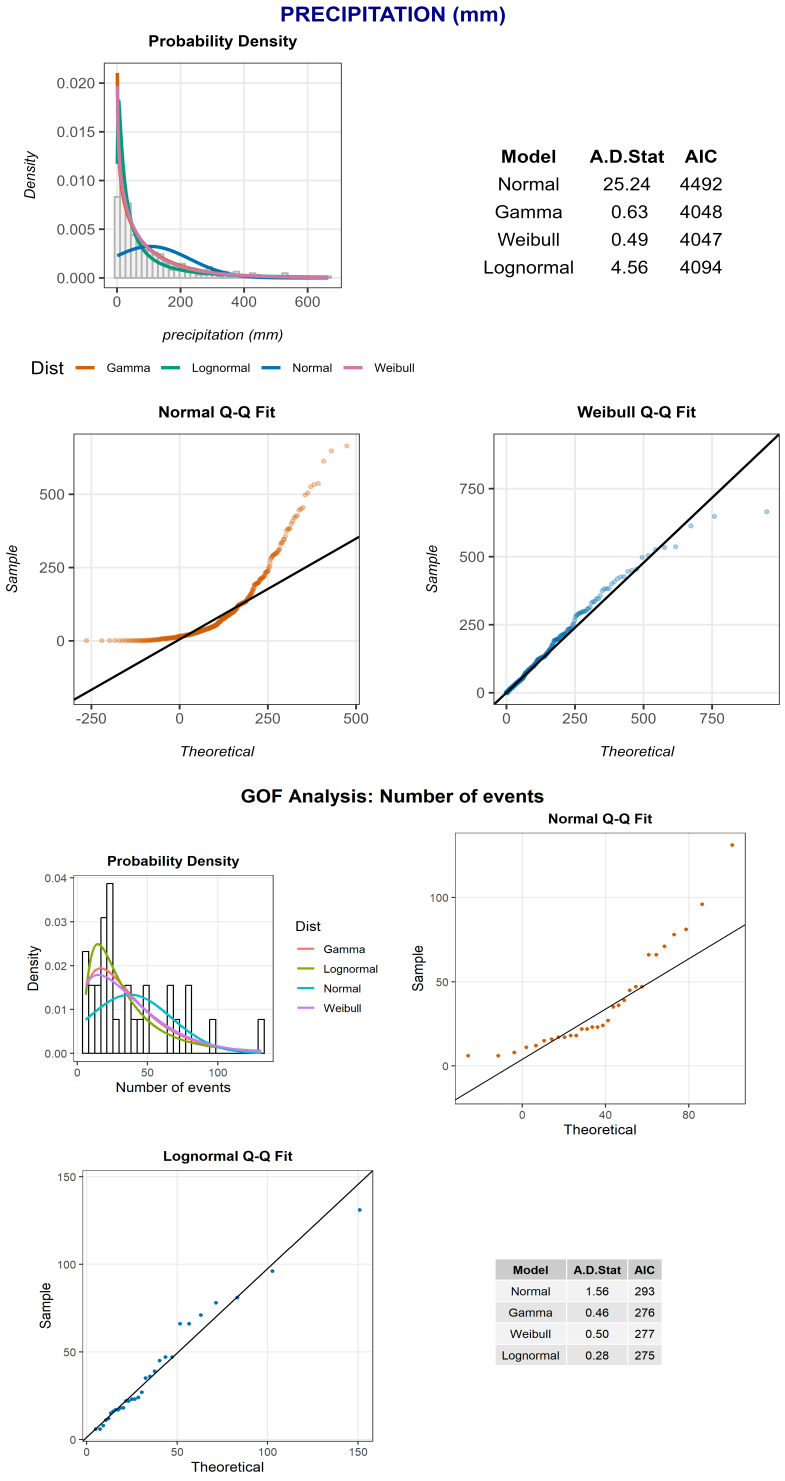


Figure 3.2 Comparative Goodness-of-Fit and Probability Distribution Analysis for Event Frequency and Precipitation Data.

The goodness-of-fit analysis shows that the distribution of most climatic and wildfire variables are not normally distributed, which is indicative of the effects of skewness, extreme values, and physical constraints in environmental datasets. This

supports the use of non-parametric statistical approaches in subsequent trend and correlation analyses. The improved performance of Weibull, lognormal and gamma distributions corroborates previous studies that indicate that climatic variables like precipitation and wind speed often have asymmetric distributions because of the irregularity of events and extreme values (Alam et al., 2018; Yonus et al., 2023). The suitability of Weibull distribution for precipitation is consistent with the monsoon-dominated rainfall pattern of the region, where rainfall is concentrated in fewer high-intensity events. Likewise, the lognormal characteristics of wind speed and wildfire frequency are related to the presence of occasional extreme events that affect the upper extreme of the distribution**.** The gamma distribution identified for wildfire-affected area is consistent with burned-area datasets, where a small number of severe wildfire events contribute a large proportion of total affected area (Malamud et al., 2005). These distribution characteristics justify the application of rank-based statistical methods in this study, as such approaches are less sensitive to non-normality and extreme observations (Hamed & Rao, 1998).

3.3 Homogeneity outcomes of climate data

This subsection examines the meteorological datasets from 1996 to 2025 for sudden, artificial shifts prior to evaluating long-term climate trends. Statistical testing identified significant structural breaks primarily within the wind speed data, along with isolated shifts in minimum temperature and relative humidity.

As detailed in primary Table 3.2, the wind speed records showed the most prominent discontinuities. Both the Pettitt and Mann-Whitney U tests mutually confirmed highly significant shifts ($p < 0.001$) in monthly wind speed during Winter wind speed in 2010. An additional shift occurred in the autumn wind speed data in 2009 ($p < 0.01$). Beyond wind variables, the tests confirmed a single break in the annual minimum temperature record in 2006 ($p < 0.05$) and another in monthly relative humidity in July 2012 ($p < 0.05$). In contrast, maximum temperature and precipitation did not exhibit any statistically significant breakpoints across any of the tested time scales. Identifying these abrupt shifts determines the specific data corrections needed before calculating the historical climate extreme indices.

Table 3.2 Test statistics for homogeneity of climate parameters.

Variable	Scale	Break_Time	Pettitt (U)	Pettitt P-val	MW (W)	MW P-val
Temp Min	Yearly	2006	135	0.03971 *	172.0	0.00393 **
Relative humidity	Monthly	2012-07	5634	0.03413 *	13202.5	0.00412 **
Wind speed	Monthly	2010-07	12121	0 ***	22248.0	0 ***
Wind speed	Winter	2010	209	0.00017 ***	217.0	2e-05 ***
Wind speed	Autumn	2009	174	0.00297 **	199.0	0.00032 ***

Note: Significance levels are indicated as * p<0.05, ** p<0.01, and *** p<0.001.

3.4 Homogenization

This subsection deals with the verification of detected station breaks by regional difference series and the statistical adjustments to the data. Wind speed was the only meteorological variable that demonstrated a statistically significant breakpoint in both the raw observations and the regional difference series. The Pettitt test (Raw p = 0.00017; Difference p = 0.00092) and the Mann-Whitney U test (Raw p = 0.00002; Difference p = 0.00010) both indicated that the break in wind speed during the winter of 2010 was highly significant in both datasets. The remaining climatic variables did not display common, mutually confirmed breakpoints across both sets of data.

Empirical Quantile Matching successfully adjusted the discontinuous records to create a uniform timeline. The raw wind speed data before 2010 contained higher baseline values, which the matching procedure reduced to align with the probability distribution of the post-2010 period as in Figure 3.3. Additionally, the visual results indicate that quantile matching was applied which raised the historical low values to match the recent station observations.

Table 3.3 Common breakpoints: Raw and Difference series.

Common Breakpoints: Raw vs. Difference Series

Variable	Scale	Break Year	Series	Pettitt P-val	MW P-val
Wind speed	Winter	2010	Raw Data	0.00017***	0.00002***
Wind speed	Winter	2010	Difference	0.00092***	0.00010***

Significance levels: *** p < 0.001

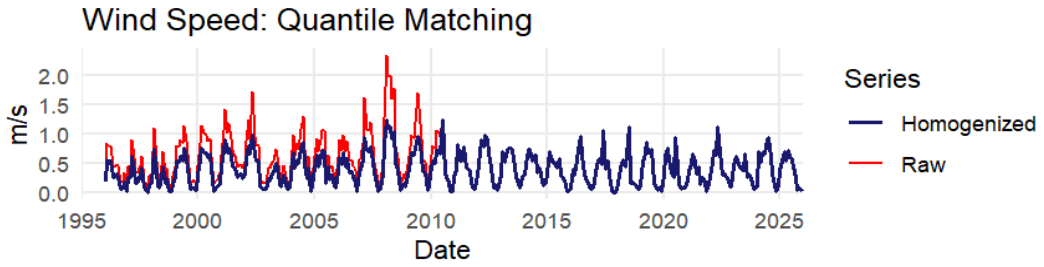


Figure 3.3 Homogenization.

The results indicate that most climatic variables were sufficiently homogeneous for long-term trend analysis, whereas wind speed required adjustment before further analysis. This is consistent with the study objective of ensuring that subsequent trend analyses reflect actual climatic variability rather than artificial changes in the observational record. Domonkos et al., (2024) reported similar results, stating that wind speed records are especially sensitive to the instrumentation and the surrounding of the sensors, and that they are more susceptible to inhomogeneity. The absence of common breakpoints in the remaining variables suggests that the detected shifts were more likely related to natural climatic variability than to station-related effects. It points to the two mechanisms showing up behind wind speed breaks: a physical move of the station, or a change in the recording instrument. Either is a plausible explanation for the Winter 2010 break found here, though without station history metadata for Islamabad, this remains an inference drawn from the general pattern rather than a confirmed local cause. Correcting the wind speed series using empirical quantile matching therefore improved the consistency of the dataset by reducing non-climatic biases while preserving the statistical distribution of the observations, providing a more reliable basis for subsequent trend and climate extreme analyses (Domonkos, 2024).

3.5 Results of autocorrelation (serial dependence)

This section presents the Lag-1 Spearman rank autocorrelation for climate and wildfire records to determine if consecutive observations were temporally related.

Wind speed exhibited persistent positive serial dependence throughout much of the year, whereas temperature, precipitation, and wildfire variables showed no significant autocorrelation outside of a few isolated periods. As detailed in Table 3.4 (a), wind speed recorded statistically significant positive autocorrelation annually (statistic = 0.656, $p < 0.001$) and across three of the four seasons, peaking in Winter (statistic = 0.615, $p < 0.001$). Monthly wind speed data showed continuous significant positive dependence from December through June. In contrast, maximum and minimum temperatures produced completely non-significant results across all time scales. Precipitation demonstrated a single significant negative autocorrelation in July (statistic = -0.378, $p = 0.042$), and humidity showed significant positive dependence only during May and the Pre-Monsoon spring season.

Table 3.4 Spearman's lag-1 Autocorrelation stats.

a) climate parameters b) fire parameters

Time Period	Precipitation			Max Temp			Min Temp			Humidity			Wind Speed		
	Statistic	P-value	AC	Statistic	P-value	AC	Statistic	P-value	AC	Statistic	P-value	AC	Statistic	P-value	AC
Jan	-0.031	0.875	No	-0.068	0.7241	No	0.03	0.879	No	0.064	0.7404	No	0.588	8e-04	Yes
Feb	-0.168	0.3835	No	-0.158	0.4141	No	-0.273	0.152	No	0.093	0.6327	No	0.395	0.0339	Yes
Mar	0.113	0.5584	No	0.06	0.7577	No	-0.154	0.4266	No	0.116	0.5496	No	0.524	0.0035	Yes
Apr	0.09	0.6409	No	0.057	0.7684	No	-0.063	0.7471	No	0.26	0.1736	No	0.408	0.0279	Yes
May	0.276	0.1475	No	0.188	0.3275	No	0.235	0.2197	No	0.454	0.0133	Yes	0.42	0.0233	Yes
Jun	-0.093	0.631	No	-0.141	0.4659	No	0.34	0.0714	No	-0.119	0.539	No	0.435	0.0182	Yes
Jul	-0.379	0.0423	Yes	-0.259	0.175	No	0.076	0.6935	No	-0.135	0.4864	No	-0.034	0.8615	No
Aug	0.215	0.2621	No	0.082	0.6731	No	-0.104	0.5905	No	-0.229	0.2318	No	0.164	0.3951	No
Sep	0.281	0.14	No	0.134	0.4883	No	0.109	0.5752	No	0.17	0.3779	No	0.071	0.7141	No
Oct	-0.232	0.2268	No	0.232	0.2259	No	0.12	0.5361	No	0.33	0.0808	No	0.264	0.1658	No
Nov	-0.18	0.351	No	0.239	0.2109	No	-0.146	0.4501	No	0.152	0.4318	No	0.271	0.1545	No
Dec	-0.153	0.4293	No	0.234	0.2217	No	-0.106	0.5849	No	-0.035	0.8551	No	0.586	8e-04	Yes
Winter	-0.122	0.5278	No	0.119	0.5396	No	0.119	0.5396	No	0.054	0.7821	No	0.615	4e-04	Yes
Pre-Monsoon / Spring	-0.198	0.3041	No	0.213	0.2677	No	0.267	0.1607	No	0.393	0.0351	Yes	0.468	0.0105	Yes
Monsoon / Summer	0.011	0.9535	No	-0.109	0.5723	No	0.184	0.3392	No	-0.101	0.6022	No	0.159	0.4093	No
Post-Monsoon / Autumn	-0.02	0.9172	No	0.312	0.0991	No	0.009	0.9616	No	0.36	0.055	No	0.439	0.0173	Yes
Annual	0.149	0.4412	No	0.311	0.1001	No	0.151	0.4337	No	0.312	0.0996	No	0.656	1e-04	Yes

(a)

Time Period	Number of Events			Area Affected (ha)		
	Statistic	P-value	AC	Statistic	P-value	AC
Jan	0.076	0.6956	No	0.085	0.6605	No
Feb	0.288	0.1297	No	0.296	0.1194	No
Mar	-0.076	0.6939	No	-0.135	0.4836	No
Apr	0.2	0.2984	No	0.213	0.2684	No
May	0.054	0.782	No	0.019	0.9232	No
Jun	-0.139	0.4714	No	-0.193	0.3153	No
Jul	0.229	0.2315	No	0.279	0.1433	No
Aug	0.215	0.2624	No	0.225	0.2403	No
Sep	-0.051	0.791	No	-0.051	0.7912	No
Oct	-0.036	0.8541	No	-0.036	0.8541	No
Nov	0.64	2e-04	Yes	0.665	1e-04	Yes
Dec	0.175	0.3629	No	0.272	0.153	No
Winter	0.091	0.6377	No	0.155	0.4206	No
Pre-Monsoon / Spring	-0.03	0.8786	No	-0.037	0.8471	No
Monsoon / Summer	0.243	0.2033	No	0.296	0.1193	No
Post-Monsoon / Autumn	0.619	3e-04	Yes	0.665	1e-04	Yes
Annual	0.014	0.9413	No	0.106	0.5828	No

(b)

For the wildfire variables, significant positive autocorrelation was strictly confined to the late-year dry season (Table 3.4 (b). Both the number of fire events and the affected area were highly auto correlated during the Post-Monsoon autumn season (events statistic = 0.619, area statistic = 0.665; both $p < 0.001$), a trend driven entirely by significant dependence in November. Every other month, season, and the annual scale for both wildfire variables yielded non-significant results. Mapping these temporal dependencies clarifies which datasets require specific statistical adjustments before the final correlation analysis between extreme climate trends and historical fires.

The clearest signal in this analysis came from wind speed, and the way the data were prepared is the most likely reason for it. The 2010 break was removed by quantile matching, and calm days recorded as 0 m/s were raised to the lowest wind speed in the record. Both steps narrow the spread of the data and leave many repeated values. Spearman's test compares ranks, so repeated values carry the same rank and match one another automatically, which lifts the coefficient. Li et al., (2022) reported that homogenising wind records lowered the standard deviation of the series across China, and Zhang and Wang (2025) found that homogenisation cut regional wind trends by about half. Since the Mann-Kendall test treats values as independent, and linked values make a

false trend more likely (Sheoran et al., 2024), the wind trend needs prewhitening or a corrected test, and this result is better read as a property of the adjusted data than of the wind itself. Temperature showed no link at any time scale, which matches the regional picture. Rashid et al., (2026) found weak and non-significant temperature trends across the Potwar Plateau for 1982–2022, and a series without a clear trend would not be expected to show linked values. It is thus possible to apply the Mann-Kendall test directly to temperature, however, a lack of correlation does not imply independence; the coefficient must be greater than approximately 0.37 for the number of pairs of data (twenty-nine).

Rainfall behaved the same way apart from one month, which is unsurprising given the number of tests run. Fire counts also start fresh each year, except in November. Fuel cannot explain this, since burning in one year would reduce the next year's fuel and give a negative value. A slow-changing human cause or a gradual shift in record keeping fits better, supported by the absence of any climate link in that month and by Tariq et al., (2022), who found that most fires in the Margalla Hills are caused by people.

3.6 Descriptive statistics results

This section outlines the descriptive statistics of the meteorological variables and wildfire records before conducting the trend analysis.

Wildfire occurrences and precipitation showed extreme seasonal variation and highly skewed data distributions, while temperature and humidity remained much more stable throughout the year. As in Table 3.5, precipitation had the highest variability among the weather variables, recording an annual mean of 1246.56 mm with a massive range between 580.80 mm and 1732.40 mm. Summer precipitation made up the bulk of the annual total with a mean of 747.04 mm, whereas autumn was the driest season averaging just 50.06 mm. The precipitation data was heavily rightward skewed during the dry winter months, peaking in December with a skewness of 2.44 and a coefficient of variation of 147.96%. Conversely, temperature profiles were highly consistent. The annual mean maximum temperature was 28.33°C, peaking in summer at a mean of 34.06°C, and maintained a very low coefficient of variation that ranged only from 2.24% to 9.02% across all individual months. Minimum temperature averaged 14.52°C annually and showed slightly higher relative variability, reaching its highest variation in January at 40.06%. Relative humidity averaged 59.15% annually, reaching its highest point in

summer at 75.11% and its lowest in spring at 55.49%, with low overall variance. Wind speed recorded an annual mean of 0.41 m/s but displayed extreme rightward skewness (2.05) and kurtosis (10.75), along with variability exceeding 100% during December and January.

Wildfire activity was overwhelmingly concentrated during the spring season. According to Fire data descriptive stats (Table 3.5), the park averaged 37.43 fire events annually, and spring accounted for 28.93 of those events on average, reaching up to 113 events in a single spring season. The area affected by fires followed the exact same seasonal pattern, averaging 102.19 hectares burned annually, with spring fires destroying an average of 82.25 hectares and reaching a maximum of 339.29 hectares. Both the number of fire events and the area affected showed massive variation over time and non-normal distributions, recording annual coefficients of variation of 81.00% and 94.23%, respectively. These fire data distributions were highly skewed with heavy tails, particularly during the off-peak autumn season where the variation for fire events reached 267.82% and the affected area kurtosis spiked to 9.62. Establishing these baseline distributions and seasonal peaks sets the necessary foundation for the trend analysis. Descriptive statistics of precipitation, relative humidity and fire parameters are given for reference in the table below while remaining parameters results are added in appendix C.

Table 3.5 Descriptive statistics climate and fire parameters (1996-2025).

Precipitation (mm)

Period	Min	Mean	Max	SD	CV (%)	Skew	Kurtosis
Jan	0.00	58.223	174.2	53.773	92.356	0.635	2.126
Feb	4.00	86.470	297.9	74.727	86.420	1.364	4.182
Mar	0.00	88.970	286.1	76.431	85.907	1.331	3.900
Apr	0.00	57.860	196.4	52.477	90.697	0.937	3.115
May	11.00	39.373	131.6	30.711	77.999	1.645	5.080
Jun	14.50	89.707	230.4	58.963	65.729	0.482	2.271
Jul	84.40	314.257	647.0	140.079	44.575	0.591	2.918
Aug	0.00	294.230	664.0	147.991	50.298	0.501	2.900
Sep	3.00	138.540	444.8	95.239	68.744	1.515	5.399
Oct	0.00	40.897	196.7	48.405	118.359	2.153	7.266
Nov	0.00	18.153	92.8	21.338	117.543	1.845	6.448
Dec	0.00	19.817	133.0	29.320	147.956	2.439	9.139
Winter	7.35	245.325	452.0	127.200	51.849	0.215	1.883
Spring	42.09	186.955	360.0	84.324	45.104	0.078	2.452
Summer	266.08	747.044	1175.0	210.161	28.132	-0.547	3.149
Autumn	0.02	59.056	208.5	50.316	85.200	1.547	5.146
Annual	580.80	1246.557	1732.4	278.137	22.312	-0.432	2.697

Relative Humidity (%)

Period	Min	Mean	Max	SD	CV (%)	Skew	Kurtosis
Jan	61.500	71.653	78.950	5.486	7.657	-0.347	1.930
Feb	52.500	67.815	78.970	5.948	8.771	-0.219	3.077
Mar	52.500	65.429	77.240	5.950	9.094	0.116	2.561
Apr	45.000	60.010	73.530	7.491	12.484	-0.276	2.350
May	36.500	51.952	64.450	6.437	12.390	-0.257	2.898
Jun	40.520	54.619	70.000	6.155	11.269	0.205	3.063
Jul	58.000	72.304	81.940	6.245	8.637	-0.847	3.407
Aug	69.500	78.339	83.420	3.041	3.882	-0.721	4.127
Sep	68.980	74.852	79.350	3.060	4.088	-0.361	2.207
Oct	60.500	72.554	79.210	4.154	5.725	-0.931	3.900
Nov	68.500	74.719	81.640	3.796	5.080	0.320	2.053
Dec	66.500	73.366	80.800	4.270	5.820	0.065	1.984
Winter	58.398	69.721	77.217	4.233	6.071	-0.537	3.061
Spring	44.577	55.488	65.319	5.427	9.780	-0.320	2.606
Summer	65.462	75.168	80.179	2.966	3.946	-0.981	5.179
Autumn	64.680	73.619	80.164	3.439	4.672	-0.228	3.099
Annual	62.270	68.159	73.100	2.762	4.052	-0.423	2.555

Number of events

Period	Min	Mean	Max	SD	CV (%)	Skew	Kurtosis
Annual	6	37.433	131	30.321	81.000	1.338	4.317
Winter	0	5.733	40	8.590	149.826	2.347	9.470
Spring	4	28.933	113	25.522	88.210	1.486	5.037
Summer	0	2.000	18	3.833	191.635	2.740	11.237
Autumn	0	0.733	8	1.964	267.824	2.935	10.468
Jan	0	0.767	7	1.695	221.152	2.747	9.816
Feb	0	1.600	9	2.387	149.172	1.476	4.342
Mar	0	1.667	20	3.845	230.681	3.929	18.730
Apr	0	4.267	21	5.232	122.627	1.390	4.587
May	0	12.133	41	11.279	92.961	1.149	3.323
Jun	0	12.533	82	17.031	135.885	2.624	10.496
Jul	0	1.667	17	3.467	208.045	3.153	13.895
Aug	0	0.267	2	0.583	218.735	2.039	5.957
Sep	0	0.067	1	0.254	380.562	0.000	0.000
Oct	0	0.067	2	0.365	547.723	0.000	0.000
Nov	0	0.667	8	1.918	287.678	3.201	11.889
Dec	0	1.733	17	3.600	207.700	2.989	12.261

Area affected (ha)

Period	Min	Mean	Max	SD	CV (%)	Skew	Kurtosis
Annual	2.12	102.185	349.40	96.294	94.234	1.059	3.247
Winter	0.00	13.223	94.44	25.235	190.847	2.409	7.642
Spring	1.72	82.245	339.29	84.221	102.402	1.183	3.926
Summer	0.00	3.750	43.27	8.827	235.421	3.434	15.009
Autumn	0.00	2.964	32.46	7.961	268.560	2.789	9.615
Jan	0.00	1.606	32.37	5.901	367.418	4.957	26.350
Feb	0.00	2.374	11.74	3.444	145.112	1.238	3.237
Mar	0.00	2.125	18.82	4.109	193.388	2.800	10.830
Apr	0.00	14.643	209.93	39.566	270.202	4.267	21.277
May	0.00	31.944	137.67	39.113	122.441	1.420	4.005
Jun	0.00	35.658	176.53	48.010	134.642	1.587	4.479
Jul	0.00	3.341	42.06	8.478	253.765	3.673	16.346
Aug	0.00	0.378	6.07	1.158	306.144	4.202	20.894
Sep	0.00	0.030	0.81	0.148	489.170	5.083	27.195
Oct	0.00	0.025	0.76	0.139	547.723	0.000	0.000
Nov	0.00	2.939	32.46	7.969	271.157	2.789	9.612
Dec	0.00	7.122	80.53	17.250	242.204	3.114	12.583

The climatic variables in this study fall into two groups based on how stable they are over time. Temperature and relative humidity change little from year to year, while precipitation and wind speed are much less stable. This distinction is important for the first objective, as it shows which variables are able to reveal a long-term signal and which are not. Maximum temperature stays fairly uniform across the months, which means that any real trend should be easy to detect through statistical testing, while minimum temperature varies a little more but is still far steadier than rainfall. Precipitation behaves in the opposite way, varying so widely that a gradual trend may be hidden by the noise. This result is consistent with Rashid et al., (2026) who investigated six meteorological

stations in the Potwar Plateau, including Islamabad and Rawalpindi, and found weak trends in temperature but strong variations in precipitation, which they termed as increasing hydroclimatic variability in the region rather than a long-term trend. The seasonal pattern seen here is also typical of the region, as summer contributed about 60% of the annual rainfall, close to the monsoon share of roughly 70.5% that Ahmad et al., (2023) reported for central Punjab. The reason for this contrast is physical: temperature follows the yearly solar cycle and repeats with little change, while rainfall arrives in separate spells that differ in frequency and strength from one year to the next. Winter rainfall in northern Pakistan is produced by western disturbances, weather systems carried within the subtropical westerly jet that bring most of the winter rain and snow to Pakistan and the western Himalaya (Hunt et al., 2025), and these are active only from December to March (Abbas et al., 2023). As a result, a given dry month may receive one or two of these systems or almost none, which produces the strong positive skew seen in the record. Because these variables depart from normality, rank-based trend tests are more suitable than parametric ones. One methodological caution concerns the coefficient of variation, which is only meaningful for variables with a true zero (Abdi, 2010); temperature in degrees Celsius does not meet this condition, so its low coefficient of variation is partly a product of the measurement unit.

Relative humidity provides the link between the climatic and wildfire records. It reaches its lowest point in spring, when temperatures rise and rainfall remains low, and the fire record follows this same window, with about three-quarters of the annual events and four-fifths of the burned area concentrated in spring alone. Wind speed completes the picture, staying low for most of the year and rising only in brief episodes; since Tariq et al., (2021) found wind speed to be strongly associated with fire severity in this park, it is these occasional gusts, rather than the low annual mean, that are likely to matter once a fire is established. Ignition is mainly anthropogenic, and Tariq et al., (2022) linked the probability of fire occurrence to site accessibility and human activity, which indicates that the fire season is set by how dry the fuel is rather than by when people are present. This provides the basis for examining wildfire occurrence against seasonal climatic conditions rather than annual means, as the second objective proposes. The observed spring peak appears to differ from Tariq et al., (2021), who assigned all 299 of their fire records to May, June and July and identified summer as the main fire season; however, the difference reflects how the seasons are defined, since May is treated as spring in the

present study and as summer in theirs. Evidence from within the park supports the earlier onset, as Sahar et al., (2024) reported a fire season running from early April to mid-July, and the same pattern is found in chir pine forests across Pakistan, which experience a long dry period from late spring to early autumn and accumulate needle litter that ignites easily (Muhammad et al., 2025). The fire record is highly uneven, driven by a small number of severe seasons, which is consistent with the unstable increasing trend Shahzad et al., (2024) reported at the national level and with the heavy-tailed distributions typical of fire regimes more generally (Malamud et al., 2005). Burned area varied more than the number of events, which indicates that the two are better treated as separate variables in the correlation analysis, while the sparse autumn observations show only that fire outside spring is rare and occasionally large rather than giving a reliable estimate.

3.7 Trend analysis of wildfire activity

This section examines the long-term patterns of wildfire activity to show how the frequency and size of fires have changed over the study period.

3.7.1 Annual trends

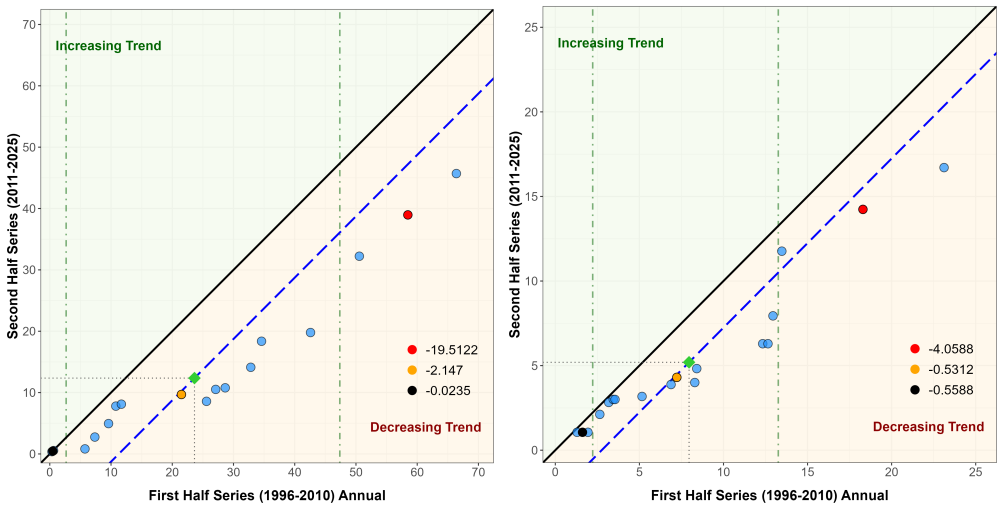
Annual wildfire frequency and total burned area exhibited overall decreasing trends over the 30-year study period.

No statistical significance was found by rank based statistical tests, but a general decrease was seen in both fire metrics. The Modified Mann-Kendall test returned a Tau of -0.162, and a Spearman’s (Rho) -0.242 for the number of annual fire events. The total annual area affected recorded an MK Tau of -0.205 and an SR Rho of -0.317. Despite the lack of statistical significance in these monotonic tests, Sen's slope estimator calculated a median annual reduction of 0.571 fire events and 2.873 hectares of burned area.

Table 3.6 Trend statistics of wildfire.

Time Period	Number of events			Area affected		
	MK Tau	SR Rho	Sen's Slope	MK Tau	SR Rho	Sen's Slope
Jan	0.163	0.187	0	0.097	0.132	0
Feb	0.008	-0.033	0	-0.068	-0.126	0
Mar	0.139	0.173	0	0.099	0.105	0
Apr	0	0.012	0	0.079	0.144	0
May	-0.014	-0.016	0	0.035	0.041	0.071
Jun	-0.084	-0.129	-0.083	-0.062	-0.091	-0.169
Jul	0.368**	0.447**	0	0.335**	0.434**	0
Aug	0.459***	0.543***	0	0.412***	0.522***	0
Sep	0.333**	0.401**	0	0.324**	0.4**	0
Oct	0.187	0.225	0	0.187	0.225	0
Nov	-0.123	-0.153	0	-0.133	-0.181	0
Dec	-0.028	-0.074	0	-0.031	-0.047	0
Winter	0.018	-0.043	0	0.01	-0.013	0
Pre-Monsoon / Spring	-0.082	-0.128	-0.185	-0.094	-0.144	-1.011
Monsoon / Summer	0.448***	0.552***	0.048	0.384***	0.504***	0
Post-Monsoon / Autumn	-0.107	-0.144	0	-0.133	-0.181	0
Annual	-0.162	-0.242	-0.571	-0.205	-0.317	-2.873

Innovative Trend Analysis (ITA) revealed highly significant negative trends for both annual metrics. Downward slopes were calculated at the 99% confidence level for the number of events (s = -0.1839) and the area affected (s = -0.7510) as shown in summary tables of ITA (visit appendix D).



(a) *(b)*

Figure 3.4 Innovative Trend Analysis annual (a) area affected (b) number of fire events.

The annual scatter plots visually confirm this decline. The distribution of data points across magnitude clusters illustrates a distinct shift in fire severity. Low-magnitude years representing the quietest fire seasons are positioned just below the 1:1 reference line, reflecting a minor decrease. However, observations in the medium and high-magnitude zones fall substantially further below the reference line. This widening gap demonstrates that the most active and expansive fire years experienced the sharpest reductions during the 2011–2025 period.

3.7.2 Seasonal trends

This section describes the changes over time in both the number of fires and the amount of area burned for the four seasons (Winter, Spring, Summer and Autumn).

Summer was the only period to show a significant rise in overall fire activity. Rank-based tests revealed strong positive correlations for both the number of events (MK Tau = 0.448; SR Rho = 0.552) and the area affected (MK Tau = 0.384; SR Rho = 0.504), as detailed in Table 3.6. The Sen's slope calculation suggested a median gain of 0.048 events annually, though the rate for the burned area remained at zero. Linear regression charts (appendix D) support this, showing a minor upward slope for fire frequency (R-squared = 0.0592) and a completely flat line for spatial extent (R-squared = 0.0011). Interestingly, while general frequency climbed, the Innovative Trend Analysis (ITA) did not find these Summer slopes to be statistically significant. A look at the seasonal ITA charts clarifies this pattern: while fires in the low-magnitude zone increased, data points in the high-magnitude zone dropped entirely below the 1:1 reference line. This indicates that the most severe summer fires actually decreased in size and frequency during the 2011–2025 period.

In contrast, Spring demonstrated clear reductions across multiple indicators. The standard statistical tests yielded non-significant negative values, but the Sen's slope estimator calculated notable annual drops of -0.185 events and -1.011 hectares. The ITA method captured this decline strongly, calculating highly significant negative slopes for both Spring fire events (-0.8622) and affected area (-3.1405). The corresponding scatter plots vividly display this shift, with almost all medium and high-magnitude observations positioned deeply below the no-trend line.

Autumn and Winter generally experienced stable or declining fire behavior. Rank-based methods produced weak, non-significant results near zero, accompanied by flat Sen's slopes. Despite this, the ITA successfully detected statistically significant negative slopes for both events and area across both seasons. The ITA graphs back this up, as the recorded events consistently fall into the lower half of the charts, safely away from the increasing trend zone. These seasonal outputs highlight that while smaller summer fires are becoming more frequent, the severity and scale of major fire events have declined considerably across all seasons.

3.7.3 Monthly trends

Monthly changes in fire-event counts and total burned area over 1996–2025 are described in this section.

Statistically significant increases in both fire-event numbers and burned area occurred only in July, August, and September (Table 3.6). Among these, August showed the strongest positive trends for both the number of events (MK Tau = 0.459; SR Rho = 0.543) and the area affected (MK Tau = 0.412; SR Rho = 0.522). July and September also displayed statistically significant positive trends across both metrics. Despite these significant rank correlations, the Sen's slope values for these three months were zero. Linear regression models further illustrated this increasing pattern; results display a clear linear rise in August fire events (R-squared = 0.3032) and area affected (R-squared = 0.1398), largely resulting from a cluster of fires between 2020 and 2025.

The remaining months did not show statistically significant trends. March and April had weak positive rank correlations for both the number of events and area affected. May recorded a minor decrease in fire events (MK Tau = -0.014) alongside a slight positive trend for the affected area (Sen's slope = 0.071). June was the only summer month with non-significant decreasing trends for both the number of events (MK Tau = -0.084) and the area burned (Sen's slope = -0.169). In autumn, October showed a weak positive trend (MK Tau = 0.187), whereas November showed a weak negative trend (MK Tau = -0.123) for fire events.

This was confirmed by Innovative Trend Analysis (ITA) results in all data zones, low, medium and high. The July, August and September values are clearly over the 1:1 reference line in all three magnitude zones, suggesting an overall trend towards more fire

events of all sizes during the 2011-2025, time period. In contrast, the ITA plots for the non-significant months do not show clear upward shifts. In March, April, and October, fire events mostly clustered in the low magnitude zone directly on or near the reference line. For historically active fire months like May and June, several data points in the medium and high magnitude zones fell below the 1:1 line, reflecting a minor decrease in severe fire years during the latter half of the study.

Annual fire frequency and burned area in Margalla Hills both declined significantly under ITA, with burned area decreasing more rapidly than fire frequency. This suggests that fires are becoming smaller rather than simply less frequent. This finding agrees with Tariq et al., (2021, 2022), who identified road proximity, forest density, and human activities as the main controls on fire severity in Margalla Hills, rather than climatic conditions. Improved fire monitoring and suppression may therefore have contributed to limiting fire spread. In contrast, Shahzad et al., (2024) reported an unstable but overall increasing trend in vegetation fires across Pakistan based on MODIS data. This difference is likely because their analysis covered a shorter and more recent period, was largely influenced by cropland burning at the national scale, and did not reflect the management conditions of a protected forest located near the capital.

Seasonally, both fire frequency and burned area declined consistently during Spring. In Summer, however, both indicators increased in rank-based terms, although the increase in burned area was minimal. This suggests that more fires were ignited, but most remained small and did not develop into extensive burn events. Autumn and Winter showed weak but consistent declines in both indicators. The observed seasonal pattern agrees with Rafaqat et al., (2022), who found that wildfire drivers vary across both geographic regions and seasons in Pakistan. Nafees et al., (2024) found that monsoon rainfall suppresses summer fires in northern Khyber Pakhtunkhwa, while winter Western Disturbances have recently increased fire risk. The contrasting pattern observed in Margalla Hills is likely related to its lower elevation and scrub-dominated vegetation, where fuels dry quickly between rainfall events and favour frequent but generally small fires.

The main departure from previous studies was the significant increase in both fire frequency and burned area during July, August, and September. This increase was concentrated in a few recent years rather than representing a gradual long-term change, and the increase in fire frequency was more pronounced than that of burned area. This

contrasts with the monsoon-related fire suppression reported by Nafees et al., (2024) for northern Pakistan. A possible explanation is that weaker or more variable monsoon rainfall over Islamabad creates short periods favourable for ignition. In addition, Tariq et al., (2021, 2022) showed that fire occurrence in Margalla Hills is strongly associated with human activities near roads and settlements, making ignitions less dependent on rainfall than in remote forest regions. At the same time, effective fire suppression likely prevents most fires from spreading over large areas. As this increase is limited to recent years, it should be regarded as an emerging pattern rather than a long-term trend.

3.8 Trends in climatic variables

This section reports significant changes in five climatic variables of study at annual, seasonal, and monthly scales. Statistic table (Table 3.7) for MMK and Spearman's rho is given in this section while for statistics table for ITA is given in appendix D.

Table 3.7: Multi temporal Trend statistics of climatic variables.

(for p-values below 0.05 and 0.01)

Time Period	Precipitation			Max Temp			Min Temp			Humidity			Wind Speed		
	MK Tau	SR Rho	Sen's Slope	MK Tau	SR Rho	Sen's Slope	MK Tau	SR Rho	Sen's Slope	MK Tau	SR Rho	Sen's Slope	MK Tau	SR Rho	Sen's Slope
Jan	-0.064	-0.081	-0.486	0.028	0.022	0.009	-0.057	-0.106	-0.013	0.184	0.279	0.154	0.397***	0.553***	0.009
Feb	-0.104	-0.145	-0.891	0.136	0.216	0.047	-0.053	-0.075	-0.014	-0.078	-0.074	-0.077	-0.117	-0.165	-0.004
Mar	0.08	0.154	0.787	0.037	0.055	0.008	-0.099	-0.16	-0.014	0.141	0.206	0.152	-0.021	-0.004	-0.001
Apr	0.124	0.188	0.784	-0.133	-0.178	-0.063	-0.278**	-0.422**	-0.059	0.145	0.2	0.207	-0.032	-0.021	-0.001
May	0.191	0.295	0.6	-0.131	-0.162	-0.053	-0.239	-0.354	-0.091	0.269**	0.366**	0.433	-0.005	0.065	0
Jun	0.099	0.136	0.841	-0.032	-0.072	-0.006	-0.301**	-0.43**	-0.067	0.076	0.14	0.085	0.099	0.155	0.012
Jul	0.2	0.303	2.86	-0.143	-0.211	-0.029	-0.291**	-0.455**	-0.028	0.192	0.288	0.098	0.241	0.363	0.015
Aug	-0.122	-0.153	-3.205	0.037	0.031	0.005	-0.012	-0.002	-0.001	-0.035	-0.053	-0.009	0.302**	0.449**	0.009
Sep	0.12	0.162	1.5	0.048	0.045	0.009	0.018	0.016	0.004	0.071	0.135	0.03	0.591***	0.763***	0.014
Oct	0.072	0.067	0.267	-0.108	-0.127	-0.029	-0.152	-0.233	-0.033	0.055	0.106	0.047	0.517***	0.609***	0.005
Nov	0.173	0.241	0.364	-0.244	-0.344	-0.06	-0.12	-0.19	-0.026	0.357***	0.479***	0.192	0.304**	0.35**	0.001
Dec	-0.035	-0.008	0	-0.092	-0.123	-0.022	-0.157	-0.241	-0.032	0.2	0.271	0.186	0.402***	0.441***	0.002
Winter	-0.025	-0.032	-0.457	0.048	0.067	0.007	-0.26**	-0.357**	-0.029	0.168	0.245	0.133	0.069	0.106	0.001
Pre-Monsoon / Spring	0.159	0.232	2.694	-0.159	-0.168	-0.038	-0.292**	-0.405**	-0.082	0.205	0.277	0.167	0.03	0.06	0.001
Monsoon / Summer	0.122	0.166	3.89	-0.053	-0.105	-0.005	-0.129	-0.219	-0.009	0.149	0.213	0.071	0.417***	0.591***	0.012
Post-Monsoon / Autumn	0.122	0.217	0.976	-0.191	-0.267	-0.039	-0.209	-0.307	-0.033	0.218	0.325	0.118	0.517***	0.686***	0.003
Annual	0.177	0.271	7.835	-0.101	-0.111	-0.016	-0.237	-0.376	-0.027	0.228	0.36	0.142	0.168	0.213	0.006

3.8.1 Trends in temperature maximum

Standard rank-based tests, including the Modified Mann-Kendall and Spearman's rank correlation, did not detect any statistically significant trends for maximum temperature during any time period.

Innovative Trend Analysis (ITA) identified broad, highly significant decreasing trends across the dataset. In this context, the ITA slope indicates the average difference in magnitude between the two halves of the study period, and a negative slope means that the overall trend is a decrease. On an annual basis, maximum temperature experienced a significant downward shift (s = -0.0279). This cooling pattern occurred across all four seasons, with Spring (s = -0.0697) and Autumn (s = -0.0481) demonstrating the sharpest significant declines, followed by Winter (s = -0.0162) and Summer (s = -0.0086).

At the monthly level, seven months produced significant negative trends. April (s = -0.0789) and November (s = -0.0691) showed the steepest drops, while January (s = -0.0201), March (s = -0.0604), May (s = -0.0606), July (s = -0.0384), and October (s = -0.0270) also recorded significant negative slopes.

No available Islamabad study covers the same 30-year window used here. Khan et al., (2022) compared 1962–1990 with 1991–2019; Rizvi et al., (2021, as cited in Khan et al., 2022) covered 1960–2013; Wasif Ali et al., (2022) used 1960–2012 PMD data plus 2000–2015 MODIS data. This period mismatch may itself explain the difference: Khan et al., (2022) show their own Karakoram stations cooled across 1962–1990 but reversed to warming by 2010–2019, so trend direction is sensitive to the window chosen. Test choice and data source may add to this. Khan et al., (2022) and Rizvi et al., (2021) used Mann-Kendall on PMD data, matching this study, so those factors are less likely to explain any gap with them. Wasif Ali et al., (2022) combined linear regression with Mann-Kendall and MODIS land surface temperature (a vegetation-sensitive measure, unlike PMD's air temperature), and at MHNP's own scale, this combination confirmed a decline rather than the citywide rise, so both method and data type could explain the difference from that study. The weather station used here sits only about 5.5 km from MHNP. This closeness means the record likely mixes some of the park's cooling with some of the surrounding city's warming, rather than cleanly representing either, which could explain why the result falls between Khan et al.'s (2022) citywide warming and Wasif Ali et al.'s (2022) park-specific decline.

3.8.2 Trends in temperature minimum

Annual minimum temperatures showed a general decreasing tendency. While standard tests did not reach statistical significance, the Sen's slope estimator indicated a median reduction of -0.027 °C per year. Innovative Trend Analysis (ITA) calculated a statistically significant annual decline with a slope of -0.0367.

Significant cooling occurred prominently during the Pre-Monsoon and Winter seasons. Both seasons recorded statistically significant declines in the standard tests, with median annual reductions of -0.062 °C for Pre-Monsoon and -0.029 °C for Winter. ITA confirmed these findings with significant negative slopes of -0.0917 and -0.0340, respectively.

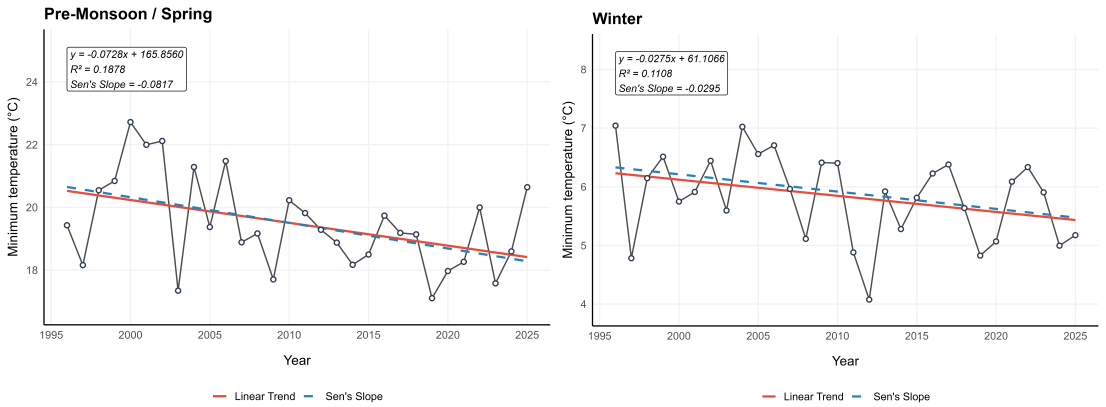


Figure 3.5 Line graphs of temperature minimum.

At the monthly scale, April, June, and July were the only months to display statistically significant negative correlations in the standard tests. April experienced the sharpest median decrease at -0.059 °C per year, followed by June (-0.057 °C) and July (-0.028 °C). ITA summary statistics matched these findings with significant negative slopes for April (-0.0773), June (-0.0601), and July (-0.0250). The ITA scatter plots for these months visually reinforce the shift, positioning all data points across the low, medium, and high clusters securely in the decreasing trend area below the reference line.

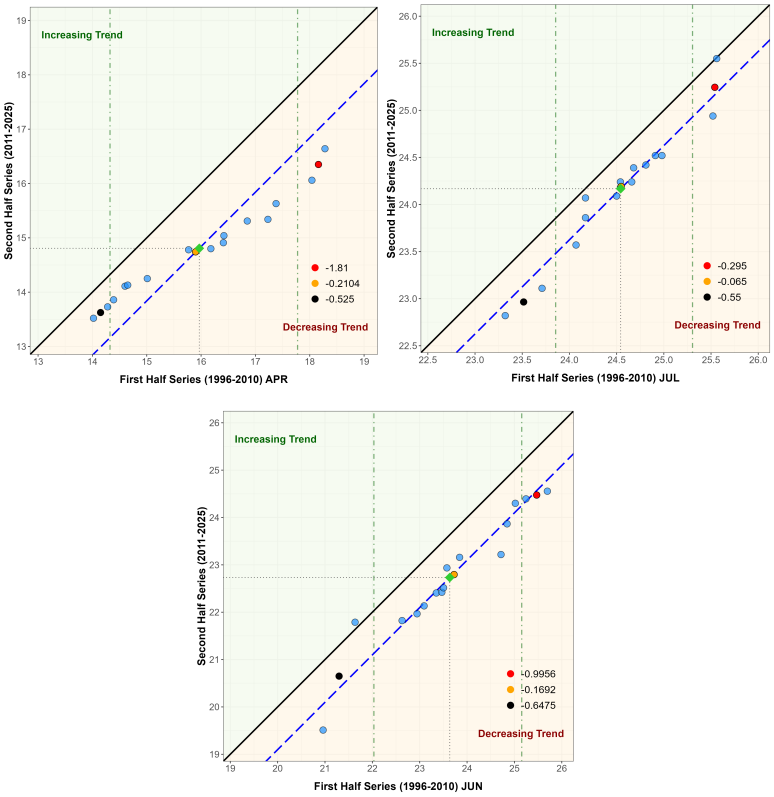


Figure 3.6 ITA graphs- temperature minimum.

Minimum temperature at MHNP shows a declining trend, although the decrease is significant only at seasonal and monthly scales in standard statistical tests. This contrasts with Islamabad's overall warming trend reported by Sajjad et al., (2020), who observed increasing minimum temperatures from 1983 to 2013 due to urban expansion in Rawalpindi and Islamabad. ITA results further indicate that the decline mainly occurred in the later years, explaining why ITA detected an annual trend while the Modified Mann-Kendall test did not. This opposite pattern is likely related to MHNP's forested land cover, which creates cooling effects compared with built-up areas, as also reported by Wasif Ali et al., (2022). Although satellite-based land surface temperature differs from recorded air temperature, the cooling trend near the monsoon onset may influence fuel moisture and temperature patterns associated with wildfire occurrence.

3.8.3 Trends of temperature based ETCCDI

This section examines the annual, seasonal, and monthly patterns of the ETCCDI temperature extreme. The trend analysis of the indices reported here is summarized in Figure 3.7(a). The daily maximum temperature (TXn) showed a significant positive yearly trend (Sen's slope of 0.100 °C per year, $p = 0.0123$). Tropical Nights (TR) showed a statistically significant annual decrease of -0.667 days per year ($p = 0.0244$), however. Both MMK and Spearman's rho confirmed that TXn and TR had statistically significant annual trends. All other annual temperature indices analyzed in this study were non-significant or produced a zero slope.

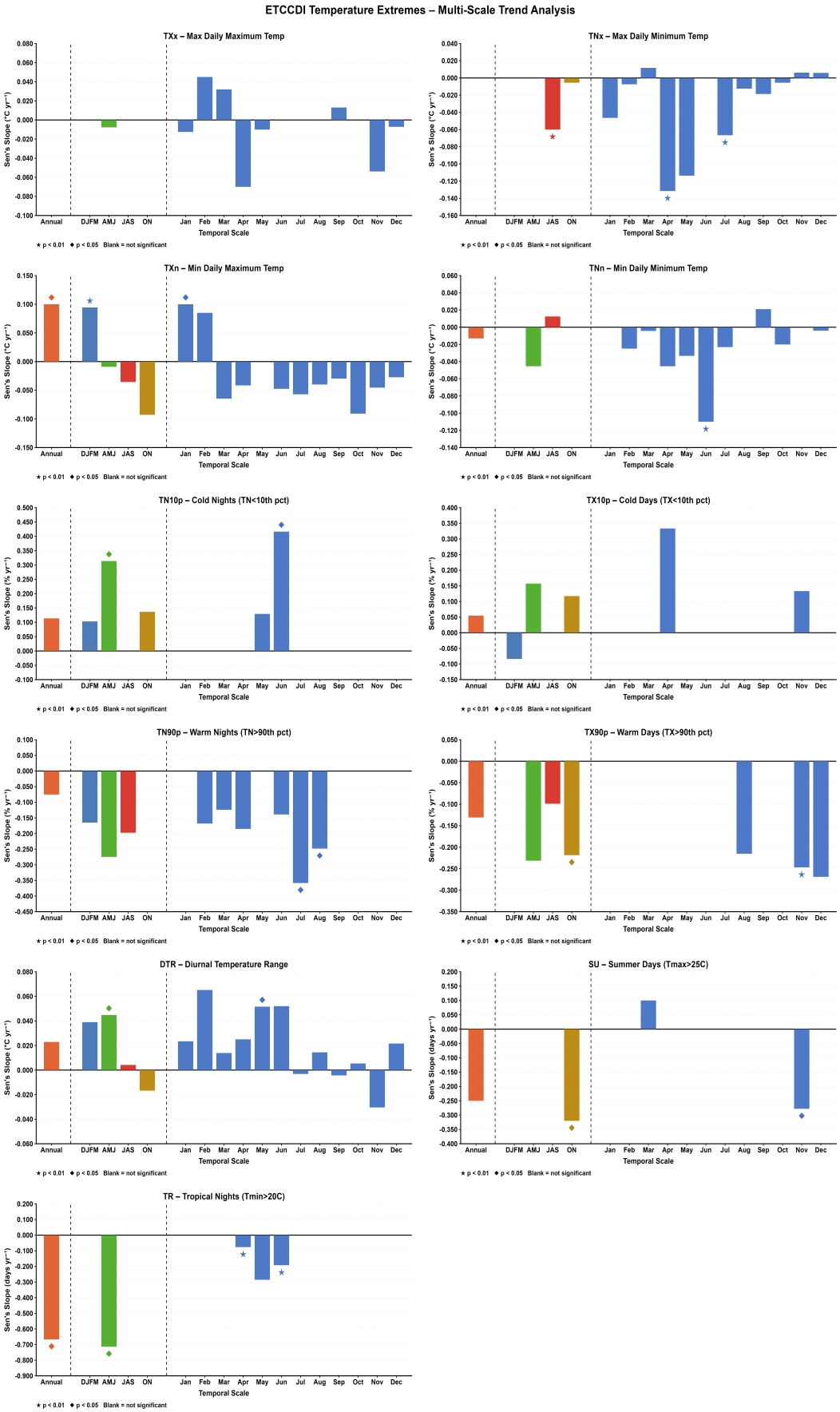


Figure 3.7(a) Sen's slope for temperature's extreme indices (1996-2025).

The intervals for these thermal shifts were provided by seasonal and monthly evaluations. The increase in TXn during the DJFM season was significant at 0.09 °C per year, which was directly related to the significant increase in January at 0.10 °C per year. The percentage of cold nights (TN10p) increased significantly by 0.31% per year in the AMJ season, and the DTR increased significantly by 0.04 °C per year, whereas the TR significantly decreased by -0.60 days per year in the AMJ season. The monthly variations during this AMJ period indicated that the maximum daily minimum temperature (TNx) had a negative trend of -0.13 °C/year during April while the TR had a negative trend of -0.10 days/year for the same month. May had a significant DTR increase of 0.05 °C per year, and June had a significant increase in TN10p (0.41% per year) with significant decreases in the lowest daily minimum temperature (TNn) of -0.11 °C per year and TR of -0.20 days per year.

TNx significantly decreased by -0.06 °C per year during the JAS season, and warm nights (TN90p) significantly decreased by -0.22% per year during the JAS season. On the monthly scale for JAS, both TNx (-0.09 °C per year) and TN90p (-0.31% per year) had significant decreases in July, and TN90p (-0.25% per year) had a significant decrease in August. Lastly, ON had large negative trends for warm days (TX90p) (slope = -0.20% per year) and SU (slope = -0.35 days per year). These seasonal declines were seen in November, with TX90p seeing a significant decrease of -0.25% per year, and SU -0.28 days per year. As in the annual results, the seasonal and monthly variations for the maximum daily maximum temperature (TXx) and cold days (TX10p) were entirely non-significant during the year. These particular temperature trends set the baseline for determining wildfire frequencies to correspond to these trends.

The annual results reveal warming of the lowest daily maximum temperature and a reduction in the number of tropical nights, suggesting non-uniform changes in temperature within MHNP. The increase in the lowest daily maximum temperature is consistent with the findings of Din et al., (2026) and Shirazi et al., (2020) for Islamabad and Potohar region, respectively, while the decrease in tropical nights is not consistent with the regional patterns.

Similar local variations have been reported in the subtropical highlands and Himalayan foothills, where topography and microclimate influence temperature patterns

(Ghanim et al., 2023; Zafar et al., 2024). This difference may reflect the cooling influence of vegetation within MHNP (Waseem & Khayyam, 2019).

During the pre-monsoon season, the diurnal temperature range increased because of cooler nights. As this period coincides with the peak wildfire season, a wider diurnal temperature range may promote daytime fuel drying, consistent with observations from Pakistan's highlands transition zones (Zafar et al., 2024). During the monsoon, TNx and TN90p decreased in July and August, contrasting with the monsoon warming reported for Islamabad (Din et al., 2026). This pattern is likely to be influenced by the presence of dense vegetation, high soil moisture, and increased cloud cover (Waseem & Khayyam, 2019). Warm days (TX90p) and summer days (SU) decreased during the post-monsoon season, while other temperature extreme indices were not statistically different, suggesting that changes were not observed in all temperature extreme indices.

3.8.4 Trends in precipitation

No statistically significant trends were found in precipitation at any annual, seasonal or monthly time scale using standard rank-based tests (MMK and Spearman's rank correlation). ITA evaluates the direction of change by comparing the mean levels of the two halves of the record. ITA showed a highly significant positive trend in mean precipitation at an annual scale with a calculated slope of 0.9383.

This substantial increase in mean precipitation was found in all four seasons. The Monsoon season (s = 1.6406), Pre-Monsoon (s = 1.0227), Post-Monsoon (s = 0.8584), and Winter (s = 0.2338) were the seasons with the highest increase.

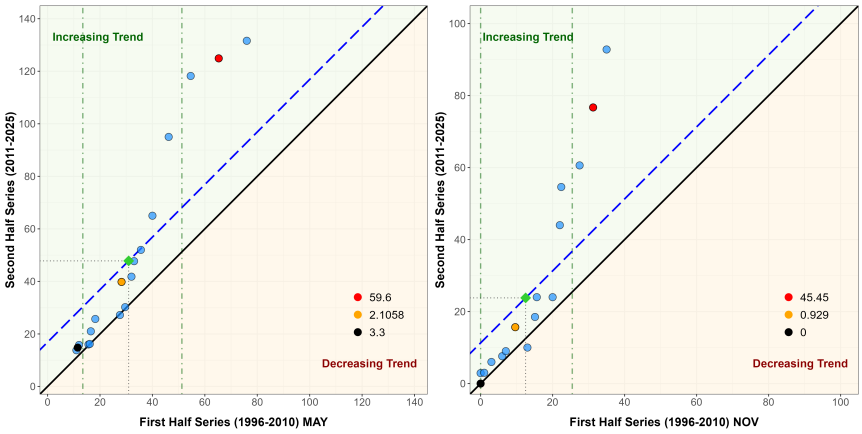


Figure 3.7 (b) ITA- precipitation.

ITA detected strong positive changes in mean precipitation in seven months at the monthly scale. September (s = 3.8027) and March (s = 2.8138) had the largest positive slopes, as did April, May, July, October, and November. The mean precipitation was significantly reduced only during the colder months, leading to negative slopes in January (s = -0.6378), February (s = -0.9987), and December (s = -0.2422). The difference between rank-based tests and ITA indicates that there has been a change towards wetter conditions at the end of the record at MHNP, rather than a general increase with time. Traditional trend tests may not be able to detect this type of irregular change, but it can be detected with ITA (Şen, 2012). Weak or insignificant rainfall trends were reported from the studies conducted in Rawalpindi, Chakwal, Islamabad and Murree, and they noted an increase in rainfall after 2015 (Miandad et al., 2025; Rashid et al., 2026). The rise is primarily in warmer months with decreases in some colder months, indicating a shift towards more irregular seasonal rainfall patterns, not a uniform rise. The change could affect the duration of the dry period of the wildfire season but the monthly ITA results should be viewed as indicating general direction rather than the exact magnitude of the change because of the 15-year periods used to divide the record.

3.8.5 Precipitation based ETCCDI trends

No statistically significant trends were found for any of the evaluated precipitation indices at the annual scale in standard rank based tests. A summary of the trend analysis of indices in this section is given in figure 3.8. The changes in precipitation persistence became significant only at the seasonal scale. The Maximum Consecutive Wet Days (CWD) experienced a statistically significant downward trend (Sen's slope of -0.048 days/year) during the DJFM season. However, the AMJ season showed a significant CWD increase, with Sen's slope equal to 0.039 days per year ($p < 0.05$). None of the other seasonal precipitation indices showed significant trends.

Statistically significant changes were identified only in May at the monthly scale. The Simple Daily Intensity Index (SDII) exhibited a statistically nonrandom increase during May with a Sen's slope of 0.16 mm day^{-1} yr^{-1} ($p < 0.05$). At the same time, May showed a significant rise in Rx1day, with Sen's slope of 0.38 mm yr^{-1} ($p < 0.05$). All other monthly differences among the evaluated precipitation indices were completely non-significant during the year. These precipitation patterns create the climatic context for evaluating their association with past fire events.

There was no significant change at the annual level for any index. When considered on an annual scale, the precipitation in MHNP has remained relatively stable in terms of both duration and intensity, only partially supporting the notion of changing climate extremes. A similar trend is observed in the area around Potohar, where the Mann-Kendall test revealed no significant trend in rainfall data from Rawalpindi and Chakwal (Miandad et al., 2025). In contrast, longer-term country-wide studies have identified trends (Bhatti et al., 2020). This variation may be due to the increased spatial extent of the national study and annual averaging of seasonal variations at MHNP.

CWD decreased in DJFM and increased in AMJ, suggesting a seasonal shift in the distribution of wet spells rather than a general increase or decrease. The winter decline is in line with the reduction in DJFM rainfall over Pakistan due to less and less intense western disturbance (Abbas et al., 2023). Statistically significant changes were identified only in May at the monthly scale. The Simple Daily Intensity Index (SDII) exhibited a significant rise during May with a Sen's slope of 0.16 mm day^{-1} yr^{-1} ($p < 0.05$). At the same time, May showed a significant rise in Rx1day, with Sen's slope of 0.38 mm yr^{-1} ($p < 0.05$). These seasonal changes can lead to decreases in soil moisture prior to the dry season and increases in fuel moisture during wet spells in AMJ. The observed change is, however, due to a fixed rainfall threshold and a single station record, which may be natural variability and not a long-term climatic trend.

Both SDII and Rx1day increased just in May. This indicates that the intensity of the rain increased during the month for each event, although the number of rainy days did not. The same trend is observed in Punjab and KPK, with Rx1day increasing by 7 to 15 percent from 1981 to 1999 and 2000 to 2022, while SDII also shows an increase, with higher rainfall per wet day (Ullah, Niaz, et al., 2026). A likely reason is more moisture and stronger convection building up before the monsoon (Ullah, Karim, et al., 2023), which packs rain into fewer, heavier bursts. This is important for the MHNP as May is immediately before the high fire season. Even without more total rain, heavier but less frequent rain can still leave longer dry gaps for fuel to dry out. As with the seasonal result, this comes from one station over 30 years, so more stations would help confirm it.

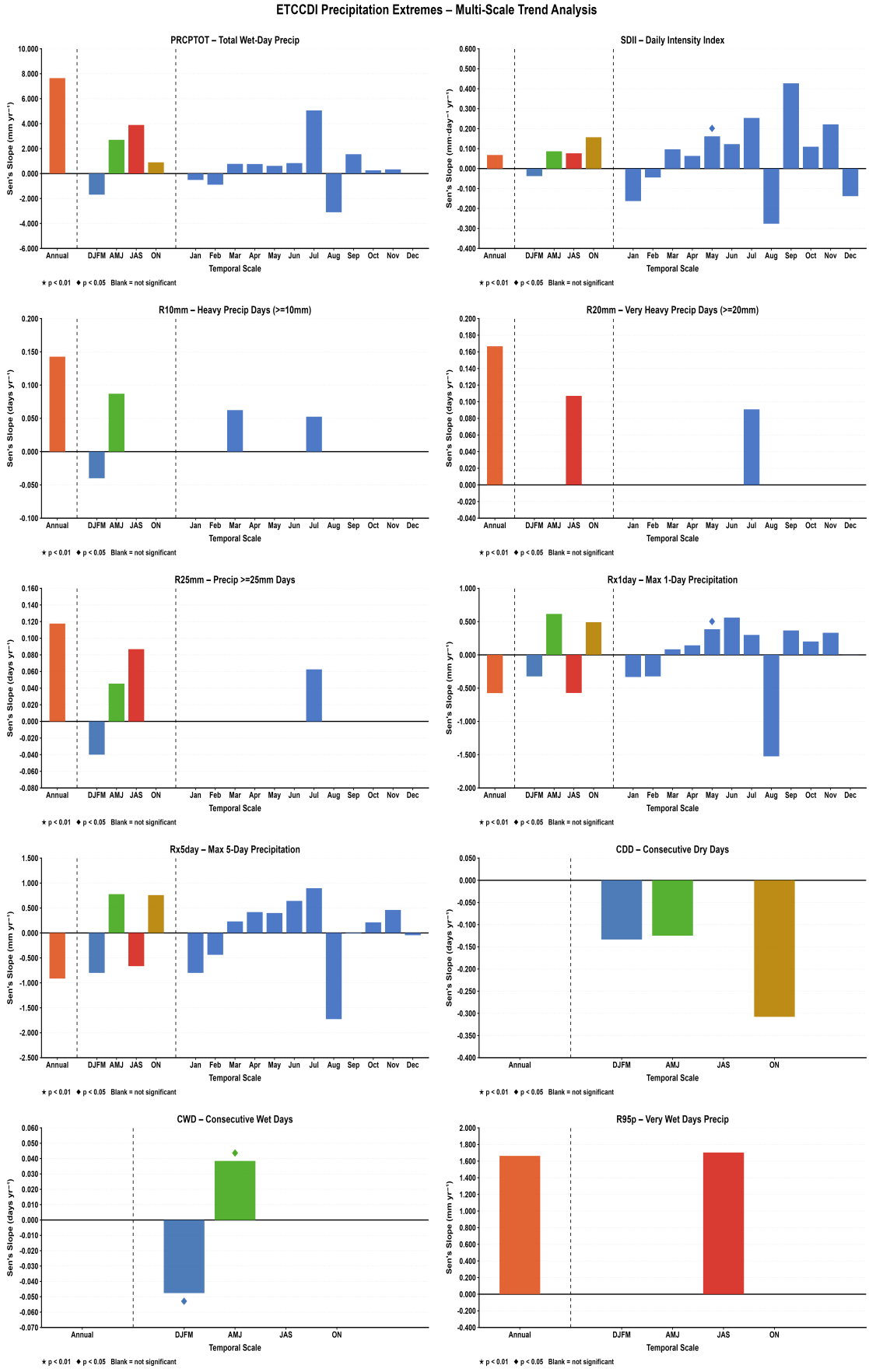


Figure 3.8 Sen's slope for precipitation extreme indices-multi scale (1996-2025).

3.8.6 Trends in relative humidity

Standard rank-based tests did not identify a statistically significant annual trend. When considered individually, the ITA that quantifies the change in the mean value between the two halves of the study period revealed a very significant increase in the mean annual relative humidity with a slope of 0.1651.

At the seasonal scale, rank-based tests also lacked significant trends. ITA calculated significant positive mean shifts across all four seasons, reaching its highest slope during the Pre-Monsoon period (s = 0.4150).

At the monthly level, rank-based tests identified statistically significant increasing trends strictly during May and November, with median annual rises of 0.433% and 0.192%, respectively. The corresponding ITA scatter plots for these two months reinforce this trend. The physical distance of these clusters from the 1:1 line indicates the severity of the shift. The data points in the higher magnitude zones move farther away from the reference line than those in the lower zones. This growing and unbalanced gap highlights the fact that the total days with the highest humidity has exhibited an increase significantly more than the number of days with the lowest humidity. In addition, ITA computed positive mean shifts for nine of the twelve months with the highest mean slopes in May (s = 0.4796) and April (s = 0.3504).

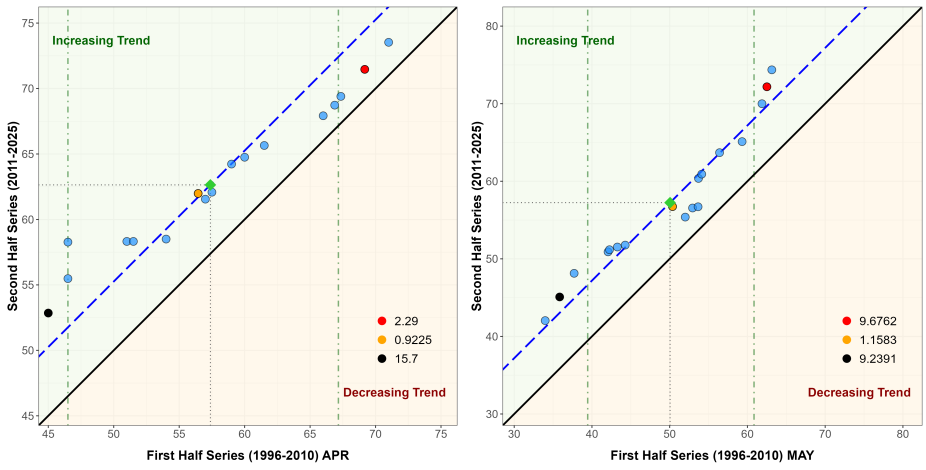


Figure 3.9 ITA- relative humidity.

This is the first site-specific assessment of relative humidity trends, as no published study has reported relative humidity trends for MHNP. The moisture pattern of humidity and precipitation is similar; both are stable in the rank-based tests, but rise in the ITA, with positive changes in May and November, and no significant change in January,

February, or December. This indicates that the changes in humidity are largely due to the availability of moisture, not just warming. The same trend was noticed by Khan et al., (2026) in the case of Upper Dir, where the humidity had a rising trend in all seasons, except winter. However, Shakoor et al., (2025) reported a reduction in humidity in the entire Punjab, including North Punjab, where warming prevails over the moisture balance. At the MHNP foothill environment, the warming effects may be offset by increased precipitation. The relevance of the wildfire is limited because the humidity increase is primarily in already humid situations and winter is relatively dry because of the lower precipitation and the lack of humidity increase.

3.8.7 Heat index results

No significant trends were identified in the Heat Index using trend analysis at the annual, seasonal or monthly time scales.

The daily Heat Index values showed significant differences between the four seasons analysed. The thermal stress was the highest during Monsoon season with a median Heat Index of 50 °C, falling in the Danger category. The Pre-monsoon season came next, with a median temperature of almost 44 °C, and that too is in the Danger classification. During both Monsoon and Pre-monsoon months, extreme observations were often recorded, in both cases exceeding the 52 °C threshold, which falls under Extreme Danger category. The Autumn season displayed moderate heat stress, recording a median value near 37 °C within the Extreme Caution category. The Winters season recorded the lowest thermal stress, maintaining a median Heat Index near 31 °C within the Caution category (Figure 3.10)

The highest mean Heat Index values occurred consistently in June, July, and August throughout the 30-year study period. May and September recorded transitional and moderate heat levels. Conditions during January, February, March, and December predominantly fell below the minimum calculation thresholds of 27 °C air temperature and 40 percent relative humidity (Figure 3.11)

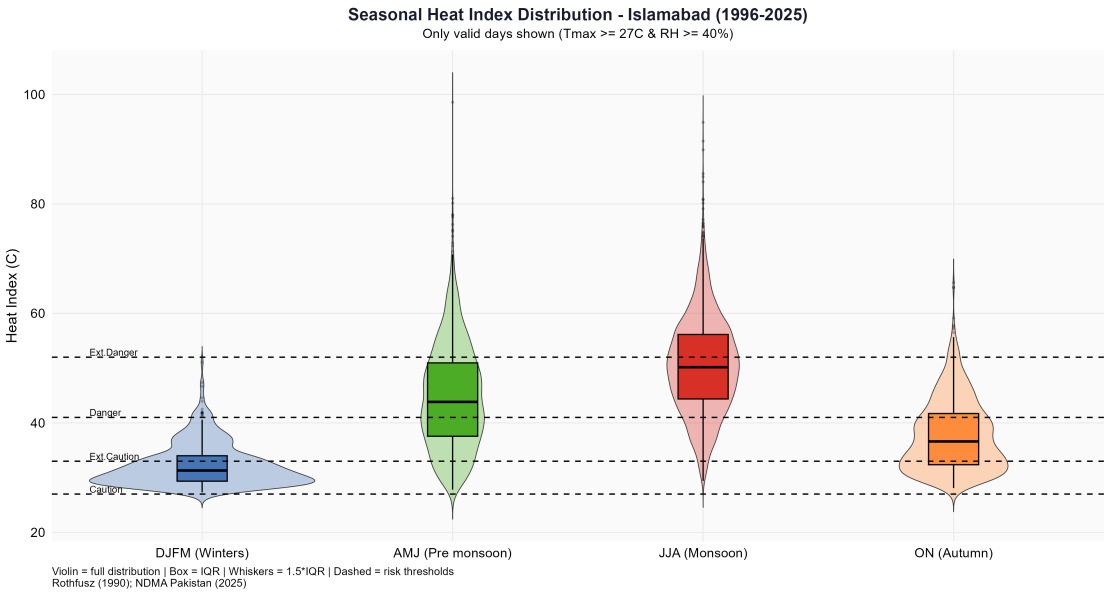


Figure 3.10 Seasonal heat index box plot.

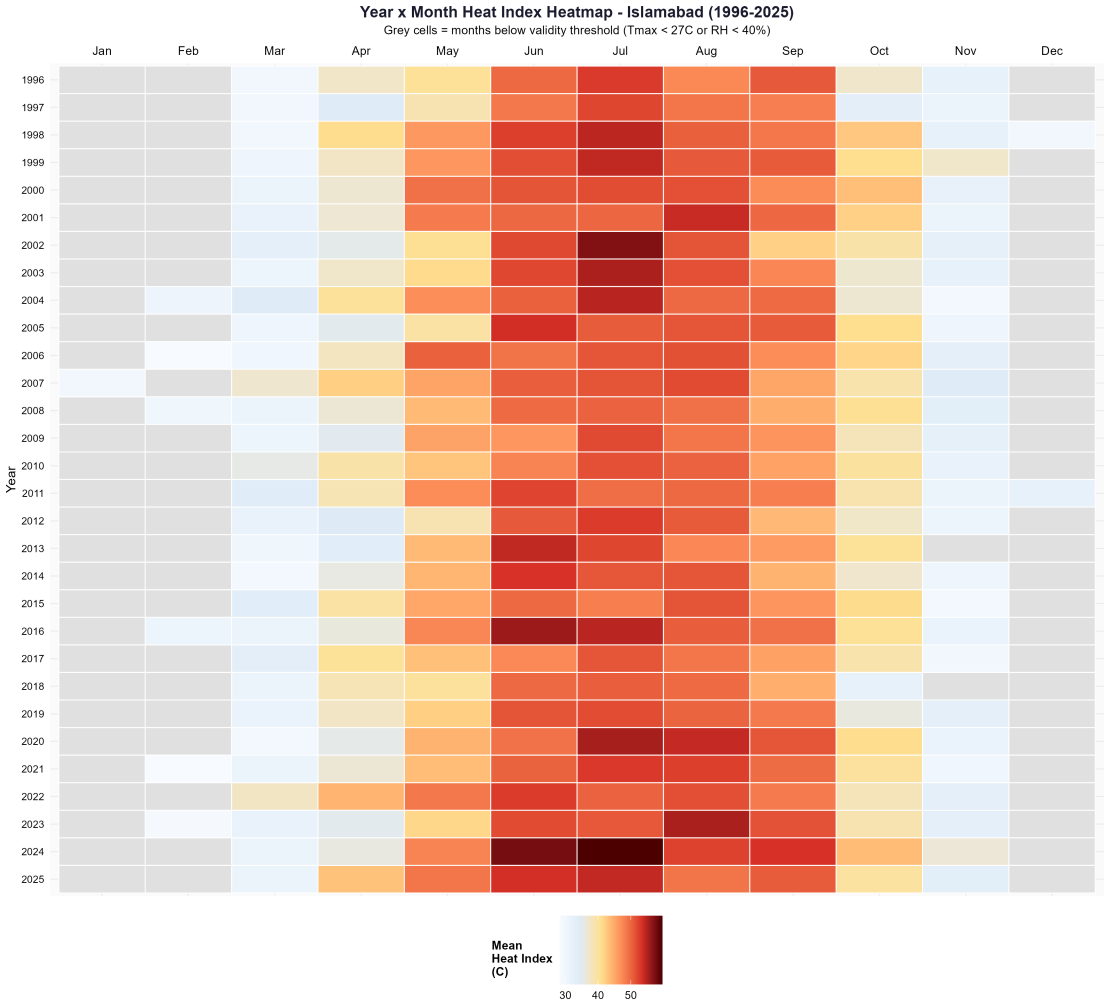


Figure 3.11 Heat index (year x month).

No clear trend was found in the Heat Index at any time scale, suggesting that heat stress at MHNP has remained broadly stable over the past 30 years. This only partly supports the idea of changing heat extremes and differs from earlier Pakistan studies that reported increasing heat-wave duration nationally (Khan et al., 2019) and a 3.5°C rise in summer Heat Index across Punjab between 1961 and 2007 (Zahid & Rasul, 2010). The difference may partly reflect the shorter record used here: the Punjab study covered 47 years, compared with 30 years in the present study, making weak or gradual changes harder to detect. Heat Index studies for Pakistani cities remain limited, with most focusing on Lahore (Khalid et al., 2025), making this the first assessment of Heat Index conditions for MHNP.

Despite the lack of a significant trend, heat stress remains high during much of the warm season. Pre-monsoon and monsoon conditions generally fall within the Danger category, with some days reaching Extreme Danger, while winter remains mostly in the Caution range. The highest values occur during June–August, when high humidity from monsoon rainfall keeps the Heat Index high even when temperatures decline slightly (Zahid & Rasul, 2010). Recent government reports also identify Islamabad as vulnerable to extreme summer heat and recognize forest fires as a heat-wave hazard in Central Pakistan (NDMA, 2025). This is important for MHNP because the period of high heat stress overlaps with the fire-risk season.

3.8.8 Trends in wind speed

Standard rank-based tests recorded no statistically significant trend for annual wind speed. The ITA was also calculated separately to estimate the mean shift between the two halves of the study period and it did not show a significant annual shift.

On the seasonal time scale, only the Monsoon and Post-Monsoon seasons showed statistically significant increasing trends, at a slope of 0.012 and 0.003 respectively. (Table 3.7) Evaluated separately, ITA calculated significant positive mean shifts for the Monsoon (s = 0.0065) and Post-Monsoon (s = 0.0050) seasons, alongside a significant negative mean shift for the Pre-Monsoon period (s = -0.0081).

At the monthly scale, standard tests recorded statistically significant increasing trends strictly during January, August, September, October, November, and December. Separately, ITA summary statistics recorded significant positive mean shifts from July

through December, peaking in September (s = 0.0173), and significant negative mean shifts from February through June.

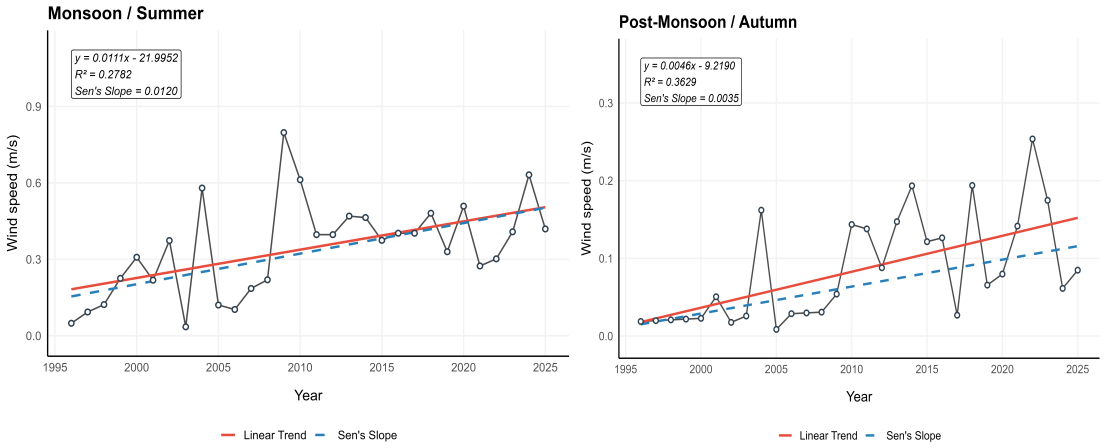


Figure 3.12 Line graphs of wind speed.

The lack of a significant annual trend indicates that wind speed at MHNP has not changed consistently, as opposing seasonal patterns offset each other. Similar results were reported for Punjab, where annual trends were weak despite increases in some northern districts, showing that changes are spatially variable rather than absent (Shakoor et al., 2025). The February–June decline may be linked to urban expansion near the park, as weak pre-monsoon winds are more affected by surface roughness. The difference between methods is expected, as rank-based tests detect consistent trends, while ITA captures shifts between two periods. Since these months' overlap with the main wildfire season (May–July) in MHNP (Tariq et al., 2021), the decline in average wind speed is unlikely to be driving fire increases, which are mainly linked to human ignition (Tariq et al., 2022). However, average trends may not reflect extreme gusts that enhance fire spread.

3.8.9 Wind speed indices

No significant trends were detected on any time scale using standard statistical tests. Historical wind profile is mostly light breezy. 95 to 100 per cent of the annual record is for the conditions below 2 m/s. Moderate winds (2-5.5 m/s) average less than 5 percent per year, and have had one high point, near 15 percent in 2008. Wind speeds of more than 5.5 meters per second make up less than 1 per cent of the record and occur only from 2024 to 2025.

This is also reflected in the seasonal and monthly distributions. Calm days make up 28-30 days per month. Moderate winds reach their peak at 3.5 days in the Pre Monsoon season, averaging 1.0 to 1.5 days/month between February and July and zero in Autumn. The stable patterns set the meteorological baseline for assessing past wildfire occurrences.

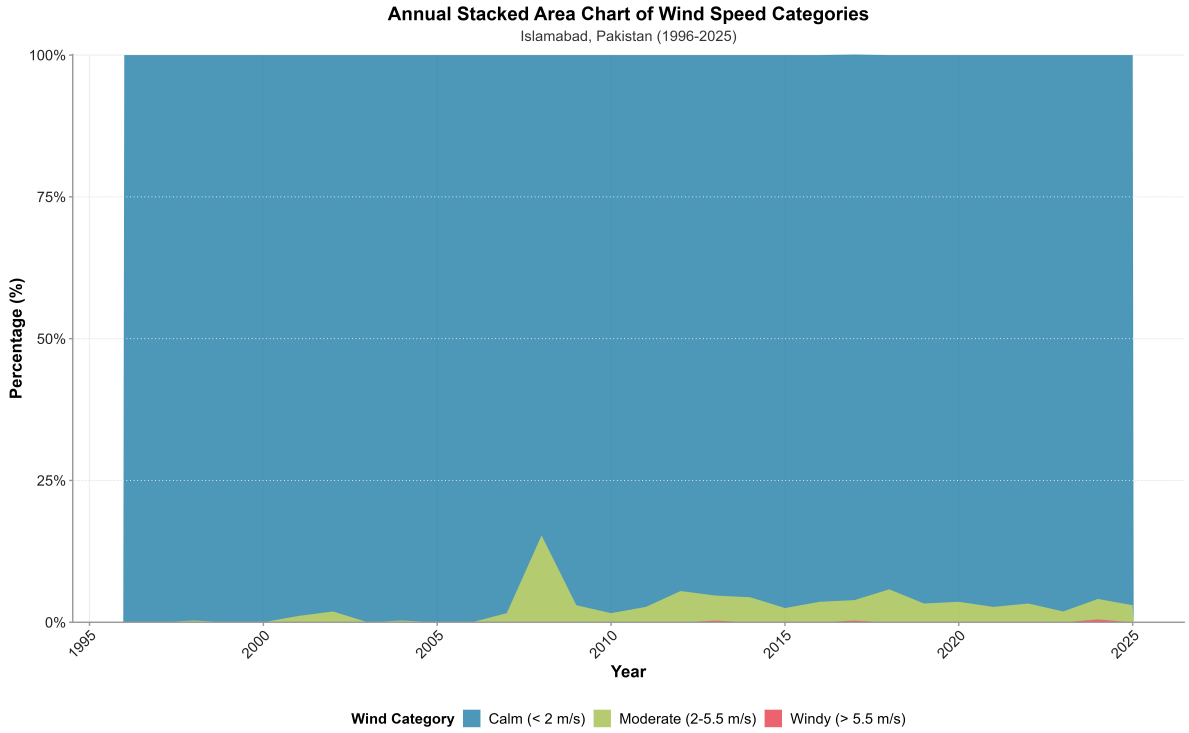


Figure 3.13 Stacked area chart of wind speed indices.

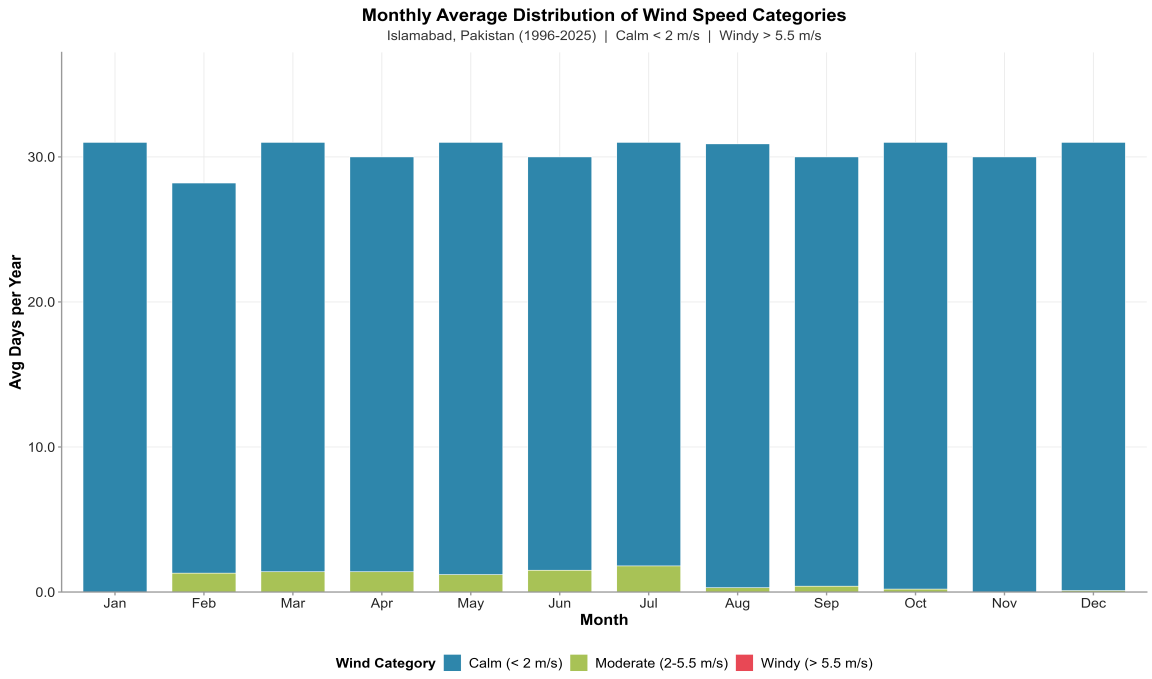


Figure 3.14 Monthly distribution of wind speed indices.

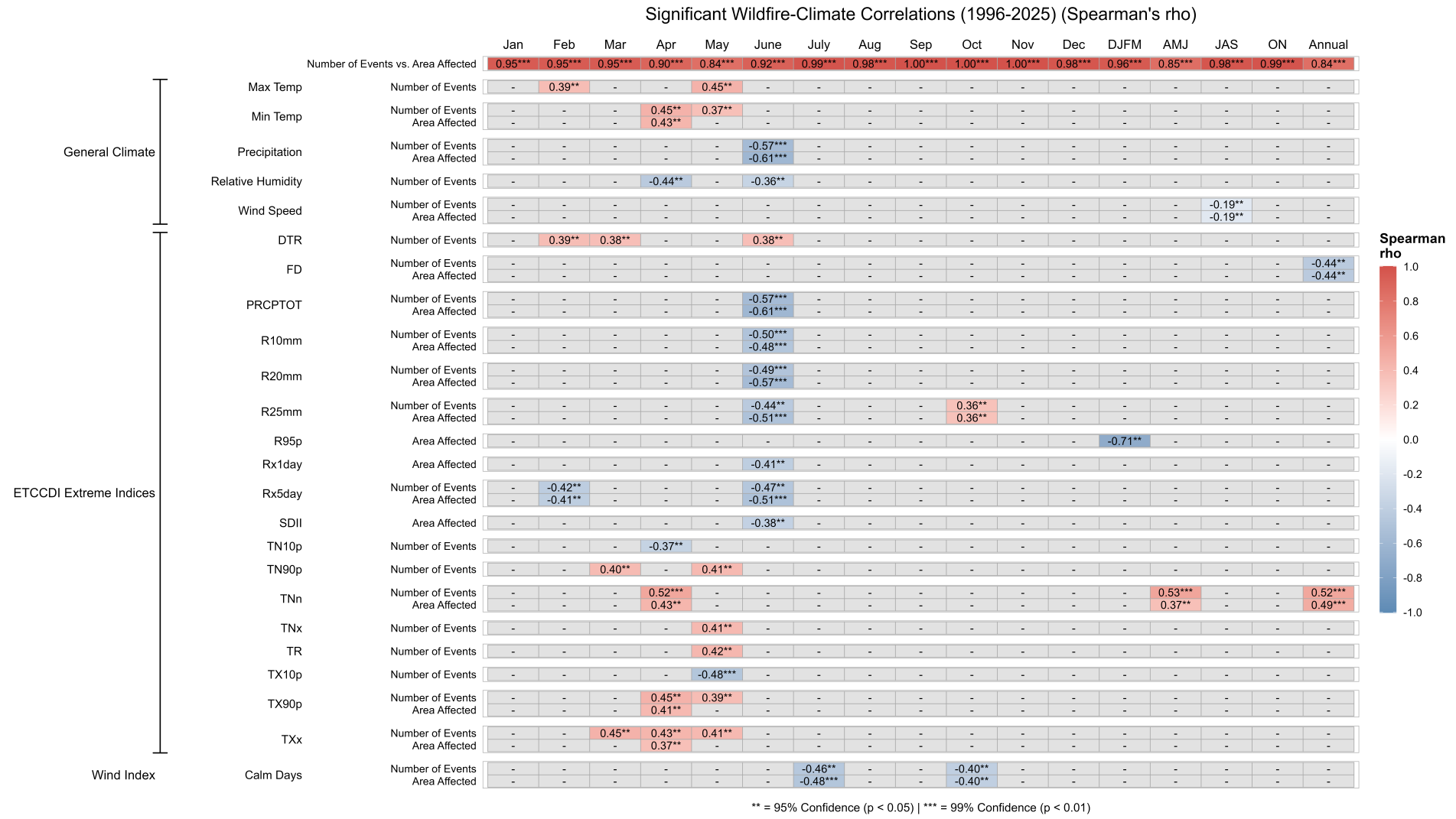
Wind at MHNP stayed calm almost every day, every month, for all 30 years. For Islamabad, and Margalla Hills, no study was found on this exact wind pattern, therefore the research from nearby mountains was used. In the Himalayan valleys of Nepal, Mikkola et al., (2023) determined that near-surface winds are weak and strongly influenced by local heating and cooling, but that differences among valleys are correlated with valley shape. The situation in the MHNP is similar, in that the local topography is hilly, and a similar pattern of calm baseline may be explained by the same relationship, which, however, was not tested by Mikkola et al., (2023) directly.

The pattern is calm and is important for fire risk. NDMA (2025) establishes 25 mph as the threshold wind speed for increasing fire hazard across the country, which is much higher than both of the thresholds used in this study. By that mark, MHNP stayed mostly clear of wind-driven fire risk for most of the 30 years, and its only windy days fell in 2024 and 2025, the same years NDMA flags Margalla Hills as at risk from wind. Older fire-behaviour studies show a similar cutoff: Cheney et al., (1998) found fires only spread steadily once wind passes about 1.4 m/s, close to this study's calm limit. Those studies used grass and shrub fuel, not MHNP's pine forest, so the figure is a rough guide, not an exact match. Even so, both point the same way: for most of the record, MHNP was not wind-ready for fire spread, which is why the rare windy days stand out.

3.9 Correlation Results

This subsection presents the statistical correlation between baseline variables, extreme climate indices, and wildfire metrics categorized by annual, seasonal and monthly timescales.

Table 3.8 Significant climate-wildfire correlation (1996-2025)



3.9.1 Correlation between temperature extremes and wildfire Activity

The lowest daily minimum temperature (TNn) had the highest positive correlation with fire events during the spring and early summer season (April to June) (rho = 0.53, p value < 0.01). The strongest inverse relationship also occurred within this period, showing that a reduction in cool days during May (TX10p) was highly correlated with an increase in fire events (rho = -0.48, p value < 0.01). While maximum temperatures, warm day indices, and other extreme metrics exhibited numerous positive relationships with fire activity from February through May, only the strongest associations are reported here; all other significant monthly and seasonal correlation coefficients are provided in Table 3.8. The diurnal temperature range (DTR) had a strong positive association to the fire events in June during the summer season.

The lowest daily minimum temperature (TNn) had a strong, positive correlation with the count of fire events and total burned area on an annual scale (rho 0.52, p value < 0.01 and rho 0.49, p value < 0.01, respectively). A study of the annual cold extremes showed that the frequency of frost days (FD) reduced as there was a significant rise in both the counts of fire events and total burned area per year (rho = -0.44, p value < 0.05). These quantitative results establish the statistical associations between seasonal temperature extremes and historical wildfire patterns in the study area.

Fire activity was linked more to the absence of cold nights than to daytime heat by itself. TNn is the coldest night of a period, so a high value means even the coldest night stayed fairly warm, and such years had more fires and a larger burned area. The negative links with cool days in May and with yearly frost days point the same way, since both values fall as the cold end of the temperature range weakens. The link is steady for the cold indices at the annual scale and in the pre-monsoon and early summer months, though the coefficients are moderate and the warm indices were linked with fire activity only between February and May.

Earlier work from the same area agrees in part. Tariq et al., (2021) found maximum temperature to be one of the main variables controlling fire severity and burned area in Margalla Hills, which fits the positive links found here for TXx and TX90p in March, April and May. Mina et al., (2023), working in Dehradun district under a similar subtropical fire season, used Kendall's tau and obtained significant positive coefficients

for maximum temperature, average temperature and diurnal range, while minimum temperature was positive but not significant. This difference may arise because TNn uses only the lowest value of the period, whereas they used the monthly average of daily minimum temperature, in which the coldest nights get smoothed out. They also linked their weak result to monthly data and suggested daily data instead. The positive correlation between DTR and June fires matches their result directly.

The probable cause of the cold-index result is night time fuel drying. Leaf litter and dry grass dry out during the day and pick up moisture at night when the air cools and dew forms, so if the coldest nights are warm, this moisture is not fully recovered and the litter will begin the following afternoon drier. Balch et al., (2022) tested this direction globally using satellite fire detections with hourly climate data and found that warmer and drier nights came first and night-time fire intensity rose as a result. The mechanism is used here only to explain why mild nights leave fuels readier to burn, not to claim that fires raised the night temperature, since TNn comes from a 30-year record for the whole park while fires are short and cover small patches. Fewer frost days act through the same process over a longer period by curing the grass layer earlier, while a wide June diurnal range means clear skies, strong sunshine and dry pre-monsoon air, which give the lowest fuel moisture of the year.

These indices also represent some of the strongest changes in this region; Saleem et al., (2021) reported higher warm nights and days and fewer cold nights and days across Pakistan, with the greatest warming occurring in spring. The useful part is the timing, since the annual links of TNn and FD suggest the cold season already carries information about the coming fire season, while the May and June links of TX10p and DTR belong to the season itself. Three limits apply. Spearman correlation shows only that two sets of values moved together, not that one caused the other. The cold indices are not independent, since TNn, FD and TN10p describe the same lower end of the range and should be read as one signal. Most fires in the park are also started by people (Tariq et al., 2022), so these indices show how ready the fuel was to burn, not how often an ignition source was present.

3.9.2 Correlation of precipitation extremes and wildfire activity

The correlations between precipitation, extreme precipitation indices and wildfire activity are provided in this subsection.

The days of very wet conditions (R95p) had the highest negative correlation with wildfire activity, during the long winter months (DJFM). Higher R95p values were associated with a smaller total area burned (rho = -0.71, p-value < 0.05). In February, the maximum 5-day precipitation (Rx5day) was also negatively correlated with both the number of fire events (rho = -0.42, p-value < 0.05) and the total area burned (rho = -0.41, p-value < 0.05). In summer, the strongest correlations were observed in June. Both total precipitation and total wet-day precipitation (PRCPTOT) were negatively correlated with the number of fire events (rho = -0.57, p-value < 0.01) and the total area burned (rho = -0.61, p-value < 0.01). Lower values of other heavy rainfall indices, including R10mm, R20mm, and Rx5day, were also significantly correlated with increased wildfire activity during June.

In contrast, the autumn pattern was different. In October, the number of extremely heavy rainfall days (R25mm) showed a positive correlation with both fire events and the total area burned (rho = 0.36, p-value < 0.05). The main correlations are presented above, while the remaining significant correlations for precipitation intensity and duration indices are listed in Table 3.8. Overall, these results indicate that historical wildfire activity was significantly correlated with changes in precipitation before and during the fire season.

There were significant decreases in burned area when more very wet days (R95p) occurred in winter and when more wet-day rain (PRCPTOT) occurred in June, indicating that increased amounts of rain before and during the fire season prevented fuels from becoming easily combustible. This backs the second objective, since it shows precipitation extremes genuinely shape fire outcomes at MHNP rather than sitting in the background. This is the same link throughout the broader Himalayan region. Both Ghanim et al., (2023) and Zafar et al., (2024) found a decreasing trend in wet-day rainfall and very-wet-day counts in the northern highlands and Himalayan region of Pakistan during the last three decades, which means the moisture that has been protecting MHNP from bigger burns may keep shrinking. In Uttarakhand, a run of low winter rain preceded an early and unusually long 2016 fire season by drying out soil and forest floor litter

(Mina et al., 2023), and in Nepal a comparable post-monsoon rainfall deficit came right before a record 2021 wildfire season (Pokharel et al., 2023). Both cases point to the same mechanism seen here: less rain in the months feeding into fire season leaves drier fuel on the ground, and fire follows.

October broke this pattern, since more extremely heavy rain days (R25mm) came with more fire, not less. Joshi et al., (2024), working in Nepal's Chure hills, found this same two-sided relationship: low-rainfall areas burn more because fuel stays dry, but high-rainfall areas also burn more over time because the extra rain grows more grass and undergrowth that later dries into fuel. That fits MHNP's October result better than a simple "more rain, less fire" rule; the heavy rain may be feeding vegetation that dries and burns once the season turns dry**.** It is sensible to use extreme indices rather than simple totals because a study of Chinese wildfires showed that extreme precipitation indices were a better explanatory variable than total precipitation for fire activity in some regions (Xing et al., 2023).

This split result matters because a single year-round precipitation-fire rule would miss the risk building through autumn. Therefore, the October relationship in MHNP may represent a lagged influence of precipitation on fuel conditions rather than a direct effect of rainfall during the same period. One limit worth flagging: this correlation cannot show whether the fuel-growth effect plays out within the same season or carries over from months earlier, since testing that would need vegetation or fuel-load data this analysis did not collect.

3.9.3 Correlation between RH, heat index and wildfire activity

This subsection presents the correlations between monthly, seasonal, and annual relative humidity, heat index and wildfire activity. Only statistically significant correlations are described here, while the complete results are provided in Table 3.8. No significant results were found for heat index correlation. Higher relative humidity during spring and early summer was significantly negatively correlated with the number of wildfire events. The relative humidity was negatively correlated with fire events (rho = -0.44, p-value < 0.05) in April. A similar negative correlation was observed in June (rho = -0.36, p-value < 0.05). These results indicate that higher atmospheric moisture during the pre-monsoon period was associated with fewer wildfire events.

Relative humidity showed a negative influence on wildfire activity, but only during April and June of the pre-monsoon period. Higher humidity was associated with fewer fire events, suggesting that atmospheric moisture mainly affects ignition success and early fire starts rather than the burned area. This is likely because humid conditions slow the drying of litter and grass fuels in MHNP. Abbas et al., (2025) found temperature and relative humidity as the primary fire drivers in the Gilgit-Baltistan region, whereas Muhammad et al., (2025) reported that moisture availability is a major factor that decreases fire risk in subtropical forests. Mina et al., (2023) also observed a negative humidity–fire relationship in the central Himalaya, although it was not significant at broader scales. The moderate correlations in MHNP may reflect the influence of human ignition sources, where climate conditions mainly affect fire development after ignition (Tariq et al., 2021; Tariq et al., 2022).

It is noteworthy that there is no significant relationship with the heat index, which means that human heat stress indicators might not be representative of wildfire conditions. Since the heat index increases with both temperature and humidity, it does not directly reflect fuel drying, where lower humidity is generally more important. This agrees with Khadke et al., (2026), who found that humidity reductions increased fire spread more strongly than temperature changes alone, while Singh et al., (2024) reported that pre-monsoon moisture conditions reduced fire occurrence in Himalayan forests. Therefore, the results support the importance of humidity as a wildfire-related variable but also show that not all temperature–humidity combinations are equally relevant for fire processes. The interpretation remains limited because monthly humidity averages may not capture short-duration humidity drops that control fuel drying, and Spearman correlation cannot detect possible threshold responses.

3.9.4 Correlation between wind extremes and wildfire activity

The number of calm days had the highest negative correlation with wildfire activity, especially in July and October. In July, a rise in calm days was found to be highly negatively correlated with the number of fire events (rho = -0.46, p-value < 0.05) and total area burned (rho = -0.48, p-value < 0.01). A similar pattern was observed in October, when an increase in calm days was negatively correlated with both fire events and the total area burned (rho = -0.40, p-value < 0.05 for both variables). Average wind speed during the monsoon season (JAS) also showed a weak but significant negative correlation with

wildfire activity. Higher seasonal wind speeds were associated with fewer fire events (rho = -0.19, p-value < 0.05) and a smaller total area burned (rho = -0.19, p-value < 0.05). Overall, the findings indicate a significant association between wind conditions and historical wildfire activity, particularly for the number of calm days.

The calm day results indicate that wind did not affect the fire initiation but rather the spread of wildfire in MHNP. In July and October, fewer calm days went with more fires and a larger burned area, and the fact that both measures reacted points to a simple physical cause. The air stirs fuel in front of the fire and brings oxygen to the flame front, which causes flames to spread into the fuel ahead, allowing a fire to burn slowly, remain small, and be easier to control when the wind is not blowing. This reading is supported by the timing of the event: July is during the monsoon season, and October is immediately following, when there is still moisture in the litter and only persistent air movement can dry it and spread fire. The association with wind was with the calm end of the wind range, not with average wind.

During the monsoon season, the opposite is true, with stronger low-level winds along the foothills of the Himalayas mainly transporting moisture, which contributes to the variability in precipitation in the upper Indus basin, accounting for more than 80% (Baudouin et al., 2020). So, wind speed in July–September is more indicative of the strength of the monsoon, and not directly of fire activity. Previous Pakistani research on fire counts showed that the wind had minimal effect, and was attributed primarily to fire spread, not ignition (Abbas et al., 2025; Muhammad et al., 2025). The calm day index is a monthly number that showed that there is a relationship between the calm day index and the average wind speed that wind speed may not be able to capture, but there are limitations as it only captures the number of days when the wind is not present, not the intensity of the wind on fire days. Trends were tested and the wind record was homogenised, while empirical quantile mapping can impact tested trends (Cannon et al., 2015).

CONCLUSION

In the time period of 1996 to 2025, the climate of Margalla Hills National Park was found to be falling below the regional warming trend observed in the Islamabad and Potohar Plateau region, with a cooling trend and an increase in moisture in the park. Similarly, fire activity decreased on yearly, seasonal and monthly time scales in both number of events and burned area. This difference in temperature suggests that moisture in the fuel is the main factor that dictates fire behavior in the park, not regional temperature.

The climate trends show a park that is different from its environment. Maximum and minimum temperatures decreased with slope −0.0279°C/yr and −0.027°C/yr respectively, primarily in the later years, and due to cooler nights during pre-Monsoon and winter. The changes were not uniform across the country – the coldest maximum temperatures went up, while the tropical and warm-night ones went down. Rainfall and humidity (ITA slope of humidity: +0.1651 %/yr) increased in the later years, but not in a regular increasing fashion, but rather towards the pre-monsoon and monsoon months. There was no apparent annual trend for heat index or wind speed and calm wind days were relatively common. The cooling effect of the park's dense vegetation, wet soil, and cloud cover is the most likely explanation for this consistent cooling and moistening, and the principal thesis is that this cooling effect is due to the park's vegetation. The same downward trend was observed for wildfire activity during these years. Fire counts and total burned area both decreased dramatically, and burned area decreased at a greater rate, so that fires were smaller, not just less frequent. Fires in the spring were less on all measures and in the summer there were more fires but most were small. The one exception is a substantial rise in fire frequency and burned area in July, August and September, which has been occurring in recent years and is best viewed as an emerging trend, rather than a stable pattern.

The lowest temperature end of the spectrum had the best climate–fire relationships having significant Spearman’s rho value of 0.52 and 0.49 for number of fire events and area affected respectively, with minimum night-time temperature and frost days being the most consistent variables annually and pre-monsoon and early summer. This is probably due to the incomplete overnight recovery of leaf litter moisture, causing fuel to be more flammable the next afternoon. Burned area was lower before and during the fire season

due to higher rainfall, except for October when higher rainfall was correlated with higher burned area later in the season, possibly because of the increased vegetation growth that was followed by drier conditions. Increased humidity during the pre-monsoon season decreased the number of ignitions and lower wind speed decreased the fire activity during the monsoon season, but the heat index did not show any relationship with fire and was not a good indicator of fuel dryness. Climate influences fire in different ways at different time scales: cold-season temperature signals the annual fire risk while moisture and wind influence fire season by season. A key limitation is that single-station data and reconstructed fire records from multiple sources may not reflect conditions across the entire park**.** The 30-year climate-fire record for Margalla Hills is presented in this thesis, which reveals that dryness of fuel, rather than ignition, is the primary driver of fire. Recent increase in late-summer fires and monitoring of cold-season temperature and pre-season moisture as early warnings should be considered as protective moisture may not persist. These findings provide park managers with a clear climate-based basis for identifying high-risk fire seasons**.**

RECOMMENDATIONS

1. Use extremes of cold season and pre-season moisture to flag high risk years and adjust risk. Ensure that crews, equipment and watchtowers are in place before the pre-monsoon and late-summer peak, not after they start.
2. Most fires are man-made, so controlling access along roads, trails and settlement edges is the best way to prevent fires; climate dictates spread, not ignition.
3. Focus on response capability on rare, non-calm days, particularly July and October when wind allows fire to develop into larger burns.
4. Do future research in creating e a locally calibrated Pakistani fire-weather index, not a Canadian, American or Australian system which could not be used here, and provide real-time feeds for operational risk projections.
5. Keep one central, up-to-date inventory of MHNP fires, rather than having the records distributed among IWMB, CDA, studies and personnel.
6. Improve monitoring: maintain complete station metadata for identification of artificial breaks, and increase the number of stations with daily records to better capture short-term, localized fire-risk events.

REFERENCES

Abatzoglou, J. T., & Williams, A. P. (2016). Impact of anthropogenic climate change on wildfire across western US forests. *Proceedings of the National Academy of Sciences*, *113*(42), 11770–11775

Abbas, A., Ullah, S., Ullah, W., Zhao, C., Karim, A., Waseem, M., Bhatti, A. S., Ali, G., Jan, M. A., & Ali, A. (2023). Characteristics of winter precipitation over Pakistan and possible causes during 1981–2018. *Water*, *15*(13), 2420

Abbas, K., Souane, A. A., Ahmad, H., Suita, F., Shu, Z., Huang, H., & Wang, F. (2025). Correlating fire incidents with meteorological variables in dry temperate forest. *Forests*, *16*(1), Article 122

Abbas, S., Waseem, M., Yaseen, M., Latif, Y., Leta, M. K., Khan, T. H., & Muhammad, S. (2023). Spatial-temporal seasonal variability of extreme precipitation under warming climate in Pakistan. *Atmosphere*, *14*(2), 210

Abdi, H. (2010). Coefficient of variation. In N. J. Salkind (Ed.), *Encyclopedia of research design* (pp. 169–171). Sage

Abubakar, S. M. (2018, June 15). Who started the fire? *The Friday Times*. https://www.thefridaytimes.com/15-Jun-2018/who-started-the-fire

Aguilar, E., Auer, I., Brunet, M., Peterson, T. C., & Wieringa, J. (2003). *Guidance on metadata and homogenization*. Expert Team on Climate Change Detection and Indices (ETCCDI)

Ahmad, I., Tang, D., Wang, T., Wang, M., Wagan, B., & Iqbal, H. (2015). Precipitation trends over time using Mann–Kendall and Spearman's rho tests in Swat River Basin, Pakistan. *Advances in Meteorology*, *2015*, Article 431860

Ahmad, K., Banerjee, A., Rashid, W., Xia, Z., Karim, S., & Asif, M. (2023). Assessment of long-term rainfall variability and trends using observed and satellite data in central Punjab, Pakistan. *Atmosphere*, *14*(1), 60

Akaike, H. (1974). A new look at the statistical model identification. *IEEE Transactions on Automatic Control*, *19*(6), 716–723

Akoglu, H. (2018). User's guide to correlation coefficients. *Turkish Journal of Emergency Medicine*, *18*(3), 91–93

Alam, M. A., Emura, K., Farnham, C., & Yuan, J. (2018). Best-fit probability distributions and return periods for maximum monthly rainfall in Bangladesh. *Climate*, *6*(1), 9

Alexander, L., & Herold, N. (2016). *ClimPACT2: Indices and software*. Commission for Climatology Expert Team on Sector-Specific Climate Indices (ET-SCI)

Alexander, L. V., Zhang, X., Peterson, T. C., Caesar, J., Gleason, B., Klein Tank, A. M. G., Haylock, M., Collins, D., Trewin, B., Rahimzadeh, F., Tagipour, A., Rupa Kumar, K., Revadekar, J., Griffiths, G., Vincent, L., Stephenson, D. B., Burn, J., ... Vazquez-Aguirre, J. L. (2006). Global observed changes in daily climate extremes of temperature and precipitation. *Journal of Geophysical Research: Atmospheres*, *111*(D5), D05109

Alifujiang, Y., Abuduwaili, J., Maihemuti, B., Emin, B., & Groll, M. (2020). Innovative trend analysis of precipitation in the Lake Issyk-Kul Basin, Kyrgyzstan. *Atmosphere*, *11*(4), 332

Aryadoust, V., & Jia, Y. (2026). Univariate normality checking practices in L2 research: An AI-assisted systematic review. *Studies in Second Language Acquisition*, *48*(2), 535–570

Aslam, I., & Yasmeen, R. (2021). Vertebrate diversity at Margalla Hills National Park, Pakistan. *Arxius de Miscel·lània Zoològica*, *19*, 237–247

Awasthi, A., Dutta, A., Pathak, V. V., Kaur, S., Kumar, V., & Lodh, A. (2026). Assessing climate change impacts on heat waves and heat index: A case study of Uttar Pradesh, India. *Frontiers in Climate*, *8*, Article 1679941

Bar, S., Parida, B. R., Roberts, G., Pandey, A. C., Acharya, P., & Dash, J. (2021). Spatio-temporal characterization of landscape fire in relation to anthropogenic activity and

climatic variability over the Western Himalaya, India. *GIScience & Remote Sensing*, *58*(2), 281–299

Batool, R., & Javaid, K. (2018). Spatio-temporal assessment of Margalla Hills forest by using Landsat imagery for year 2000 and 2018. *The International Archives of the Photogrammetry, Remote Sensing and Spatial Information Sciences*, *XLII-3*, 69–76

Baudouin, J.-P., Herzog, M., & Petrie, C. A. (2020). Contribution of cross-barrier moisture transport to precipitation in the upper Indus River basin. *Monthly Weather Review*, *148*(7), 2801–2818

Bera, A. K. (1981). Efficient tests for normality, homoscedasticity and serial independence of regression residuals: Monte Carlo evidence. *Economics Letters*, *7*(4), 313–318

Berlinger, M., Kolling, S., & Schneider, J. (2021). A generalized Anderson–Darling test for the goodness-of-fit evaluation of the fracture strain distribution of acrylic glass. *Glass Structures & Engineering*, *6*(2), 195–208

Bhatti, A. S., Wang, G., Ullah, W., Ullah, S., Fiifi Tawia Hagan, D., Kwesi Nooni, I., et al., (2020). Trend in extreme precipitation indices based on long term in situ precipitation records over Pakistan. *Water*, *12*(3), 797

Bowman, D. M. J. S., Balch, J. K., Artaxo, P., Bond, W. J., Carlson, J. M., Cochrane, M. A., D'Antonio, C. M., DeFries, R. S., Doyle, J. C., Harrison, S. P., Johnston, F. H., Keeley, J. E., Krawchuk, M. A., Kull, C. A., Marston, J. B., Moritz, M. A., Prentice, I. C., Roos, C. I., Scott, A. C., ... Pyne, S. J. (2009). Fire in the Earth system. *Science*, *324*(5926), 481–484

Cannon, A. J., Sobie, S. R., & Murdock, T. Q. (2015). Bias correction of GCM precipitation by quantile mapping: How well do methods preserve changes in quantiles and extremes? *Journal of Climate*, *28*(17), 6938–6959

Caussinus, H., & Mestre, O. (2004). Detection and correction of artificial shifts in climate series. *Journal of the Royal Statistical Society: Series C (Applied Statistics)*, *53*(3), 405–425

Chandio, S. H., Sanjrani, M. A., Bhutto, S. U. A., Sanjrani, M. A., & Khaskheli, N. A. (2019). Impact of natural events and anthropogenic activities on the biodiversity of Margallah Hills National Park Islamabad (MHNP). *North American Academic Research*, *2*(3), 20–32.

Charak, A. S., Kumar, R., Verma, A. K., Kumar, B. R., & Kumar, S. (2026). Bioclimatic, anthropogenic and topographical drivers of forest fire dynamics in the Western Himalaya. *Trees, Forests and People*, *25*, 101258

Chen, J., Saunders, K., & Whan, K. (2021). Quality control and bias adjustment of crowdsourced wind speed observations. *Quarterly Journal of the Royal Meteorological Society*, *147*(740), 3647–3664

Cheney, N. P., Gould, J. S., & Catchpole, W. R. (1998). Prediction of fire spread in grasslands. *International Journal of Wildland Fire*, *8*(1), 1–13

Collaud Coen, M., Andrews, E., Bigi, A., Martucci, G., Romanens, G., Vogt, F. P. A., & Vuilleumier, L. (2020). Effects of the prewhitening method, the time granularity, and the time segmentation on the Mann–Kendall trend detection and the associated Sen's slope. *Atmospheric Measurement Techniques*, *13*(12), 6945–6964

Cooley, A. K., & Chang, H. (2021). Detecting change in precipitation indices using observed (1977–2016) and modeled future climate data in Portland, Oregon, USA. *Journal of Water and Climate Change*, *12*(4), 1135–1153

de Winter, J. C. F., Gosling, S. D., & Potter, J. (2024). Comparing the Pearson and Spearman correlation coefficients across distributions and sample sizes: A tutorial using simulations and empirical data. *Psychological Methods*. Advance online publication

Delignette-Muller, M. L., & Dutang, C. (2015). fitdistrplus: An R package for fitting distributions. *Journal of Statistical Software*, *64*(4), 1–34

Della-Marta, P. M., & Wanner, H. (2006). A method of homogenizing the extremes and mean of daily temperature measurements. *Journal of Climate*, *19*(17), 4179–4197

Diaconescu, E., Sankare, H., Chow, K., Murdock, T. Q., & Cannon, A. J. (2023). A short note on the use of daily climate data to calculate Humidex heat-stress indices. *International Journal of Climatology*, *43*(2), 837–849

Din, R. U., Hussain, S., Khan, A. A., Anjum, M. N., Rahman, A. T. M. S., & Ullah, S. (2026). Assessing nonstationary hydroclimatic impacts on streamflow in the Soan River Basin, Pakistan, using Mann-Kendall test and artificial neural network technique. *Hydrology*, *13*(4), Article 106

Domonkos, P. (2021). Efficiency of time series homogenization: Method comparison with 12 monthly temperature test datasets. *Journal of Climate*, *34*(8), 3049–3063

Domonkos, P. (2024). Relative homogenization of climatic time series. *Atmosphere*, *15*(8), 957

Domonkos, P., & Joelsson, L. M. T. (2024). ANOVA (Benova) correction in relative homogenization: Why it is indispensable. *International Journal of Climatology*, *44*(12), 4515–4528

Dunn, R. J. H., Donat, M. G., Alexander, L. V., et al., (2022). Comparing extremes indices in recent observational and reanalysis products. *Frontiers in Climate*, 4, 989505

Dunn, R. J. H., Herold, N., Alexander, L. V., Donat, M. G., Allan, R., Bador, M., Contractor, S., Lewis, S. C., Perkins-Kirkpatrick, S. E., Shah, H. L., Trewin, B., Zhang, X., & Fischer, E. M. (2024). Observed global changes in sector-relevant climate extremes indices an extension to HadEX3. *Earth and Space Science*, 11(3), e2023EA003279

Elhassnaoui, I. (n.d.). Statistical descriptive analysis of three climate variables: Precipitation, temperature and relative humidity. Study cases (Innaouene watershed; Morocco). *E3S Web of Conferences*

Emerson, R. W. (2023). Mann–Whitney U test and t-test. *Journal of Visual Impairment & Blindness*, *117*(1), 99–100

European Climate Assessment & Dataset. (2025). *Algorithm Theoretical Basis Document (ATBD)* (Version 11). Royal Netherlands Meteorological Institute (KNMI)

Flannigan, M. D., Krawchuk, M. A., de Groot, W. J., Wotton, B. M., & Gowman, L. M. (2009). Implications of changing climate for global wildland fire. *International Journal of Wildland Fire*, *18*(5), 483–507

Ghanim, A. A. J., Anjum, M. N., Rasool, G., Saifullah, Irfan, M., Rahman, S., Mursal, S. N. F., & Niazi, U. M. (2023). Assessing spatiotemporal trends of total and extreme precipitation in a subtropical highland region: A climate perspective. *PLOS ONE*, *18*(8), e0289570

Giglio, L., Boschetti, L., Roy, D. P., Humber, M. L., & Justice, C. O. (2018). The Collection 6 MODIS burned area mapping algorithm and product. *Remote Sensing of Environment*, *217*, 72–85

Gocic, M., & Trajkovic, S. (2013). Analysis of changes in meteorological variables using Mann-Kendall and Sen's slope estimator statistical tests in Serbia. *Global and Planetary Change*, *100*, 172–182

Goss, M., Swain, D. L., Abatzoglou, J. T., Sarhadi, A., Kolden, C. A., Williams, A. P., & Diffenbaugh, N. S. (2020). Climate change is increasing the likelihood of extreme autumn wildfire conditions across California. *Environmental Research Letters*, *15*(9), 094016

Government of Pakistan. (2020). *Pakistan environmental year book 2019–20*. Ministry of Climate Change.

Government of Pakistan. (2022). *Pakistan environmental year book 2022–23*. Ministry of Climate Change & Environmental Coordination.

Gul, S., Ren, J., Xiong, N., & Khan, M. A. (2021). Design and analysis of statistical probability distribution and non-parametric trend analysis for reference evapotranspiration. *PeerJ*, *9*, e11597

Hair, J. F., Black, W. C., Babin, B. J., & Anderson, R. E. (2010). *Multivariate data analysis: A global perspective*. Pearson Prentice Hall.

Hamadeh, N., Karouni, A., Daya, B., & Chauvet, P. (2017). Using correlative data analysis to develop weather index that estimates the risk of forest fires in Lebanon &

Mediterranean: Assessment versus prevalent meteorological indices. *Case Studies in Fire Safety*, *7*, 8–22

Hamed, K. H., & Rao, A. R. (1998). A modified Mann-Kendall trend test for autocorrelated data. *Journal of Hydrology*, *204*(1–4), 182–196

Haseeb, F., Ali, S., Ahmed, N., Alarifi, N., & Youssef, Y. M. (2025). Comprehensive probabilistic analysis and practical implications of rainfall distribution in Pakistan. *Atmosphere*, *16*(2), 122

Hunt, K. M. R., Baudouin, J.-P., Turner, A. G., Dimri, A. P., Jeelani, G., Pooja, Chattopadhyay, R., Cannon, F., Arulalan, T., Shekhar, M. S., Sabin, T. P., & Palazzi, E. (2025). Western disturbances and climate variability: A review of recent developments. *Weather and Climate Dynamics*, *6*(1), 43–112

Intergovernmental Panel on Climate Change. (2021). Summary for policymakers. In V. Masson-Delmotte et al., (Eds.), *Climate change 2021: The physical science basis. Contribution of Working Group I to the Sixth Assessment Report of the Intergovernmental Panel on Climate Change*. Cambridge University Press

Jolly, W. M., Cochrane, M. A., Freeborn, P. H., Holden, Z. A., Brown, T. J., Williamson, G. J., & Bowman, D. M. J. S. (2015). Climate-induced variations in global wildfire danger from 1979 to 2013. *Nature Communications*, *6*, 7537

Jones, M. W., Abatzoglou, J. T., Veraverbeke, S., Andela, N., Lasslop, G., Forkel, M., Smith, A. J. P., Burton, C., Betts, R. A., van der Werf, G. R., Sitch, S., Canadell, J. G., Santín, C., Kolden, C., Doerr, S. H., & Le Quéré, C. (2022). Global and regional trends and drivers of fire under climate change. *Reviews of Geophysics*, *60*(3), e2020RG000726

Joshi, K. P., Adhikari, G., Bhattarai, D., Adhikari, A., & Lamichanne, S. (2024). Forest fire vulnerability in Nepal's Chure region: Investigating the influencing factors using generalized linear model. *Heliyon*, *10*(7), e28525

Junaidi, I., & Shahid, J. (2021, May 30). Around 90pc fires in Margalla Hills work of villagers: IWMB. *Dawn*. https://www.dawn.com/news/1626403

Kalashnikov, D. A., Abatzoglou, J. T., Williams, E. L., Yin, C., Gurazada, M., Kumar, M., Thomas, A. P., & Ebiendele, P. E. (2026). Heatwaves enable wildfire activity in the western United States. *Science Advances*, *12*(25), eaea1277

Kartal, V., Nones, M., Topcu, E., & Ariman, S. (2024). Comparison of different techniques in determining groundwater levels trends in Türkiye. *Hydrological Processes*, *38*(8), e15244

Khadke, L., Mukherjee, S., & Ghosh, S. (2026). Simulating forest fires in Uttarakhand: Uncovering the role of meteorological variables. *Journal of Earth System Science*, *135*, Article 18

Khalid, A., Dahlan, N. D., Shahidan, M. F., Ahmad, K. A. B., & Abas, M. F. B. (2025). Outdoor standard evaluation of heat index and climate parameters for Lahore, Pakistan. *Sustainable Cities and Society: Advances*, *2*(1)

Khalid, N., Ahmad, S. S., Erum, S., & Butt, A. (2015). Monitoring forest cover change of Margalla Hills over a period of two decades (1992–2011): A spatiotemporal perspective. *Journal of Ecosystem & Ecography*, *6*(1), 1–8.

Khan, F., Ali, S., Mayer, C., Ullah, H., & Muhammad, S. (2022). Climate change and spatio-temporal trend analysis of climate extremes in the homogeneous climatic zones of Pakistan during 1962–2019. *PLOS ONE*, *17*(7), e0271626

Khan, M. A., & Gadiwala, M. S. (2013). A study of drought over Sindh (Pakistan) using standardized precipitation index (SPI) 1951–2010. *Pakistan Journal of Meteorology*, *10*(19), 25–36.

Khan, N., Shahid, S., Ismail, T., Ahmed, K., & Nawaz, N. (2019). Trends in heat wave related indices in Pakistan. *Stochastic Environmental Research and Risk Assessment*, *33*(1), 287–302

Khan, R., Alwabel, A. S. A., Ahmad, A., Helal, M. M., Rafiq, M., Rahman, W. U., Mehmood, A., Khalil, M. N., Ahmad, R., & Gurmani, A. R. (2026). Assessment of climatic parameter variation and its impact on sustainable agriculture in Dir Upper Pakistan with mitigation and adaptation strategies. *Scientific Reports*, *16*(1), 9576

Klein Tank, A. M. G., Zwiers, F. W., & Zhang, X. (2009). *Guidelines on analysis of extremes in a changing climate in support of informed decisions for adaptation* (WCDMP-No. 72, WMO-TD No. 1500). World Meteorological Organization

Kocsis, T., Kovács-Székely, I., & Anda, A. (2020). Homogeneity tests and non-parametric analyses of tendencies in precipitation time series in Keszthely, Western Hungary. *Theoretical and Applied Climatology*, *139*(3–4), 849–859

Kumar, S., & Kumar, A. (2022). Hotspot and trend analysis of forest fires and its relation to climatic factors in the western Himalayas. *Natural Hazards*, *114*(3), 3529–3544

Lanzante, J. R. (1996). Resistant, robust and non-parametric techniques for the analysis of climate data: Theory and examples, including applications to historical radiosonde station data. *International Journal of Climatology*, *16*(11), 1197–1226

Lee, C., Park, S., & Jeong, J. (2016). Comprehensive comparison of normality tests: Empirical study using many different types of data. *Journal of the Korean Data and Information Science Society*, *27*(5), 1399–1412

Lewis, C. H. M., Little, K., Graham, L. J., Kettridge, N., & Ivison, K. (2024). Diurnal fuel moisture content variations of live and dead Calluna vegetation in a temperate peatland. *Scientific Reports*, *14*(1), Article 4815

Li, M., Shen, Y., Yao, J., Ye, D., Fan, J., & Simmonds, I. (2022). An assessment of observed wind speed and wind power density over China for 1980–2021. *Wind Energy*, *25*(12), 2052–2070.

Lu, Y.-C., & Romps, D. M. (2022). Extending the heat index. *Journal of Applied Meteorology and Climatology*, *61*(10), 1367–1383

Mahmood, R., & Jia, S. (2016). Quality control and homogenization of daily meteorological data in the trans-boundary region of the Jhelum River basin. *Journal of Geographical Sciences*, *26*(12), 1661–1674

Malamud, B. D., Millington, J. D. A., & Perry, G. L. W. (2005). Characterizing wildfire regimes in the United States. *Proceedings of the National Academy of Sciences*, *102*(13), 4694–4699

Malik, A., & Kumar, A. (2020). Spatio-temporal trend analysis of rainfall using parametric and non-parametric tests: Case study in Uttarakhand, India. *Theoretical and Applied Climatology*, *139*(1), 577–595

Mardia, K. V., Kent, J. T., & Taylor, C. C. (2024). *Multivariate analysis*. Academic Press.

Matthews, S. (2014). Dead fuel moisture research: 1991–2012. *International Journal of Wildland Fire*, *23*(1), 78–92

Mauget, S. A. (2003). Multidecadal regime shifts in U.S. streamflow, precipitation, and temperature. *Journal of Climate*, *16*(14), 2360–2374.

Mehmood, K., Anees, S. A., Luo, M., Akram, M., Zubair, M., Khan, K. A., & Khan, W. R. (2024). Assessing Chilgoza Pine (*Pinus gerardiana*) forest fire severity: Remote sensing analysis, correlations, and predictive modeling for enhanced management strategies. *Trees, Forests and People*, *16*, 100521

Menne, M. J., & Williams, C. N., Jr. (2009). Homogenization of temperature series via pairwise comparisons. *Journal of Climate*, *22*(7), 1700–1717

Miandad, M., Ansar, A., Rahman, G., Munawar, S., & Dawood, M. (2025). Spatio-temporal impact of climate variability on crop production of Potohar Region, Pakistan (1990–2017). *Ecological Questions*, *36*(1), 1–25

Mikkola, J., Sinclair, V. A., Bister, M., & Bianchi, F. (2023). Daytime along-valley winds in the Himalayas as simulated by the Weather Research and Forecasting (WRF) model. *Atmospheric Chemistry and Physics*, *23*(2), 821–842

Mina, U., Dimri, A. P., & Farswan, S. (2023). Forest fires and climate attributes interact in central Himalayas: An overview and assessment. *Fire Ecology*, *19*(1), Article 14.

Ministry of Climate Change and Environmental Coordination. (2025). *Climate change: Past and future trends* (Chapter 6). Government of Pakistan

Muhammad, S., Nizami, S. M., Jiang, Q., Mehmood, K., Hussain, M., Anees, S. A., Shahzad, F., & Khan, W. R. (2025). Machine learning-based forest fire vulnerability assessment in subtropical chir pine forests of Pakistan. *Fire Ecology*, *21*(1), Article 72

Nafees, M., Rashid, W., Sultan, H., Khan, N. H., Khurshid, M., Ali, W., & Bohnett, E. (2024). Occurrence, probable causes, and management of forest wildfires in the Northern Highlands of Pakistan. *Environmental Challenges, 15,* Article 100930

National Disaster Management Authority. (2025). *Forest fire guidelines*. Government of Pakistan

National Disaster Management Authority. (2025). *Heatwave guidelines 2025*. National Emergencies Operation Center, NDMA, Pakistan.

National Disaster Management Authority. (2025, May). *Heatwave outlook 2025*. Government of Pakistan

Nerantzaki, S. D., & Papalexiou, S. M. (2022). Assessing extremes in hydroclimatology: A review on probabilistic methods. *Journal of Hydrology*, *605*, 127302

O, S., Hou, X., & Orth, R. (2020). Observational evidence of wildfire-promoting soil moisture anomalies. *Scientific Reports*, *10*, 11008

Ouyang, X., Liao, W., & Luo, M. (2024). Change of probability density distributions of summer temperatures in different climate zones. *Frontiers of Earth Science*, *18*(1), 1–16

Pal, I., & Al-Tabbaa, A. (2011). Assessing seasonal precipitation trends in India using parametric and non-parametric statistical techniques. *Theoretical and Applied Climatology*, *103*(1), 1–11

Pokharel, B., Sharma, S., Stuivenvolt-Allen, J., Wang, S.-Y. S., LaPlante, M., Gillies, R. R., Khanal, S., Wehner, M., Rhoades, A., Hamal, K., Hatchett, B., Liu, W.-Y., Mukherjee, S., & Aryal, D. (2023). Amplified drought trends in Nepal increase the potential for Himalayan wildfires. *Climatic Change*, *176*(2), 17

Pokhrel, S., Thakuri, S., Subedi, C. K., Kunwar, R. M., Sharma, K. P., Chaudhary, R. P., & Ghimire, S. K. (2026). Spatiotemporal impacts of forest fires on mountain vegetation: A case study from Langtang National Park, Nepal Himalaya. *Ecology and Evolution*

Qudratullah, D. (2024, September 3). *Analysis of Islamabad's wildfire fighting capabilities* (ISSRA Insight). Institute for Strategic Studies, Research and Analysis. https://issra.pk/pub/insight/2024/Analysis-of-Islamabads-Wildfire-Fighting-Capabilities/Insight.html

Rafaqat, W., Iqbal, M., Kanwal, R., & Song, W. (2022). Study of driving factors using machine learning to determine the effect of topography, climate, and fuel on wildfire in Pakistan. *Remote Sensing*, *14*(8), 1918

Rahman, M. M., Rahman, M. M., Ahmed, F., & Islam, M. N. (2017). Analysis and prediction of rainfall trends over Bangladesh using Mann–Kendall, Spearman's rho tests and ARIMA model. *Meteorology, Hydrology and Water Management*, *5*(2), 47–56.

Rai, P., Bangelesa, F., Abel, D., Ziegler, K., Huang, J., Schaffhauser, T., Pollinger, F., Disse, M., & Paeth, H. (2024). Extreme precipitation and temperature indices under future climate change in central Asia based on CORDEX-CORE. *Theoretical and Applied Climatology*, *155*(7), 6015–6039

Rais, M., Ahmed, J., Naveed, A., Batool, A., Shahzad, A., Bibi, R., & Sajjad, A. (2021). Field surveys along habitat gradients revealed differences in herpetofauna assemblage in Margalla Hills National Park, Islamabad, Pakistan. *Biodiversity Data Journal*, *9*, e61541

Rais, M., Mahmood, T., Ali, S., et al., (2021). Field surveys along habitat gradients revealed differences in herpetofauna assemblage in Margalla Hills National Park, Islamabad, Pakistan. *Biodiversity Data Journal*, *9*, e62312.

Rashid, A., Ali, M., & Wang, Q. (2026). Long-term trends and variability of air temperature and precipitation across the Potwar Plateau region, northern Pakistan (1982–2022). *AIMS Geosciences*, *12*(3), 628–663

Reinders, J. B., & Muñoz, S. E. (2024). Accounting for hydroclimatic properties in flood frequency analysis procedures. *Hydrology and Earth System Sciences*, *28*, 217–227

Rizvi, F. F., Ahmed, B., Hussain, S., Khan, A., Raza, M., & Shahid, M. (2021). Assessment of climate extremes from historical data (1960–2013) of Soan River Basin in Pakistan. *International Journal of Global Warming*, *25*(1), 1–37

Rothfusz, L. P. (1990). *The heat index "equation" (or, more than you ever wanted to know about heat index)* (Technical Attachment SR 90-23). National Oceanic and Atmospheric Administration, National Weather Service

Sahar, K., Aslam, S., Ali, S., Riaz, A., Murtaza, G., & Mirza, Z. B. (2024). Exploring soil invertebrate responses to forest fires in Margalla Hills National Park (MHNP), Islamabad: An inquiry into survival strategies beneath the ash. *Journal of Environment and Ecology*, *15*(1), 21

Sajjad, S. H., Shahzad, K., Iqbal, T., & Ashraf, N. (2020). Impact of urban evolution on local temperature trends of Rawalpindi and Islamabad. *European Journal of Climate Change*, *2*(2), 33–46

Sarfaraz, S., Arsalan, M. H., & Fatima, H. (2014). Regionalizing the climate of Pakistan using Köppen classification system. *Pakistan Geographical Review*, *69*(2), 111–132

Schroeder, W., Oliva, P., Giglio, L., & Csiszar, I. A. (2014). The new VIIRS 375 m active fire detection data product: Algorithm description and initial assessment. *Remote Sensing of Environment*, *143*, 85–96

Sen, P. K. (1968). Estimates of the regression coefficient based on Kendall's tau. *Journal of the American Statistical Association*, *63*(324), 1379–1389

Şen, Z. (2012). Innovative trend analysis methodology. *Journal of Hydrologic Engineering*, *17*(9), 1042–1046

Şen, Z. (2017). Innovative trend significance test and applications. *Theoretical and Applied Climatology*, *127*(3–4), 939–947

Seneviratne, S. I., Zhang, X., Adnan, M., Badi, W., Dereczynski, C., Di Luca, A., Ghosh, S., Iskandar, I., Kossin, J., Lewis, S., Otto, F., Pinto, I., Satoh, M., Vicente-Serrano, S. M., Wehner, M., & Zhou, B. (2021). Weather and climate extreme events in a changing climate. In V. Masson-Delmotte et al., (Eds.), *Climate change 2021: The*

physical science basis. Contribution of Working Group I to the Sixth Assessment Report of the Intergovernmental Panel on Climate Change (pp. 1513–1766). Cambridge University Press

Shahzad, F., Mehmood, K., Hussain, K., Haidar, I., Anees, S. A., Muhammad, S., Ali, J., Adnan, M., Wang, Z., & Feng, Z. (2024). Comparing machine learning algorithms to predict vegetation fire detections in Pakistan. *Fire Ecology*, *20*(1), Article 57

Shakoor, A., Shah, S. A., Sattar, M. N., Ogunrinde, A. T., Alharbi, R. S., & Rehman, F. u. (2025). Hydroclimate drivers and spatiotemporal dynamics of reference evapotranspiration in a changing climate. *Water*, *17*(17), 2586

Sheoran, R., Dumka, U. C., Tiwari, R. K., & Hooda, R. K. (2024). An improved version of the prewhitening method for trend analysis in the autocorrelated time series. *Atmosphere*, *15*(10), 1159.

Shirazi, S. A., Abbas, S., Shakarullah, K., Yaseen, M., Mazhar, N., Wahla, S. S., & Khurshid, M. (2020). Trends and variability of temperature time series over the Kanshi catchment in the Potohar region of Punjab-Pakistan. *Pakistan Journal of Science*, *72*(3), 241–248.

Sillmann, J., Kharin, V. V., Zhang, X., Zwiers, F. W., & Bronaugh, D. (2013). Climate extremes indices in the CMIP5 multimodel ensemble: Part 1. Model evaluation in the present climate. *Journal of Geophysical Research: Atmospheres*, *118*(4), 1716–1733

Singh, R. D., Gumber, S., Sundriyal, R. C., Ram, J., & Singh, S. P. (2024). Chir pine forest and pre-monsoon drought determine spatial, and temporal patterns of forest fires in Uttarakhand Himalaya. *Tropical Ecology*, *65*(1), 32–42

Šrajbek, M., Đurin, B., Gnjato, S., & Popov, T. (2025). Regional innovative trend analysis of annual and seasonal discharges of rivers in Bosnia and Herzegovina. *Earth*, *6*(2), 30

Swain, D. L., Abatzoglou, J. T., Albano, C. M., Brunner, M., Diffenbaugh, N. S., Kolden, C., Prein, A. F., Singh, D., Skinner, C. B., Swetnam, T. W., & Touma, D. (2025). Increasing hydroclimatic whiplash can amplify wildfire risk in a warming climate. *Global Change Biology*, *31*(2), e70075

Tariq, A., Shu, H., Gagnon, A. S., Li, Q., Mumtaz, F., Hysa, A., Siddique, M. A., & Munir, I. (2021). Assessing burned areas in wildfires and prescribed fires with spectral indices and SAR images in the Margalla Hills of Pakistan. *Forests*, *12*(10), 1371

Tariq, A., Shu, H., Saddiqui, S., Mousa, B. G., Munir, I., Nasri, A., Waqas, H., Baqa, M. F., & Lu, L. (2021). Forest fire monitoring using spatial-statistical and geo-spatial analysis of factors determining forest fire in Margalla Hills, Islamabad, Pakistan. *Geomatics, Natural Hazards and Risk, 12*(1), 1212–1233

Tariq, A., Shu, H., Siddiqui, S., Munir, I., Sharifi, A., Li, Q., & Lu, L. (2022). Spatio-temporal analysis of forest fire events in the Margalla Hills, Islamabad, Pakistan using socio-economic and environmental variable data with machine learning methods. *Journal of Forestry Research*, *33*(1), 183–194

Tomšik, R. (2019). Power comparisons of Shapiro–Wilk, Kolmogorov–Smirnov and Jarque–Bera tests. *Scholars Journal of Research in Mathematics and Computer Science*, *3*(3), 238–244.

Turco, M., Rosa-Cánovas, J. J., Bedia, J., Jerez, S., Montávez, J. P., Llasat, M. C., & Provenzale, A. (2018). Exacerbated fires in Mediterranean Europe due to anthropogenic warming projected with non-stationary climate-fire models. *Nature Communications*, *9*, 3821

Uhm, T., & Yi, S. (2023). A comparison of normality testing methods by empirical power and distribution of P-values. *Communications in Statistics–Simulation and Computation*, *52*(9), 4445–4458

Ullah, H., Niaz, R., Hussain, I., Alshanbari, H. M., & Almazah, M. M. A. (2026). Assessment of climatological trends, spatial distribution and driving forces of extreme daily precipitation events. *Pure and Applied Geophysics*, *183*(7), 3545–3579

Ullah, W., Karim, A., Ullah, S., Rehman, A.-U., Bibi, T., Wang, G., Ullah, S., Bhatti, A. S., Ali, G., Abbas, A., Hagan, D. F. T., Nooni, I. K., Zhu, C., & Hussain, A. (2023). An increasing trend in daily monsoon precipitation extreme indices over Pakistan and its relationship with atmospheric circulations. *Frontiers in Environmental Science*, *11*, Article 1228817

Venema, V., Trewin, B., Wang, X. L., Szentimrey, T., Lakatos, M., Aguilar, E., Auer, I., Guijarro, J. A., Menne, M., Oria, C., Louamba, S. R. L., & Rasul, G. (2018). *Guidance on the homogenization of climate station data*

Wan, H., Wang, X. L., & Swail, V. R. (2010). Homogenization and trend analysis of Canadian near-surface wind speeds. *Journal of Climate*, *23*(5), 1209–1225

Wang, F., Shao, W., Yu, H., Kan, G., He, X., Zhang, D., Ren, M., & Wang, G. (2020). Re-evaluation of the power of the Mann–Kendall test for detecting monotonic trends in hydrometeorological time series. *Frontiers in Earth Science*, *8*, Article 14

Wang, W., Chen, Y., Becker, S., & Liu, B. (2015). Linear trend detection in serially dependent hydrometeorological data based on a variance correction Spearman rho method. *Water*, *7*(12), 6673–6695

Wang, X. L., & Feng, Y. (2013). *RHtestsV4 user manual*. Climate Research Division, Atmospheric Science and Technology Directorate, Environment Canada.

Wang, Y., Wu, Y., Cui, H., Liu, Y., Li, M., Yang, X., Zhao, J., & Yu, Q. (2025). Extreme climate drivers and their interactions in lightning-ignited fires: Insights from machine learning models. *Forests*, *16*(12), 1861

Wang, Y., Xu, Y., Tabari, H., Wang, J., Wang, Q., Song, S., & Hu, Z. (2020). Innovative trend analysis of annual and seasonal rainfall in the Yangtze River Delta, eastern China. *Atmospheric Research*, *231*, 104673

Waseem, S., & Khayyam, U. (2019). Loss of vegetative cover and increased land surface temperature: A case study of Islamabad, Pakistan. *Journal of Cleaner Production*, *234*, 972–983

Wasif Ali, N. u. A. B., Amir, S., Iqbal, K. M. J., Shah, A. A., Saqib, Z., Akhtar, N., Ullah, W., & Tariq, M. A. U. R. (2022). Analysis of land surface temperature dynamics in Islamabad by using MODIS remote sensing data. *Sustainability*, *14*(16), Article 9894

Weaver, K. F., Morales, V., Dunn, S. L., Godde, K., & Weaver, P. F. (2017). *An introduction to statistical analysis in research: With applications in the biological and life sciences*. John Wiley & Sons

Welham, S. J., Gezan, S. A., Clark, S. J., & Mead, A. (2014). *Statistical methods in biology: Design and analysis of experiments and regression*. CRC Press.

Westerling, A. L., Hidalgo, H. G., Cayan, D. R., & Swetnam, T. W. (2006). Warming and earlier spring increase western U.S. forest wildfire activity. *Science, 313*(5789), 940–943

Wijngaard, J. B., Klein Tank, A. M. G., & Können, G. P. (2003). Homogeneity of 20th century European daily temperature and precipitation series. *International Journal of Climatology, 23*(6), 679–692

Williams, A. P., Abatzoglou, J. T., Gershunov, A., Guzman-Morales, J., Bishop, D. A., Balch, J. K., & Lettenmaier, D. P. (2019). Observed impacts of anthropogenic climate change on wildfire in California. *Earth's Future, 7*(8), 892–910

Xing, H., Fang, K., Yao, Q., Zhou, F., Ou, T., Liu, J., Zhou, S., Jiang, S., Chen, Y., Bai, M., & Chen, J. M. (2023). Impacts of changes in climate extremes on wildfire occurrences in China. *Ecological Indicators, 157,* Article 111288

Xu, W. R., Dixon, K. W., Zenes, N., & Adams-Smith, D. (2025). Sometimes missing the heat: The risk of underestimating extreme heat days with daily maximum heat index approximation. *International Journal of Biometeorology, 69*(11), 2967–2981

Yaseen, Z. M., Kisi, O., Deo, R. C., Demir, V., Al-Ansari, N., & Shahid, S. (2020). Spatiotemporal variability in the hydrometeorological time-series over Upper Indus River Basin of Pakistan. *Advances in Meteorology, 2020,* Article 5852760

Yonus, M., Jan, B., Khan, H., Nawaz, F., & Ali, M. (2023). Study the seasonal trend analysis and probability distribution functions of rainfall for atmospheric region of Pakistan. *MethodsX, 10,* 102058

Yue, S., Pilon, P., & Cavadias, G. (2002). Power of the Mann–Kendall and Spearman's rho tests for detecting monotonic trends in hydrological series. *Journal of Hydrology, 259*(1–4), 254–271.

Zacharakis, I., & Tsihrintzis, V. A. (2023). Environmental forest fire danger rating systems and indices around the globe: A review. *Land, 12*(1), Article 194.

Zafar, U., Anjum, M. N., Hussain, S., Sultan, M., Rasool, G., Riaz, M. Z. B., Shoaib, M., & Asif, M. (2024). Analyzing the spatiotemporal changes in climatic extremes in cold and mountainous environment: Insights from the Himalayan Mountains of Pakistan. *Atmosphere*, *15*(10), 1221.

Zahid, M., & Rasul, G. (2010). Rise in summer heat index over Pakistan. *Pakistan Journal of Meteorology*, *6*(12), 85–96.

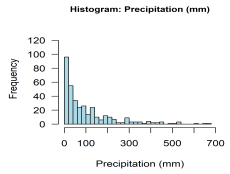
Zhang, X., Alexander, L., Hegerl, G. C., Jones, P., Klein Tank, A., Peterson, T. C., Trewin, B., & Zwiers, F. W. (2011). Indices for monitoring changes in extremes based on daily temperature and precipitation data. *Wiley Interdisciplinary Reviews: Climate Change*, *2*(6), 851–870.

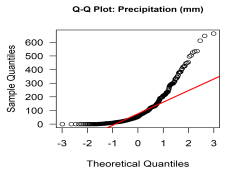
Zhang, Z., & Wang, K. (2025). Homogenization of surface wind speed over global land from 1973 to 2022. *Journal of Geophysical Research: Atmospheres*, *130*, e2024JD042939.

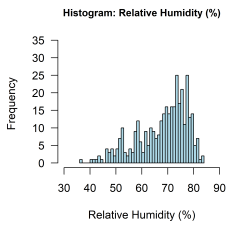
APPENDIX

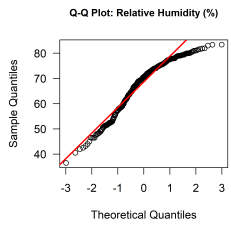
A1. Normality test results for monthly climate data.

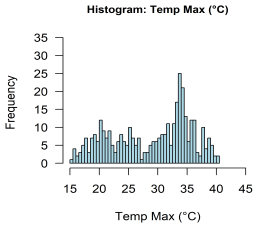
Variable	A2	p-value	D	p-value	JB	p-value	W2	p-value	Verdict
Precipitation (mm)	25.24	3.7e-24	0.2001	9.5e-40	438.6	0e+00	4.478	7.4e-10	Not Normal
Temp Max (°C)	8.61	6e-21	0.1288	9.3e-16	27.1	1.3e-06	1.540	7.4e-10	Not Normal
Temp Min (°C)	10.17	3.7e-24	0.1262	4.1e-15	32.1	1.1e-07	1.470	7.4e-10	Not Normal
Relative Humidity (%)	8.06	1.1e-19	0.1182	3.8e-13	39.8	2.2e-09	1.381	7.4e-10	Not Normal
Wind Speed (m/s)	14.20	3.7e-24	0.1807	4.1e-32	1867.2	0e+00	2.073	7.4e-10	Not Normal

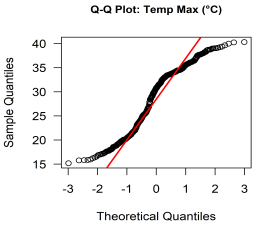


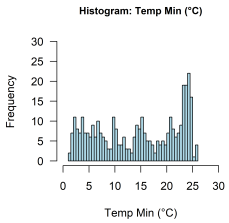


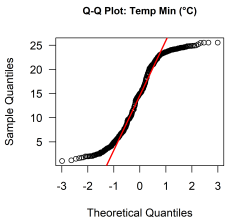


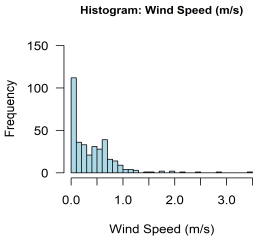


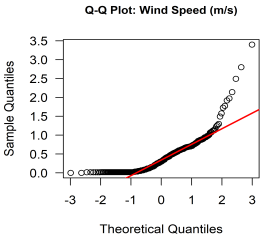




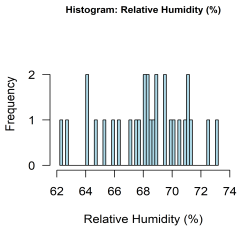


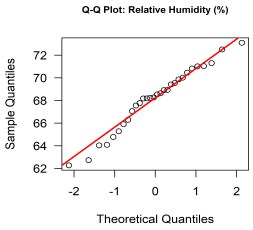


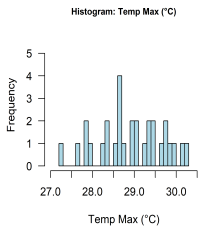


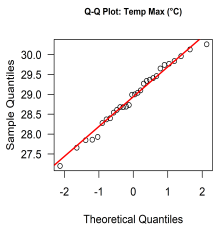


A2. Normality test results for yearly climate data.

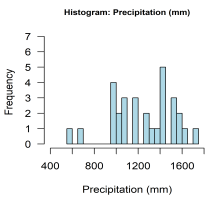


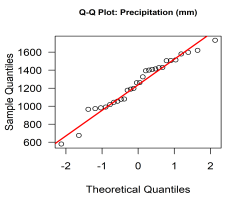


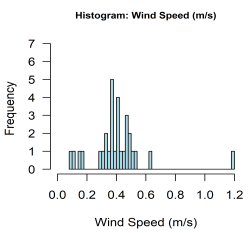


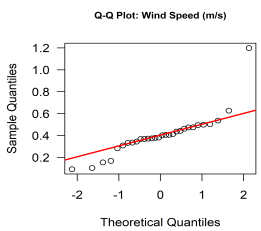


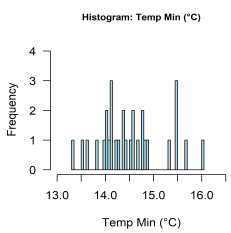
Variable	A2	p-value	D	p-value	JB	p-value	W2	p-value	Verdict
Precipitation (mm)	0.41	0.3226	0.1347	0.1782	1.0	0.5925	0.062	0.3399	Normal
Temp Max (°C)	0.19	0.8908	0.0709	0.963	0.8	0.6626	0.027	0.8793	Normal
Temp Min (°C)	0.47	0.2309	0.0983	0.6485	1.2	0.5417	0.077	0.2206	Normal
Relative Humidity (%)	0.37	0.4001	0.1364	0.1652	1.1	0.5645	0.065	0.3146	Normal
Wind Speed (m/s)	1.73	0.0001482***	0.2084	0.002154**	96.1	0***	0.290	0.0003802***	Not Normal

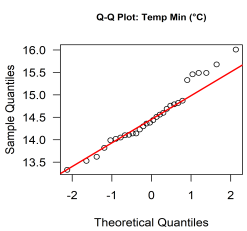






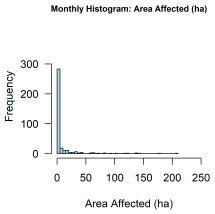


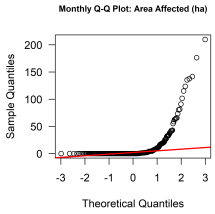


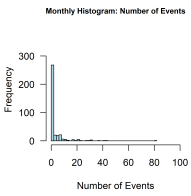


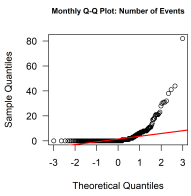
A3. Normality test results for monthly and yearly fire data.

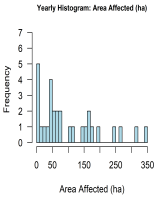
Scale	Variable	A2	p1	D	p2	JB	p3	W2	p4	Verdict
Monthly	number of events	64.77	< 0.0001***	0.3415	< 0.0001***	22167.6	< 0.0001***	12.983	< 0.0001***	Not Normal
Monthly	area affected (ha)	82.40	< 0.0001***	0.3662	< 0.0001***	10676.5	< 0.0001***	17.034	< 0.0001***	Not Normal
Yearly	Number of events	1.55	4e-04***	0.2045	0.0025**	11.1	0.0038**	0.277	5e-04***	Not Normal
Yearly	Area affected (ha)	1.25	0.0025**	0.2022	0.0030**	5.7	0.0583	0.210	0.0036**	Not Normal

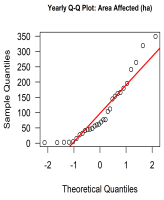


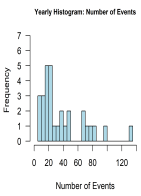


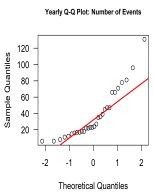




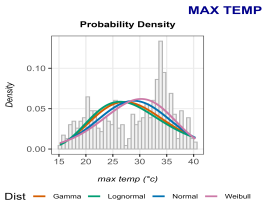




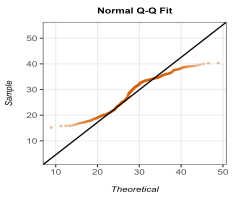


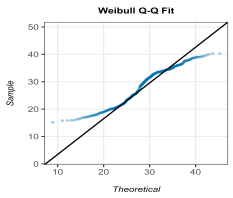


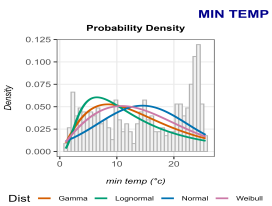
B1. Goodness-of-Fit results for climate data.



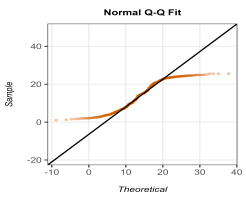
Model	A.D.Stat	AIC
Normal	8.65	2393
Gamma	10.50	2412
Weibull	7.64	2373
Lognormal	11.67	2429

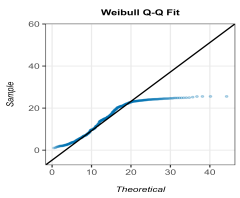


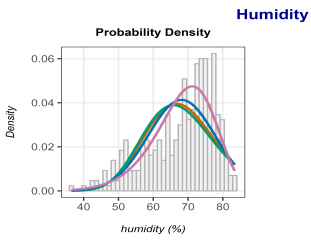




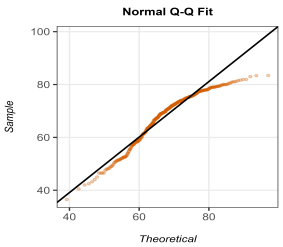
Model	A.D.Stat	AIC
Normal	10.22	2504
Gamma	12.16	2525
Weibull	11.71	2492
Lognormal	15.65	2592

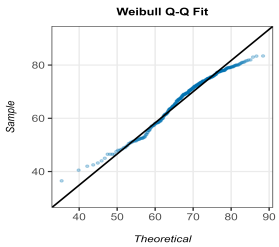


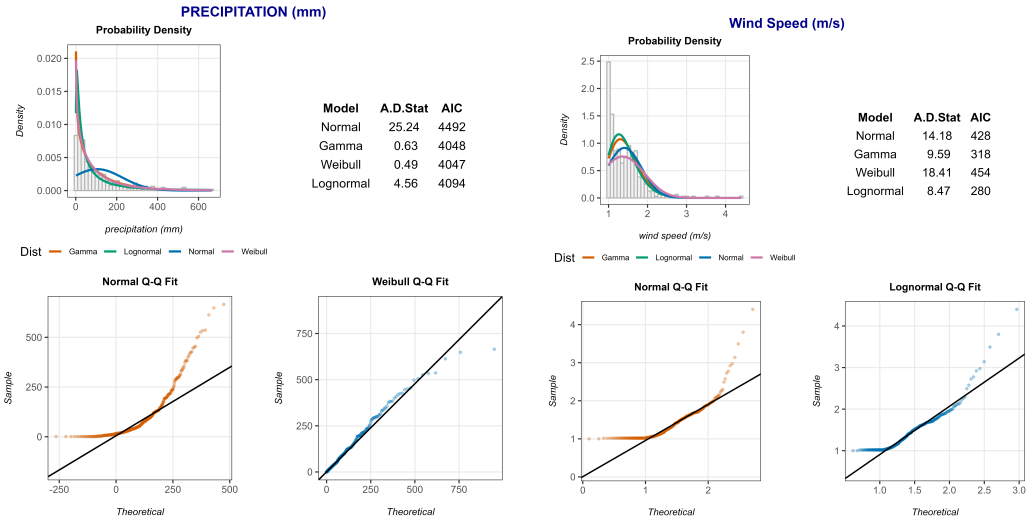




Model	A.D.Stat	AIC
Normal	8.08	2659
Gamma	10.57	2691
Weibull	4.25	2605
Lognormal	11.95	2710



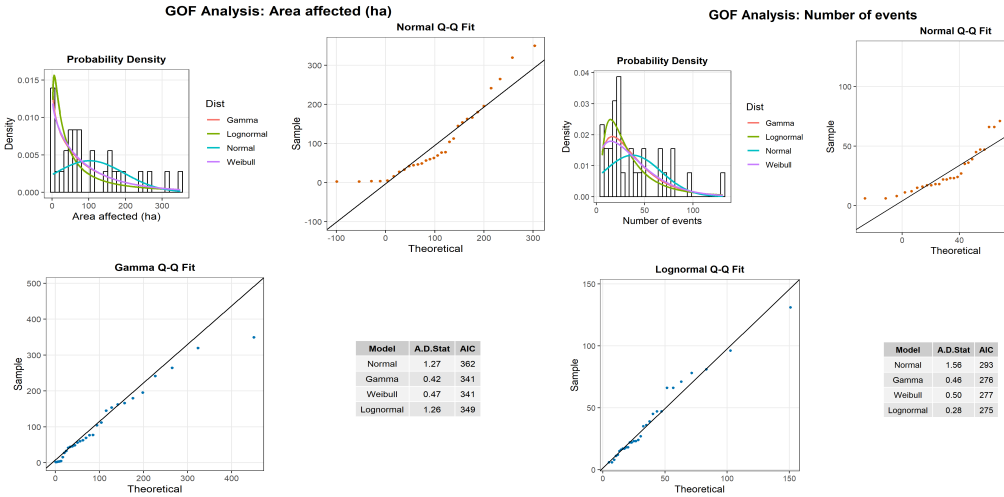




Model	A.D.Stat	AIC
Normal	25.24	4492
Gamma	0.63	4048
Weibull	0.49	4047
Lognormal	4.56	4094

Model	A.D.Stat	AIC
Normal	14.18	428
Gamma	9.59	318
Weibull	18.41	454
Lognormal	8.47	280

B2. Goodness-of-Fit results for fire data.



Model	A.D.Stat	AIC
Normal	1.27	362
Gamma	0.42	341
Weibull	0.47	341
Lognormal	1.26	349

Model	A.D.Stat	AIC
Normal	1.56	293
Gamma	0.46	276
Weibull	0.50	277
Lognormal	0.28	275

C. Descriptive statistics results for climate data

Max Temperature (°C)

Period	Min	Mean	Max	SD	CV (%)	Skew	Kurtosis
Jan	15.190	18.012	21.460	1.655	9.190	0.302	2.167
Feb	15.970	20.448	24.650	1.941	9.491	0.039	2.932
Mar	21.610	25.221	30.130	2.276	9.023	0.500	2.492
Apr	26.720	30.990	35.760	2.226	7.183	0.261	2.252
May	31.610	35.872	39.660	2.006	5.593	0.105	2.483
Jun	34.510	37.810	40.320	1.448	3.830	-0.284	2.445
Jul	32.900	35.127	38.980	1.357	3.862	0.796	3.702
Aug	31.780	33.657	35.150	0.755	2.243	-0.096	3.161
Sep	31.490	33.362	34.880	0.966	2.895	-0.486	2.193
Oct	26.900	30.589	32.860	1.393	4.555	-0.711	3.164
Nov	22.830	25.192	27.900	1.240	4.921	-0.043	2.409
Dec	17.290	20.481	23.550	1.403	6.848	-0.246	2.968
Winter	18.622	21.065	23.169	1.140	5.412	-0.383	2.877
Spring	31.555	34.901	37.571	1.495	4.283	-0.154	2.538
Summer	32.800	34.056	35.276	0.605	1.776	0.109	2.214
Autumn	25.179	27.935	29.736	1.118	4.003	-0.393	2.744
Annual	27.200	28.927	30.260	0.775	2.680	-0.257	2.372

Min Temperature (°C)

Period	Min	Mean	Max	SD	CV (%)	Skew	Kurtosis
Jan	1.040	2.845	4.980	1.140	40.062	0.517	2.237
Feb	3.400	6.085	9.910	1.221	20.059	0.558	4.992
Mar	8.570	10.739	12.760	1.026	9.552	0.106	2.319
Apr	13.520	15.387	18.280	1.305	8.483	0.608	2.404
May	16.610	19.805	24.570	2.025	10.226	0.725	2.983
Jun	20.280	23.268	25.560	1.196	5.141	-0.207	2.911
Jul	22.820	24.355	25.560	0.655	2.690	-0.224	3.130
Aug	22.510	23.758	24.840	0.522	2.198	0.022	3.012
Sep	19.370	21.187	22.820	0.894	4.218	-0.032	2.362
Oct	11.680	14.636	16.990	1.336	9.125	-0.510	2.562
Nov	6.280	8.156	10.670	1.154	14.149	0.348	2.228
Dec	1.740	3.612	5.520	1.073	29.704	0.124	2.176
Winter	4.076	5.795	7.043	0.744	12.838	-0.342	2.330
Spring	17.401	19.490	22.480	1.340	6.874	0.612	2.656
Summer	21.892	23.121	23.883	0.434	1.875	-0.772	3.608
Autumn	9.392	11.448	13.677	1.009	8.811	-0.202	2.805
Annual	13.330	14.521	16.010	0.660	4.545	0.456	2.615

Wind Speed (m/s)

Period	Min	Mean	Max	SD	CV (%)	Skew	Kurtosis
Jan	0.019	0.210	1.266	0.233	110.993	3.200	15.166
Feb	0.024	0.642	3.400	0.560	87.265	4.091	21.096
Mar	0.071	0.715	2.494	0.485	67.881	2.078	7.749
Apr	0.035	0.681	2.800	0.453	66.615	3.362	17.344
May	0.019	0.692	1.973	0.433	62.577	1.062	4.627
Jun	0.019	0.714	2.140	0.467	65.404	1.198	5.350
Jul	0.019	0.596	1.576	0.380	63.785	0.597	3.187
Aug	0.019	0.283	0.692	0.181	63.893	0.279	2.335
Sep	0.019	0.145	0.411	0.128	88.636	0.437	1.745
Oct	0.019	0.096	0.265	0.085	88.491	0.496	1.638
Nov	0.000	0.042	0.120	0.035	83.278	1.020	2.658
Dec	0.000	0.058	0.265	0.061	104.028	1.669	5.651
Winter	0.017	0.389	1.768	0.290	74.562	3.521	17.856
Spring	0.030	0.695	2.217	0.398	57.273	1.646	8.457
Summer	0.035	0.343	0.798	0.185	53.990	0.255	2.698
Autumn	0.019	0.070	0.194	0.053	76.227	0.640	2.237
Annual	0.092	0.405	1.199	0.194	47.933	2.053	10.747

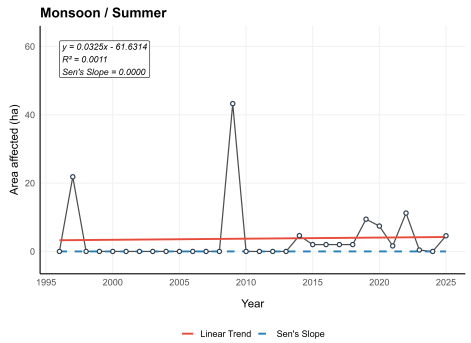
D1. ITA results for fire and climate data.

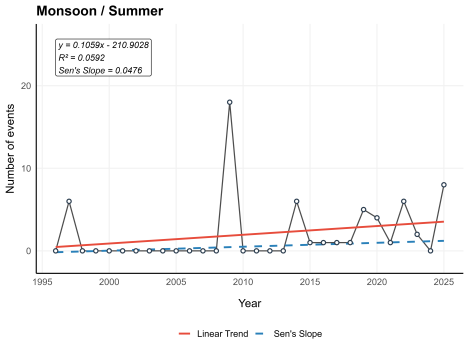
Statistics on the monthly, seasonal and annual ITA - Area affected (ha)

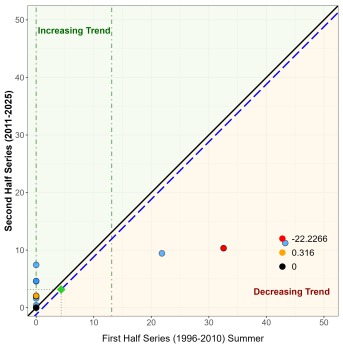
Period	Slope s	Correlation ρy1y2	Slope Std. Dev.	Sig. Level 95%	Sig. Level 99%
January	-0.1042 *	0.7647	0.0493	±0.0966	±0.1269
February	-0.0954 **	0.8814	0.0204	±0.0400	±0.0526
March	-0.1002 **	0.9324	0.0184	±0.0360	±0.0474
April	-0.9669 **	0.9199	0.1927	±0.3777	±0.4964
May	-0.9589 **	0.9736	0.1094	±0.2144	±0.2818
June	-1.2146 **	0.9859	0.0980	±0.1920	±0.2524
July	-0.1226	0.7661	0.0706	±0.1383	±0.1818
August	0.0397 **	0.9457	0.0046	±0.0091	±0.0120
September	0.0040	0.0000	0.0026	±0.0050	±0.0066
October	0.0034	0.0000	0.0024	±0.0047	±0.0062
November	-0.2738 **	0.9012	0.0431	±0.0845	±0.1111
December	-0.4945 **	0.9348	0.0758	±0.1486	±0.1953
Winter	-0.7948 **	0.9140	0.1274	±0.2497	±0.3282
Spring	-3.1405 **	0.9608	0.2870	±0.5625	±0.7393
Summer	-0.0789	0.7927	0.0692	±0.1356	±0.1782
Autumn	-0.2705 **	0.9280	0.0368	±0.0721	±0.0947
Annual	-0.7510 **	0.9563	0.0616	±0.1207	±0.1586

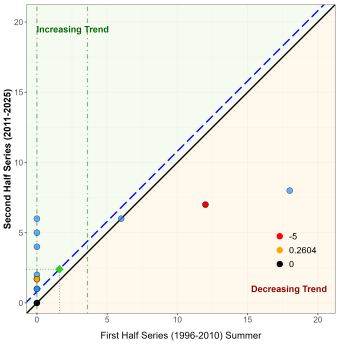
Statistics on the monthly, seasonal and annual ITA - Number of events

Period	Slope s	Correlation ρy1y2	Slope Std. Dev.	Sig. Level 95%	Sig. Level 99%
January	0.0133 *	0.9564	0.0061	±0.0119	±0.0157
February	-0.0267 **	0.9585	0.0084	±0.0164	±0.0216
March	-0.0889 **	0.8884	0.0221	±0.0433	±0.0569
April	-0.1689 **	0.9615	0.0177	±0.0346	±0.0455
May	-0.3200 **	0.9321	0.0506	±0.0992	±0.1303
June	-0.3733 **	0.9333	0.0757	±0.1484	±0.1951
July	0.0178	0.6965	0.0329	±0.0644	±0.0847
August	0.0267 **	0.5707	0.0066	±0.0129	±0.0169
September	0.0089 *	0.0000	0.0044	±0.0086	±0.0112
October	0.0089	0.0000	0.0063	±0.0123	±0.0162
November	-0.0533 **	0.9024	0.0103	±0.0202	±0.0266
December	-0.1067 **	0.9395	0.0152	±0.0299	±0.0393
Winter	-0.2133 **	0.9042	0.0458	±0.0897	±0.1179
Spring	-0.8622 **	0.9392	0.1083	±0.2123	±0.2790
Summer	0.0533	0.6839	0.0371	±0.0727	±0.0955
Autumn	-0.0444 **	0.9722	0.0056	±0.0110	±0.0145
Annual	-0.1839 **	0.9530	0.0198	±0.0388	±0.0510









ITA: Area affected *Number of fire event*

Innovative Trend Analysis (ITA) Statistics

(* significant at 95% level, ** significant at 99% level)

Variable	Statistic	Jan	Feb	Mar	Apr	May	Jun	Jul	Aug	Sep	Oct	Nov	Dec	Winter	Pre-Monsoon	Monsoon	Post-Monsoon	Annual
PRECIPITATION (mm)	Slope s	-0.6378 **	-0.9987 *	2.8138 **	0.9200 **	1.1253 **	0.1102	1.4928 **	1.1569	3.8027 **	0.9640 **	0.7529 **	-0.2422 *	0.2338 **	1.0227 **	1.6406 **	0.8584 **	0.9383 **
	Correlation ρ	0.9431	0.8564	0.9243	0.9415	0.9643	0.9896	0.9862	0.8938	0.9267	0.8539	0.9398	0.9625	0.9643	0.9746	0.9383	0.9460	0.9739
	Slope Std.Dev	0.2208	0.4875	0.3621	0.2184	0.0999	0.1036	0.1872	0.8300	0.4439	0.3185	0.0901	0.0977	0.0877	0.0859	0.1951	0.1006	0.0572
	Sig. Level 95%	±0.4328	±0.9555	±0.7097	±0.4281	±0.1958	±0.2030	±0.3670	±1.6268	±0.8700	±0.6243	±0.1766	±0.1916	±0.1719	±0.1684	±0.3823	±0.1972	±0.1121
	Sig. Level 99%	±0.5688	±1.2559	±0.9327	±0.5626	±0.2573	±0.2668	±0.4823	±2.1381	±1.1434	±0.8205	±0.2321	±0.2518	±0.2260	±0.2213	±0.5025	±0.2592	±0.1474
MAX TEMP (°C)	Slope s	-0.0201 **	0.0154	-0.0604 **	-0.0789 **	-0.0606 **	0.0094	-0.0384 **	-0.0005	-0.0050	-0.0270 **	-0.0691 **	0.0004	-0.0162 **	-0.0697 **	-0.0086 **	-0.0481 **	-0.0279 **
	Correlation ρ	0.9734	0.9325	0.9074	0.8047	0.9639	0.9464	0.9786	0.9226	0.9431	0.8566	0.9594	0.9455	0.9713	0.8708	0.9431	0.9335	0.9558
	Slope Std.Dev	0.0046	0.0087	0.0119	0.0169	0.0066	0.0058	0.0034	0.0036	0.0040	0.0091	0.0043	0.0056	0.0032	0.0118	0.0025	0.0050	0.0028
	Sig. Level 95%	±0.0091	±0.0170	±0.0234	±0.0332	±0.0129	±0.0113	±0.0067	±0.0071	±0.0078	±0.0178	±0.0084	±0.0110	±0.0063	±0.0231	±0.0050	±0.0097	±0.0055
	Sig. Level 99%	±0.0120	±0.0224	±0.0307	±0.0436	±0.0169	±0.0149	±0.0088	±0.0093	±0.0102	±0.0234	±0.0111	±0.0145	±0.0083	±0.0304	±0.0066	±0.0128	±0.0072
MIN TEMP (°C)	Slope s	-0.0280 **	-0.0334 **	-0.0381 **	-0.0773 **	-0.1061 **	-0.0601 **	-0.0250 **	-0.0116 **	0.0128 **	-0.0185 **	-0.0191 **	-0.0363 **	-0.0340 **	-0.0917 **	-0.0210 **	-0.0188 **	-0.0367 **
	Correlation ρ	0.9222	0.8706	0.9568	0.9847	0.9804	0.9579	0.9735	0.8936	0.9599	0.9489	0.9832	0.9509	0.9017	0.9600	0.9050	0.9761	0.9653
	Slope Std.Dev	0.0055	0.0076	0.0037	0.0028	0.0049	0.0048	0.0018	0.0029	0.0031	0.0052	0.0026	0.0041	0.0039	0.0053	0.0031	0.0027	0.0021
	Sig. Level 95%	±0.0107	±0.0148	±0.0072	±0.0054	±0.0096	±0.0095	±0.0036	±0.0057	±0.0060	±0.0102	±0.0050	±0.0080	±0.0076	±0.0104	±0.0061	±0.0053	±0.0042
	Sig. Level 99%	±0.0141	±0.0195	±0.0095	±0.0072	±0.0126	±0.0124	±0.0047	±0.0076	±0.0079	±0.0134	±0.0066	±0.0105	±0.0100	±0.0137	±0.0080	±0.0069	±0.0055
Humidity (%)	Slope s	0.2025 **	0.0815 *	0.2236 **	0.3504 **	0.4796 **	0.0650	0.1635 **	0.0049	0.0878 **	0.0488	0.1814 **	0.0923 **	0.1499 **	0.4150 **	0.0803 **	0.1151 **	0.1651 **
	Correlation ρ	0.9714	0.8868	0.9677	0.9793	0.9622	0.8265	0.9098	0.9306	0.9554	0.8471	0.9371	0.9408	0.9096	0.9156	0.9829	0.9249	0.9611
	Slope Std.Dev	0.0160	0.0344	0.0184	0.0186	0.0313	0.0441	0.0323	0.0138	0.0111	0.0280	0.0164	0.0179	0.0182	0.0385	0.0068	0.0162	0.0100
	Sig. Level 95%	±0.0313	±0.0675	±0.0361	±0.0364	±0.0613	±0.0865	±0.0633	±0.0270	±0.0218	±0.0548	±0.0321	±0.0351	±0.0356	±0.0754	±0.0134	±0.0318	±0.0196
	Sig. Level 99%	±0.0412	±0.0887	±0.0474	±0.0478	±0.0806	±0.1137	±0.0832	±0.0355	±0.0286	±0.0720	±0.0422	±0.0461	±0.0468	±0.0991	±0.0176	±0.0417	±0.0257
Wind Speed (m/s)	Slope s	0.0041	-0.0161 **	-0.0167 **	-0.0082 **	-0.0080 **	-0.0076 *	0.0074 **	0.0090 **	0.0173 **	0.0073 **	0.0027 **	0.0055 **	-0.0058	-0.0081 **	0.0065 **	0.0050 **	-0.0003
	Correlation ρ	0.6873	0.6141	0.7696	0.8471	0.9840	0.9396	0.9769	0.9238	0.6966	0.6821	0.4681	0.8543	0.6549	0.9296	0.9654	0.7538	0.8830
	Slope Std.Dev	0.0022	0.0060	0.0055	0.0031	0.0009	0.0030	0.0010	0.0009	0.0017	0.0011	0.0004	0.0006	0.0032	0.0018	0.0008	0.0006	0.0013
	Sig. Level 95%	±0.0044	±0.0117	±0.0107	±0.0060	±0.0018	±0.0059	±0.0019	±0.0017	±0.0034	±0.0021	±0.0009	±0.0011	±0.0063	±0.0036	±0.0016	±0.0011	±0.0025
	Sig. Level 99%	±0.0058	±0.0154	±0.0141	±0.0079	±0.0024	±0.0078	±0.0026	±0.0022	±0.0045	±0.0028	±0.0011	±0.0014	±0.0083	±0.0047	±0.0021	±0.0014	±0.0033

D2. Mann–Kendall test statistics ETCCDI indices (1996-2025)

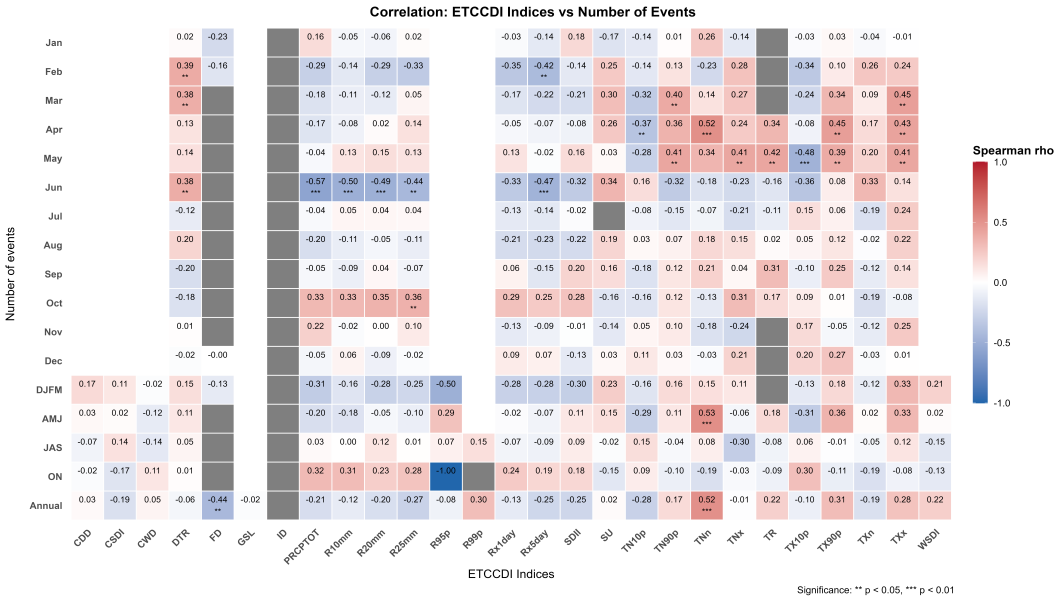
Trends of temperature based Indices

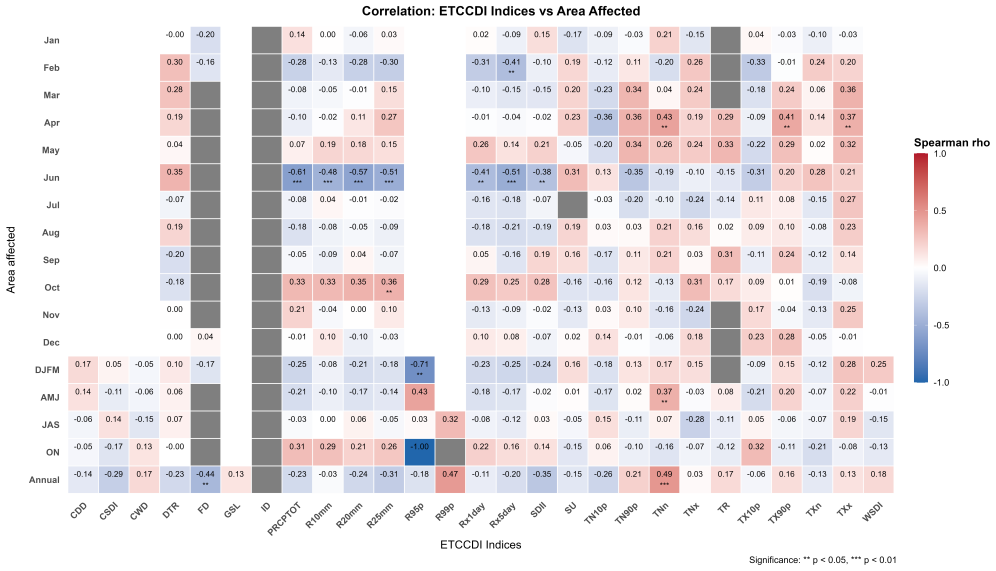
Index	Description	Unit	Mean	Min	Max	Sen's slope	τ	p-value	Sig.
TXx	TXx – Annual Max. Daily Maximum Temp.	Tmax (°C)	43.38	39.10	46.60	0.000	-0.014	0.9288	ns
TNx	TNx – Annual Max. Daily Minimum Temp.	Tmin (°C)	29.69	27.50	31.70	0.000	-0.077	0.5748	ns
TXn	TXn – Annual Min. Daily Maximum Temp.	Tmax (°C)	10.34	7.20	14.00	0.100	0.329	0.0123	*
TNn	TNn – Annual Min. Daily Minimum Temp.	Tmin (°C)	-0.79	-2.80	1.30	-0.013	-0.098	0.4720	ns
TN10p	TN10p – Cold Nights (TN < 10th percentile)	Days (%)	8.24	1.92	20.55	0.114	0.201	0.1247	ns
TX10p	TX10p – Cold Days (TX < 10th percentile)	Days (%)	9.37	4.37	21.64	0.055	0.088	0.5090	ns
TN90p	TN90p – Warm Nights (TN > 90th percentile)	Days (%)	8.81	3.56	21.92	-0.075	-0.149	0.2600	ns
TX90p	TX90p – Warm Days (TX > 90th percentile)	Days (%)	8.52	1.64	21.37	-0.131	-0.154	0.2388	ns
WSDI	WSDI – Warm Spell Duration Index	Days	3.43	0.00	19.00	0.000	-0.309	0.0330	*
CSDI	CSDI – Cold Spell Duration Index	Days	3.90	0.00	25.00	0.000	0.003	1.0000	ns
DTR	DTR – Mean Diurnal Temperature Range	Temperature (°C)	14.41	12.83	15.32	0.023	0.228	0.0804	ns
FD	FD – Frost Days (Tmin < 0°C)	Days	3.60	0.00	17.00	0.000	0.131	0.3425	ns
SU	SU – Summer Days (Tmax > 25°C)	Days	244.90	213.00	268.00	-0.250	-0.118	0.3719	ns
ID	ID – Ice Days (Tmax < 0°C)	Days	0.00	0.00	0.00	0.000	1.000	1.0000	ns
TR	TR – Tropical Nights (Tmin > 20°C)	Days	122.67	82.00	147.00	-0.667	-0.295	0.0244	*
GSL	GSL – Growing Season Length	Days	364.13	360.00	365.00	0.000	-0.031	0.8573	ns

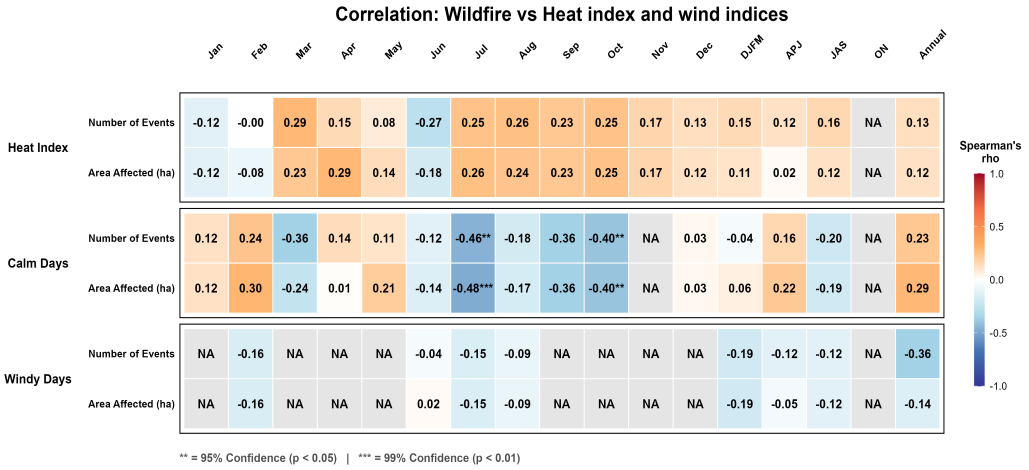
Trends of precipitation based Indices

Index	Description	Unit	Mean	Min	Max	Sen's slope	τ	p-value	Sig.
PRCPTOT	PRCPTOT – Annual Total Wet-Day Precipitation	Precipitation (mm)	1244.83	580.50	1730.40	7.650	0.172	0.1868	ns
SDII	SDII – Simple Daily Intensity Index	Intensity (mm day^{-1})	17.11	11.39	22.49	0.068	0.154	0.2390	ns
CDD	CDD – Maximum Consecutive Dry Days	Days	45.00	21.00	86.00	0.000	0.016	0.9145	ns
CWD	CWD – Maximum Consecutive Wet Days	Days	5.27	3.00	9.00	0.000	-0.097	0.5019	ns
R10mm	R10mm – Heavy Precipitation Days (≥10 mm)	Days	34.77	17.00	55.00	0.143	0.140	0.2981	ns
R20mm	R20mm – Very Heavy Precipitation Days (≥20 mm)	Days	20.13	8.00	28.00	0.167	0.238	0.0731	ns
R25mm	R25mm – Precipitation ≥25 mm Days	Days	16.17	7.00	23.00	0.118	0.179	0.1835	ns
Rx1day	Rx1day – Maximum 1-Day Precipitation	Precipitation (mm)	121.32	50.00	243.00	-0.574	-0.097	0.4644	ns
Rx5day	Rx5day – Maximum 5-Day Precipitation	Precipitation (mm)	199.70	85.70	333.00	-0.913	-0.057	0.6685	ns
R95p	R95p – Very Wet Day Precipitation Total	Precipitation (mm)	326.49	0.00	604.80	1.663	0.060	0.6554	ns
R99p	R99p – Extremely Wet Day Precipitation Total	Precipitation (mm)	108.08	0.00	321.00	0.000	-0.052	0.7199	ns

E. Spearman's correlations results




Correlation: ETCCDI Indices vs Area Affected
Area affected
Jan
Feb
Mar
Apr
May
Jun
Jul
Aug
Sep
Oct
Nov
Dec
DJFM
AMJ
JAS
ON
Annual
CDD
CSDI
CWD
DTR
FD
GSL
ID
PRCPTOT
R10mm
R20mm
R25mm
R95p
R99p
Rx1day
Rx5day
SDII
SU
TN10p
TN90p
TNn
TNx
TR
TX10p
TX90p
TXn
TXx
WSDI
ETCCDI Indices
Spearman rho
1.0
0.5
0.0
-0.5
-1.0
Significance: ** p < 0.05, *** p < 0.01


Correlation: Wildfire vs Heat index and wind indices
Jan
Feb
Mar
Apr
May
Jun
Jul
Aug
Sep
Oct
Nov
Dec
DJFM
APJ
JAS
ON
Annual
Heat Index
Number of Events
-0.12 -0.00 0.29 0.15 0.08 -0.27 0.25 0.26 0.23 0.25 0.17 0.13 0.15 0.12 0.16 NA 0.13
Area Affected (ha)
-0.12 -0.08 0.23 0.29 0.14 -0.18 0.26 0.24 0.23 0.25 0.17 0.12 0.11 0.02 0.12 NA 0.12
Calm Days
Number of Events
0.12 0.24 -0.36 0.14 0.11 -0.12 -0.46** -0.18 -0.36 -0.40** NA 0.03 -0.04 0.16 -0.20 NA 0.23
Area Affected (ha)
0.12 0.30 -0.24 0.01 0.21 -0.14 -0.48*** -0.17 -0.36 -0.40** NA 0.03 0.06 0.22 -0.19 NA 0.29
Windy Days
Number of Events
NA -0.16 NA NA NA -0.04 -0.15 -0.09 NA NA NA NA -0.19 -0.12 -0.12 NA -0.36
Area Affected (ha)
NA -0.16 NA NA NA 0.02 -0.15 -0.09 NA NA NA NA -0.19 -0.05 -0.12 NA -0.14
Spearman's rho
1.0
0.5
0.0
-0.5
-1.0
** = 95% Confidence (p < 0.05) | *** = 99% Confidence (p < 0.01)

12% Overall Similarity

The combined total of all matches, including overlapping sources, for each database.

Filtered from the Report

- Bibliography
- Quoted Text

Match Groups

227 Not Cited or Quoted 8%
Matches with neither in-text citation nor quotation marks

118 Missing Quotations 4%
Matches that are still very similar to source material

0 Missing Citation 0%
Matches that have quotation marks, but no in-text citation

0 Cited and Quoted 0%
Matches with in-text citation present, but no quotation marks

Top Sources

6% Internet sources
7% Publications
8% Submitted works (Student Papers)

Integrity Flags

0 Integrity Flags for Review

Our system's algorithms look deeply at a document for any inconsistencies that would set it apart from a normal submission. If we notice something strange, we flag it for you to review.

A Flag is not necessarily an indicator of a problem. However, we'd recommend you focus your attention there for further review.

Match Groups

- **227** Not Cited or Quoted 8%
  Matches with neither in-text citation nor quotation marks
- **118** Missing Quotations 4%
  Matches that are still very similar to source material
- **0** Missing Citation 0%
  Matches that have quotation marks, but no in-text citation
- **0** Cited and Quoted 0%
  Matches with in-text citation present, but no quotation marks

Top Sources

- 6% Internet sources
- 7% Publications
- 8% Submitted works (Student Papers)

Top Sources

The sources with the highest number of matches within the submission. Overlapping sources will not be displayed.

1	Internet	
www.mdpi.com		<1%
2	Student papers	
Royal Veterinary College on 2022-08-04		<1%
3	Internet	
link.springer.com		<1%
4	Internet	
www.nepjol.info		<1%
5	Internet	
neptjournal.com		<1%
6	Student papers	
Universidad de Lleida on 2026-07-08		<1%
7	Internet	
krex.k-state.edu		<1%
8	Internet	
mdpi-res.com		<1%
9	Student papers	
University of Durham on 2021-08-09		<1%
10	Internet	
ebin.pub		<1%